

Inês Rodrigues Padrão

Licenciada em Bioquímica

Multicomponent Chemically and Physically Cross-linked Hydrogels

Dissertação para Obtenção do Grau de Mestre em Biotecnologia

Orientador: Dr. Ana Cecília Afonso Roque, FCT NOVA

Co-orientador: Dr. Ana Sofia Fidalgo Pombo Mendes Pina, FCT

NOVA

Setembro de 2019



Inês Rodrigues Padrão

Licenciada em Bioquímica

Multicomponent Chemically and Physically Cross-linked Hydrogels

Dissertação para obtenção do Grau de Mestre em Biotecnologia

Orientador: Dr. Ana Cecília Afonso Roque, FCT NOVA

Co-orientador: Dr. Ana Sofia Fidalgo Pombo Mendes Pina, FCT NOVA

Faculdade de Ciências e Tecnologia

Universidade Nova de Lisboa

Setembro de 2019

Multicomponent Chemically and Physically Cross-linked Hydrogels Copyright © Inês Rodrigues Padrão, Faculdade de Ciências e Tecnologia, Universidade Nova de Lisboa. A Faculdade de Ciências e Tecnologia e a Universidade Nova de Lisboa têm o direito, perpétuo e sem limites geográficos, de arquivar e publicar esta dissertação através de exemplares impressos reproduzidos em papel ou de forma digital, ou por qualquer outro meio conhecido ou que venha a ser inventado, e de a divulgar através de repositórios científicos e de admitir a sua cópia e distribuição com objetivos educacionais ou de investigação, não comerciais, desde que seja dado crédito ao autor e editor.

Acknowledgments

Walking down this path was only possible with the support, energy and strength of many people, especially of my advisor Professor Cecilia Roque, who so kindly welcomed me in her laboratory and believed in me. I appreciate the exemplary orientation marked by a high scientific rigor, a permanent interest and great dedication.

It is true that walking through new stages in life is always challenging and it is easy to have some reservations. Therefore, I also want to thank my co-advisor Dr. Ana Pina, who was always ready to share her knowledge and to give very thoughtful advices, making everything much easier. I feel like I grew up as a scientist and person this past year. This growth was the result of being surrounded by very competent people. For that, I thank you very much.

A big thanks to the people who are part of the Biomolecular Engeneering Lab, especially to Carina Esteves for always brightening my day and spending so many hours with me in the rheology lab, to Claudia Fernandes who had a lot of patience when introducing me to the world of protein expression and Ugi reactions, to Henrique Costa for being a fantastic "guru", to Manuel Matos for always stealing my pipette tips and to Gonçalo Teixeira who did a great job at keeping our moral up. Claudia "1984", Iana Lychko, Sara Carvalho and Gonçalo Santos I thank you for always being there for me when I needed it. And finally, to the incredible "Late Shift", Beatriz Mariz and Fernando Nunes, thank you for being the best thesis buddies ever!

Thank you to D. Palminha, Dr. Inês Grilo, Cecília Bonifácio and Elizabete Ferreira for all of the help and availability.

Jorge, Ruben and Your Excellency Dr. Claudia Vi., I am forever grateful for making my breaks so interesting and for giving me the courage to keep on fighting. Thank you, Mary, Bia, and Marta, the best friends I could have ever wanted.

Thank you, Mariana for going on both running and writing marathons with me, for being my friend and especially my "sister".

Finally, a big thank you to the most important people of my life, my parents, my brother, my beautiful grandmother (the greatest warrior I have ever met) and Francisco. You are my everything.

Abstract

Hydrogels are an emerging class of functional and tunable biomaterials. The hydrogel network can be maintained by chemical or physical interactions that are established between polymeric chains.

The aim of this work is to develop polyethylene glycol (PEG)-based hydrogels using innovative methods based on chemical and physical interactions.

A new chemical strategy for the production of hydrogels using a multicomponent reaction was shown for the first time. Here, 4-arm star-shaped PEG molecules, with suitable end functionalities, were used to form mechanically stiff chemically cross-linked hydrogels. The possibility of incorporating different molecular moieties into the network allowed the creation of functional and tunable hydrogels.

The other approach of the work focused on physically cross-linked hydrogels. Here, the interaction between two affinity pairs was exploited to form physically crosslinked hydrogels. The first affinity pair studied was a peptide-inspired WW domain and its natural binding partner (PPxY peptide). Multivalency was created by conjugating both components of the affinity pair into 8-arm star-shaped PEG polymers. Once mixed, a new soft affinity-triggered assembly was formed, and the mechanical properties of these hydrogels were characterized, and shown to be similar to hydrogels that contain the full version of the WW peptide in tandem.

The second affinity pair studied was the Green Fluorescent Protein (GFP) and a *de novo* designed ligand. In this case, multivalency was generated by the tandem arrangement of GFP in 3 and 5 repeats. GFP in tandem was intercalated with a hydrophilic spacer and recombinantly expressed in two *E. coli* strains. The obtained crude extracts were further processed to purify the GFP protein using immobilized metal affinity chromatography, anion exchange and size-exclusion chromatography.

Keywords: Hydrogel; PEG; Ugi reaction; WW domain; GFP; tandem.

Resumo

Os hidrogéis são uma classe emergente de biomateriais funcionais e ajustáveis. A rede do hidrogel pode ser mantida por interações químicas ou físicas que são estabelecidas entre as cadeias poliméricas.

O objetivo deste trabalho é desenvolver hidrogéis à base de polietileno glicol (PEG) usando métodos inovadores baseados em interações químicas e físicas.

Uma nova estratégia química para a produção de hidrogéis usando uma reação multicomponente foi mostrada pela primeira vez. Aqui, moléculas de PEG em forma de estrela de 4 braços, com funcionalidades finais adequadas, foram usadas para formar hidrogéis quimicamente reticulados que são mecanicamente rígidos. A possibilidade de incorporar diferentes porções moleculares na rede permitiu a criação de hidrogéis funcionais e ajustáveis.

Outra abordagem do trabalho focou-se em hidrogéis fisicamente reticulados. Aqui, a interação entre dois pares de afinidade foi explorada para formar hidrogéis fisicamente reticulados. O primeiro par de afinidade estudado foi um péptido inspirado no domínio WW e o seu par de ligação natural (péptido PPxY). A multivalência foi criada conjugando os péptidos a polímeros de PEG em forma de estrela de 8 braços. Uma vez misturados, forma-se instantaneamente um novo gel. As propriedades mecânicas destes hidrogéis foram caracterizadas e demonstradas serem semelhantes aos hidrogéis que contêm a versão completa do péptido WW em conjunto.

O segundo par de afinidade estudado foi a proteína fluorescente verde (GFP) e um ligando de afinidade desenhado *de novo*. Neste caso, a multivalência foi gerada pelo arranjo da GFP em 3 e 5 repetições. A GFP multivalente foi intercalada com um espaçador hidrofílico e expressa por via recombinante em duas estirpes de *E. coli*. Os extratos brutos obtidos foram posteriormente processados para purificar a proteína GFP utilizando várias técnicas cromatográficas.

Palavras-chave: Hidrogel; PEG; Reação de Ugi; Domínio WW; GFP; tandem

Table of Contents

Acknowledgments	VI
Abstract	IX
Resumo	X
Table of Contents	XIII
Index of Tables	xv
Index of Figures	XVI
Abbreviations	XIX
1 . Literature Review	23
1.1. Hydrogels	23
1.1.1. Hydrogel Classification	
1.2. Research Strategy	
2 . Multifunctional Chemical Hydrogels	33
2.1. Hydrogels Formed by Polymer Polycondensation via the Ugi Reaction	33
2.1.1. Ugi Reaction	
2.1.2. Ugi Reaction and Hydrogel Formation	
2.2. Research Strategy	
2.3. Materials and Methods	
2.3.1. Materials	37
2.3.2. Methods	37
2.4. Results and Discussion	40
2.4.1. Hydrogel Formation Conditions	
2.5. Conclusions	61
3 . Affinity Triggered Hydrogels	65
3.1. Affinity Pair: WW Domain and PPxY	65
3.2. Affinity Pair: Green Fluorescent Protein and A4C7	
3.2.1. Green Fluorescent Protein	
3.2.2. A4C7: Small synthetic ligand for GFP purification	67
3.2.3. Introducing Multivalency by Incorporating Multi-arm PEG Molecules	
3.3. Research Strategy	68
3.4. Materials and Methods	70
3.4.1. Materials	
3.4.2. Methods	
3.5 Results and Discussion	
3.5.1 Affinity-triggered Assemblies Based on a Peptide-Peptide Affinity Pair	78

3.5.2 Affinity-triggered Assemblies Based on a Protein-synthetic ligand Affinity Pair Conclusions	
onclusions and Future Perspectives	
ography	

Index of Tables

Table 1.1 – Different approaches for creating chemically cross-linked hydrogels	24
Table 1.2 – Examples of ligand-receptor pairs exploited to create affinity-triggered hydrogels	27
Table 1.3 – Ligand-receptor pairs and multimerization strategy to form affinity-triggered hydrogels	28
Table 2.1 – Hydrogels synthetized by polymer condensation via the Ugi reaction	35
Table 2.2 – Parameter determination of different hydrogels formed by polymer polycondensation by the	
Ugi reaction at different temperatures and with different isopropyl isocyanide and propionaldehyde	
molar excess in comparison to the amines in the system	
Table 2.3 – Parameter determination of different hydrogels formed by polymer polycondensation by the	
Ugi reaction in different solvents.	
Table 2.4 – Parameter determination of different polymer concentrations formed by polymer	
polycondensation by the Ugi reaction.	47
Table 2.5 – Components introduced into the mixture of different hydrogel to understand the influence of	
the Ugi reaction	50
Table 2.6 – Parameter determination of different hydrogels formed by polymer polycondensation by the	
Ugi reaction using varied carboxylic acids.	52
Table 2.7 – Parameter determination of different hydrogels formed by polymer polycondensation by the	
Ugi reaction using varied isocyanides	54
Table 2.8 – Parameter determination of different hydrogels formed by polymer polycondensation by the	
Ugi reaction using varied aldehydes.	56
Table 3.1 – Comparison between the affinity constant of minimalist version and the full version of WW	
domain towards the PPxY domain	78
Table 3.2 – Comparison of storage modulus between different affinity-triggered hydrogels comprising of	:
the pair WW and PPxY domains	79
Table 3.3 – Quantification and purity evaluation of the DNA extracted with the MiniPrep Kit	80
Table 3.4 – Molecular weight of the tandem GFP protein	82
Table 3.5 – Concentration of GFP in tandem display on the various stages of fractioning	84
Table 3.6 – Concentration of GFP in tandem display on the various stages of fractioning	86
Table 3.7 – Percentage of the protein of interest expressed in the soluble form	86
Table 3.8 – Concentration of GFP in tandem display on the various stages of fractionation	88
Table 3.9 – Concentration of GFP in tandem display expressed using different strains and culture volum	nes
Table 3.10 – Molecular weight and isoelectric point of each tandem GFP protein	91
Table 3.11 – Yield associated with each purification step	94

Index of Figures

Figure 1.1 – Schematic representation of a hydrogel and its network	23
Figure 1.2 – Different approaches for creating chemically cross-linked hydrogels	25
Figure 1.3 – Schematic representation of the formation of an affinity-triggered hydrogel	27
Figure 1.4 – Schematic representation of the strategies to create multivalency of the affinity pair	
components	28
Figure 1.5 – Schematic representation of the research strategy.	30
Figure 2.1 – Ugi reaction mechanism.	33
Figure 2.2 – Starting components for the formation of hydrogels via Ugi condensation reaction	40
Figure 2.3 – Sample characterization by ATR-FTIR spectra to confirm functionalization	41
Figure 2.4 – Schematic representation of the optimization conditions process	41
Figure 2.5 – Hydrogels formed by polymer polycondensation by the Ugi reaction with different isopropyl isocyanide and propionaldehyde molar excess at 60 °C.	
Figure 2.6 – Rheological analysis: Frequency sweeps of the hydrogels' samples from the studies on the effect of the isocyanide and aldehyde excess	
Figure 2.7 – Hydrogels formed by polymer polycondensation by the Ugi reaction with different solvents. Figure 2.8 – Rheological analysis: Frequency sweeps of the hydrogels' samples from the solvent effect	.46
studies Figure 2.9 – Hydrogels formed by polymer polycondensation by the Ugi reaction with different PEG	46
concentrations	48
Figure 2.10 – Rheological analysis: Frequency sweeps of the hydrogels' samples from the critical gel concentration studies.	48
Figure 2.11 – Sample characterization by ATR-FTIR spectra of different hydrogels formulated by the starting conditions.	49
Figure 2.12 – Chemical components that can be altered to introduce functionality	50
Figure 2.13 – Reaction between NHS group and an amine	51
Figure 2.14 – Compounds used for the incorporation into PEG-[NHS] ₄ .	51
Figure 2.15 – Isocyanide compounds used to formulate the hydrogels	51
Figure 2.16 – Sample characterization by ATR-FTIR spectra	52
[COOH] ₄	53
Figure 2.18 – Rheological analysis: Frequency sweeps of the hydrogels' samples with different PEG-COOH.	53
Figure 2.19 – Hydrogels formed by polymer polycondensation by the Ugi reaction with different isocyanides.	54
Figure 2.20 – Sample characterization by ATR-FTIR spectra of the hydrogels formulated to incorporate function of conductivity.	the
Figure 2.21 – Rheological analysis: Frequency sweeps of the conductive hydrogels' samples	
Figure 2.22 – Aldehyde compounds used to formulate the hydrogels.	
Figure 2.23 – Hydrogels formed by polymer polycondensation by the Ugi reaction with different aldehyd	es.
Figure 2.24 – Sample characterization by ATR-FTIR spectra of the hydrogels formulated to incorporate new functionalities.	

Figure 2.26 – Rheological analysis: Frequency sweeps of the antimicrobial hydrogels' samples	58
Figure 2.26 - Schematic representation of the hydrogel obtained by polycondensation via the Ugi re	action.
	59
Figure 2.27 – Antimicrobial activity of hydrogels against Escherichia coli K-12 and Staphylococcus a	nureus
ATCC 25923 after 24 hours of incubation	60
Figure 2.28 – Biofilm formation in the absence and presence of hydrogels against <i>Escherichia coli</i> K	(-12
and Staphylococcus aureus ATCC 25923 after 1 hour of incubation.	60
Figure 3.1 – WW domain prototype proposed by Macias et al via NMR experiments. ^[112] Protein Data	a Bank
ID: 1E0M	
Figure 3.2 – GFP structure proposed by Yang et al.[115] Protein Data Bank ID: 1GFL.	66
Figure 3.3 – Chemical structure of A4C7.	67
Figure 3.4 – Schematic representation of 2-arm PEG, 4-arm PEG and 8-arm PEG molecules	
Figure 3.5 – Schematic representation of an affinity triggered assembly formed by PEG-[PPxY] $_8$ and	I PEG-
[mWW] ₈	
Figure 3.6 – Schematic representation of an affinity triggered assembly formed by PEG-[A4C7] $_4$ and	
in tandem display.	
Figure 3.7 – Graphic representation of the plasmid carrying the [GFP-HS] gene	
Figure 3.8 – WW domain prototype proposed by Macias et al.[112] Protein Data Bank ID: 1E0M	
Figure 3.9 – Frequency sweeps of the hydrogel and the control.	
Figure 3.10 – Integrity evaluation of plasmid DNA	
Figure 3.11 – Expression of tandem proteins [GFP-HS] $_3$ and [GFP-HS] $_5$ in Rosetta cells	
Figure 3.12 – Expression of tandem proteins [GFP-HS] $_3$ and [GFP-HS] $_5$ in BLR (DE3) cells in 1 L of	culture
volume	
Figure 3.13 – Expression of tandem proteins [GFP-HS] $_3$ and [GFP-HS] $_5$ in BLR (DE3) cells in b5 L $_5$	
culture volume	
Figure 3.14 – Schematic of the purification steps of [GFP-HS] ₃ crude extract	
Figure 3.15 – Chromatogram of immobilized affinity chromatography of the [GFP-HS] ₃ soluble fraction	on89
Figure 3.16 – Chromatogram of size-exclusion chromatography of the [GFP-HS] ₃ soluble fraction from the figure 3.16 – Chromatogram of size-exclusion chromatography of the [GFP-HS] ₃ soluble fraction from the figure 3.16 – Chromatography of the [GFP-HS] ₃ soluble fraction from the figure 3.16 – Chromatography of the [GFP-HS] ₃ soluble fraction from the figure 3.16 – Chromatography of the [GFP-HS] ₃ soluble fraction from the figure 3.16 – Chromatography of the [GFP-HS] ₃ soluble fraction from the figure 3.16 – Chromatography of the [GFP-HS] ₃ soluble fraction from the figure 3.16 – Chromatography of the [GFP-HS] ₃ soluble fraction from the figure 3.16 – Chromatography of the [GFP-HS] ₃ soluble fraction from the figure 3.16 – Chromatography of the figure 3.16 – Chromato	
expression in BLR (DE3) cells.	
Figure 3.17 – Evaluation of the samples purified by size-exclusion	
Figure 3.18 – Chromatogram of anion exchange chromatography of the [GFP-HS] ₃ soluble fraction to	
the expression in BLR (DE3) cells.	
Figure 3.19 – Evaluation of the purification methods used for [GFP-HS] ₃	
Figure 3.20 – Schematic of the purification steps of [GFP-HS] ₅ crude extract	
Figure 3.21 – Chromatogram of size-exclusion chromatography of the [GFP-HS] $_5$ soluble fraction from the figure 3.21 – Chromatogram of size-exclusion chromatography of the [GFP-HS] $_5$ soluble fraction from the figure 3.21 – Chromatography of the [GFP-HS] $_5$ soluble fraction from the figure 3.21 – Chromatography of the [GFP-HS] $_5$ soluble fraction from the figure 3.21 – Chromatography of the [GFP-HS] $_5$ soluble fraction from the figure 3.21 – Chromatography of the [GFP-HS] $_5$ soluble fraction from the figure 3.21 – Chromatography of the [GFP-HS] $_5$ soluble fraction from the figure 3.21 – Chromatography of the [GFP-HS] $_5$ soluble fraction from the figure 3.21 – Chromatography of the [GFP-HS] $_5$ soluble fraction from the figure 3.21 – Chromatography of the [GFP-HS] $_5$ soluble fraction from the figure 3.21 – Chromatography of the figure 3.	
expression in BLR (DE3) cells.	
Figure 3.22 – Chromatogram of size-exclusion chromatography of the [GFP-HS] $_3$ soluble fraction from the figure 3.22 – Chromatogram of size-exclusion chromatography of the [GFP-HS] $_3$ soluble fraction from the figure 3.22 – Chromatography of the [GFP-HS] $_3$ soluble fraction from the figure 3.22 – Chromatography of the [GFP-HS] $_3$ soluble fraction from the figure 3.22 – Chromatography of the [GFP-HS] $_3$ soluble fraction from the figure 3.22 – Chromatography of the [GFP-HS] $_3$ soluble fraction from the figure 3.22 – Chromatography of the [GFP-HS] $_3$ soluble fraction from the figure 3.22 – Chromatography of the [GFP-HS] $_3$ soluble fraction from the figure 3.22 – Chromatography of the [GFP-HS] $_3$ soluble fraction from the figure 3.22 – Chromatography of th	
expression in BLR (DE3) cells.	
Figure 3.23 – Evaluation of the purification methods used for [GFP-HS] ₅	94

Abbreviations

A4 – 1-Pyrenemethylamine Hydrochloride

ATR-FTIR – Attenuated Total Reflection–Fourier Transform Infrared

BI - Before Induction

C.V. - Column Volume

C7 - Phenylacetic Acid

G' - Elastic or Storage moduli

G" - Viscous or Loss moduli

GAMBA – 4-(aminomethyl)benzoic acid

GF - Gel Fraction

GFP - Green Fluorescent Protein

[GFP-HS]₁ – 1 repeat of the GFP followed by the hydrophilic spacer complex

[GFP-HS]₂ – 2 repeats of the GFP followed by the hydrophilic spacer complex

[GFP-HS]₃ – 3 repeats of the GFP followed by the hydrophilic spacer complex

[GFP-HS]₄ – 4 repeats of the GFP followed by the hydrophilic spacer complex

[GFP-HS]₅ – 5 repeats of the GFP followed by the hydrophilic spacer complex

 $[GFP-HS]_x - x$ repeats of the GFP followed by the hydrophilic spacer complex

IMAC – Immobilized Metal Affinity Chromatography

IPTG – isopropyl β-D-1 thiogalactopyranoside

k_A – Affinity constant

LB - Luria-Bertani

MM - Molecular Marker

mWW - Minimalist version of the WW peptide

NHS - N-Hydroxysuccinimide

NHS - N-Hydroxysuccinimide

O.D._{600nm} - Optical density at 600 nm

PAMBA – 4-(aminomethyl)benzoic acid

PC - Pellet collected after the first centfugation

PEG - Polyethylene Glycol

PEG-[A4C7]₄ – Synthetic ligand A4C7 functionalized on a 4-arm PEG molecule.

PEG-[COOH]₄ – carboxylic acid functionalized on a 4-arm PEG molecule

PEG-[GABA]₄ – Gamma-amino-butyric acid functionalized on 4-arm PEG molecule

PEG-[Mal]₈ – Maleimide-terminated 8-arm PEG

 $\mathsf{PEG}\text{-}[\mathsf{mWW}]_8-\mathsf{Minimalist}$ version of the WW peptide functionalized on an 8-arm PEG molecule

PEG-[NH₂]₄ – 4-arm PEG functionalized with NH₂

PEG-[NHS]₄ – 4-arm PEG functionalized with NHS moiety

PEG-[NHS]₈ – N-hydroxysuccinimide-terminated 8-arm PEG

PEG-[PAMBA]₄ – 4-(aminomethyl)benzoic acid functionalized on 4-arm PEG molecule

PEG-[PPxY]₈ – Peptide PPxY functionalized on a 8-arm PEG molecule

PU - Pellet collected after the ultracentrifugation

SC – Supernadant collected after the first centfugation

SDS-PAGE - Sodium Dodecyl Sulfate-Polyacrylamide Gel Electrophoresis

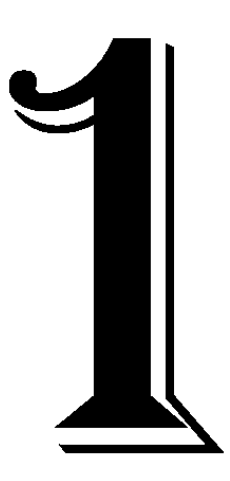
SEC - Size-exclusion chromatography

SU - Supernadant collected after the ultracentrifugation

TIP1 – Tax-interactive protein-1

Wg – Total dried hydrogel weight

Wr - Total dried hydrogel weight after regular replace of water



LITERATURE REVIEW

1. Literature Review

1.1. Hydrogels

Hydrogels are three-dimensional, hydrophilic and insoluble polymeric networks (Figure 1.1). They absorb water and biological fluids without losing their structural integrity due to their physical or chemical cross-linking.^[1,2] The cross-linking provides mechanical strength, stability and enables the hydrogels to be water insoluble.^[3,4]

Hydrogels were first developed in 1960 with the goal of creating more biocompatible contact lenses.^[5]. As the strategy to produce hydrogels has been in constant evolution, the importance of these hydrophilic structures on the biomedical field has also been increasing.^[6]. The major developments in hydrogel research led to the categorization of three hydrogel generations^[7]. The first generation comprised simple, water-swollen, chemically cross-linked hydrogels mostly prepared by polymerization of water-soluble monomers such as vinyl monomers^[8] or by the cross-link of hydrophilic polymers like Poly(vinyl alcohol)^[9]. Afterwards, in the 1970s, the second generation of hydrogels arrived when hydrogels began to respond to environmental triggers such as temperature^[10], pH^[11] or molecule concentration^[12]. Most recently, in the 1990s, new cross-linking methods were introduced. Examples include peptide interactions^[13], metal-ligand coordination^[14] and stereocomplexation^[15] resulting in enhanced hydrogel properties.

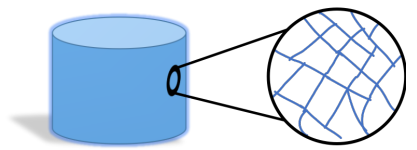


Figure 1.1 – Schematic representation of a hydrogel and its network.

1.1.1. Hydrogel Classification

Hydrogels can be categorized based on source, polymeric composition, physical appearance, type of cross-linking, physical state, network electrical charge, or the stimuli the hydrogels respond to.^[3,16,17] Herein, the hydrogels' classification will be based on the preparation method, more specifically on their cross-linking nature, and divided into two main categories: chemically cross-linked hydrogels and physically cross-linked hydrogels.

Chemically and physically cross-linked hydrogels have many differences namely due to the strength of the bonds that contribute to their formation^[18]. These characteristics are exploited to create hydrogels for a wide range of applications mainly on the biomedical field from drug delivery to tissue engineering.^[16]

1.1.1.1 Chemically Cross-linked Hydrogels

When synthetizing chemically cross-linked hydrogels, covalent bonds are formed between the polymeric chains. In result, chemically cross-linked hydrogels are so stable that only when the covalent points are cleaved, the hydrogels can be dissolved. Usually, these hydrogels present higher mechanical strength and its degradation times can be extended for long periods of time, depending on the type of chemical bonds.^[3] Moreover, unlike physically cross-linked hydrogels, it is possible to control the network's pore size.^[16]

There are many different methods for creating chemically cross-linked hydrogels (see Table 1.1 and Figure 1.2). These methods rely on the polymer's properties, namely the existence of compatible functional groups that form a covalent bond with the aid of a cross-linking agent. [16]

Table 1.1 – Different approaches for creating chemically cross-linked hydrogels.

Method	Methodology	Polymers	Application	Ref.
Chemical graft- ing	Activation of macromolecular backbones by a chemical agent	Chitosan-cellulose	Agricultural	[19]
Condensation reaction	Most common: Ugi /Passerini reaction. Chemical reaction between two smaller molecules to form a larger molecule	Alginate	Biological	[20]
High-energy ra- diation	Polymerization of unsaturated compounds using gamma or electron beam radiation	Poly(vinyl methyl ether)	Biological	[21]
Radiation graft- ing	Polymerization of a polymer's monomer using of high energy radiation	Carboxymethyl cellu- lose and styrene sul- fonate	Water purifica- tion	[22]
Radical polymerization	Successive addition of free-radi- cal low molecular weight mono- mers aided by a cross-linking agent	Poly(ethylene gly- col)methyl ether methacrylate	Anti-fouling	[23]

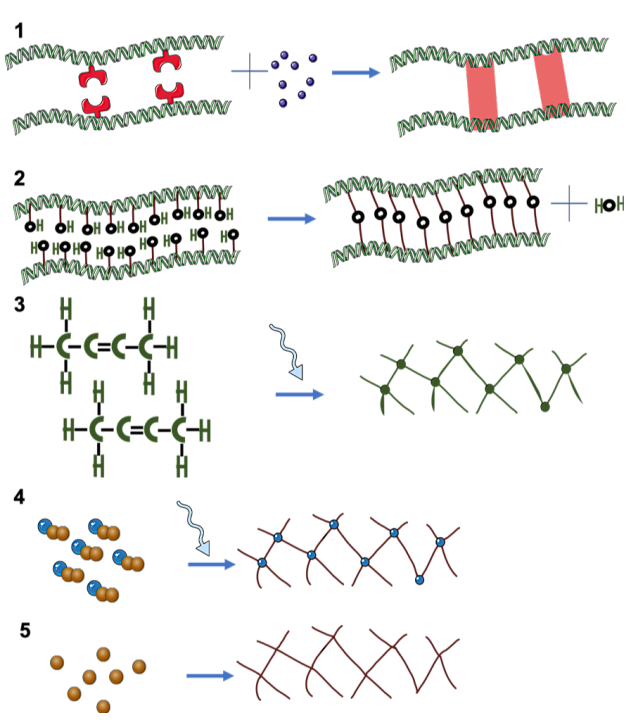


Figure 1.2 – Different approaches for creating chemically cross-linked hydrogels.

Legend: 1 – Chemical grafting; 2 – Condensation reaction; 3 – High-energy radiation; 4 – Radiation grafting; 5 – Radical polymerization.

1.1.1.2 Physically Cross-linked Hydrogels

Physically cross-linked hydrogels maintain their integrity due to physical interactions (ionic^[24], hydrophobic^[25] or hydrogen bonds^[26]) that occur between the various polymer chains.^[3] A major advantage of these gels is the lack of need for chemical cross-linking agents and so, they are highly requested to be applied in the pharmaceutical and biomedical field.^[16]

The dependence of the precursors for the gelation restricts the ability to tune the hydrogels' properties because they are dependent on the polymers' intrinsic properties. [27] Moreover, the ratio in which the precursors are introduced to the mixture is also of great importance. As an example, Zhang [28] reported that introducing the precursors with a ratio of 7.5:2.5 or 9:0.5 to form a non-covalent hydrogel lead to a difference of 100 Pa of the gels' stiffness which is important when considering the suitability of the hydrogels to different applications.

One of the most prominent examples of the formation of a physically cross-linked hydrogel is through the establishment of ionic interactions between alginate molecules and calcium ions. [16] As the formation conditions are very mild – room temperature and physiological pH – these hydrogels are highly used as a matrix for cell encapsulation. [29,30]

Hydrogen bonds are often exploited to design physically cross-linked gel-like structures. For instance, when combining gelatin and agar, a physically cross-linked hydrogel can be created via the formation of hydrogen bonds between the two components. However, these networks are very reliant on the solution's pH and they can dilute and disperse when in contact with an inflow of water.^[16]

Another example of a mean to form physically cross-linked hydrogels is by using hydrophobic interactions. These hydrogels are formed when an amphiphilic polymer – present in concentrations as low as 0.25 % (weight percentage) – interacts with water.^[16,31–33] There is a plethora of combinations between different polymers that can resort into hydrogels that can solubilize at different temperatures and acquire different shapes.^[31]

1.1.1.2.1. Hydrogel Formation Triggers

The self-assembly of polymers is a common method of physically cross-linked hydrogels' formation. The network formation can be triggered by several stimulus such as pH^[34], the presence of an enzyme to convert a precursor into a hydrogel^[35] or by the affinity between precursors^[36].

Chiu^[34] developed hydrogels based on a chitosan conjugated hydrophobic side chains that are triggered by a balance between charge repulsion and hydrophobic interactions at **pH 7.4**. The storage modulus (G') is of 27 kPA at pH 7.4.

Toledano^[35] developed **enzyme-sensitive** hydrogels in which N-(fluorenylmethoxycarbonyl) coupled with an amino acid and a dipeptide were set in a solution with a protease. The enzyme will activate by reverse hydrolysis the N-(fluorenylmethoxycarbonyl)-amino acid moiety and a N-(fluorenylmethoxycarbonyl)-dipeptide hydrogel was formed.

There are some reports in the literature where a hydrogel is formed due to the implementation of two triggers. For silk fibroin hydrogels to gelate, it is important to either increase the **temperature** or to reduce the solution's **pH** to promote a bigger water desorption and to decrease the repulsion between the β -sheets. This way, the protein chains assemble into hydrogels.^[37]

For detailed reviews on the promotion of physically cross-linked hydrogels by these external triggers, see [38,39].

Affinity-triggered hydrogels

The affinity constant (k_A) is a kinetic parameter that describes the association dynamics of a system. It is connected to the binding and unbinding reaction of two different molecules – the receptor and the ligand. The stronger the binding ligand and the target molecule (receptor) are attracted towards each other and bind, more intramolecular interactions are established and the greater the affinity constant will be. $^{[40,41]}$

Noncovalent intermolecular forces are essential for molecular recognition and consequent complex formation. These noncovalent interactions such as hydrogen bonding, ionic and Van der Waals interactions are relatively weak (0.5 to 10 kcal mol⁻¹) and so, a stable complex is often formed by a combination of multiple interactions. Moreover, both the binding and the target molecules need to be in close proximity because the noncovalent forces feature a short range.^[41]

For the hydrogel network to be formed, the presence of at least two binding participants is necessary (Figure 1.3). One well-known example of an interaction responsible for the formation/destruction of a network is the interaction established between an antibody and an antigen (k_A 8.9x10⁸ M⁻¹). An antibody and an antigen were grafted to a polymer and their affinity towards each other leads to the formation of an network.^[42] For more examples of ligand-receptor pairs used to create affinity triggered hydrogels, see Table 1.2.



Figure 1.3 – Schematic representation of the formation of an affinity-triggered hydrogel

Table 1.2 – Examples of ligand-receptor pairs exploited to create affinity-triggered hydrogels.

Binding participant I	Binding participant II	Affinity constant k _A (M ⁻¹)	Ref.
Glucose	Concanavalin A	6.61x10 ²	[43,44]
Proline-rich peptide	WW domain CC43	2.2x10 ⁵	[36]
Proline-rich peptide	WW domain Nedd4.3	1.6x10⁴	[36]
Heparin	Heparin-binding, coiled-coil peptide	1x10 ⁵	[28]
Low-molecular-weight heparin- functionalized star PEG	Heparin-binding, coiled-coil peptide- functionalized star PEG	8.7x10 ⁷	[28]
Gyrase	Coumermycin	1x10 ⁸	[45]
Rabbit IgG	Goat anti-rabbit IgG	2.61x10 ⁸	[42]
Avidin	Biotin	1x10 ¹⁴	[46]

Besides the affinity pairs, the affinity constant (k_A) determined for the interaction between the two components is also indicated. These hydrogels are used for either drug delivery or tissue engineering.

When determining affinity-triggered hydrogels' properties, there are some factors to take into account: Not only will the concentration and the binding affinity of the hydrogel's components affect its mechanical properties, but their molecular weight will have an important role as well. When decreasing the molecular weight and increasing the binding strength, stiffer hydrogels will be formed.^[1,47]

When creating affinity-triggered hydrogels, the affinity pairs need to be arranged in a multivalent way. Otherwise, the network with none or only one multivalent affinity pair will not be formed. [48] Multivalency allows for strong, reversible and dynamic interactions between different interfaces and molecules. [49]

The affinity constant of the affinity pair and the multivalency strategy will have an effect on the stiffness of the hydrogel (see Table 1.3).

Table 1.3 – Ligand-receptor pairs and multimerization strategy to form affinity-triggered hydrogels.

Binding participant I	Binding participant II	k _A (M ⁻¹)	Storage Modulus (G') (Pa)	Ref.
TIP1 fused to tri-	TIP1-binding peptide fused to a trimeric protein	2.3 x10 ⁶	262	[50]
meric protein	TIP1-binding peptide conjugated to a multimeric PEG	2.3 x10 ⁶	35	[51]
TIP1 fused to tetram- eric protein	TIP1 -binding peptide conjugated to multimeric PEG	1.5 x10 ⁸	80	[52]

Besides the affinity pairs, the affinity constant (k_A) determined for the interaction between the two components and the storage modulus of the hydrogel formed are also indicated. In bold, the multimerization strategy employed. TIP1 – tax-interactive protein-1.

There are three different strategies to ensure the multivalency of the affinity pairs (Figure 1.4): 1) Tandem display of the affinity pairs 2) Multimeric polymers to immobilize the affinity pairs, or 3) Multimeric proteins.

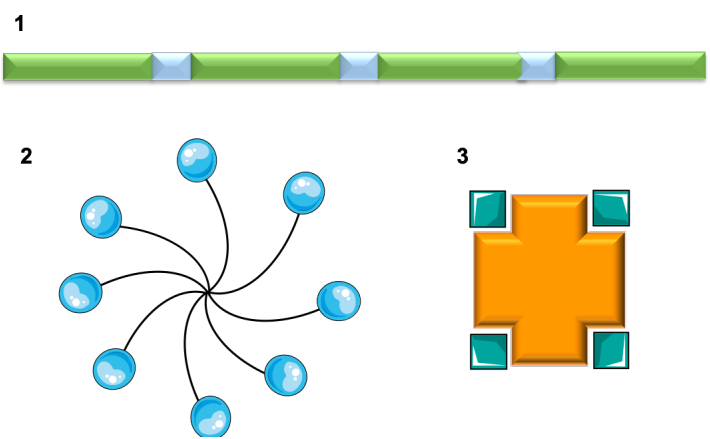


Figure 1.4 – Schematic representation of the strategies to create multivalency of the affinity pair components.

Legend: 1 – Tandem display separated by a spacer (blue); 2 – Branched polymer; 3 – Multimeric proteins.

1. Affinity pairs with tandem display

Tandem display is a result of the design of a gene construct involving a pre-defined number of repeats of the same protein/protein domain.^[47]

Using repeat proteins or peptides as building blocks designed by a variable number of tandem repeats, grants the capacity to manipulate the behaviour and/or properties of a given protein-based material.^[53] However, the production of stable and soluble tandem repeat proteins either synthetically or biologically is a big hurdle to overcome but it is overshadowed by the possibility to select the number of repeats and the function of each linker introduced between the repeats.^[54] This allows to construct affinity pairs tailored to the need of the user such as introducing arginine-glycine-aspartate peptides to promote cell adhesion combined with heparin binding factors to facilitate the delivery of growth factors.^[55] There are also reported examples of affinity

pairs with tandem display coupled by the introduction of spacers. Seven repeats of the WW domain were linked together by hydrophilic spacers aiming to confer flexibility to the protein chains so the WW domain would become more assessible to a proline-rich peptide domain (PPxY domain). [36] Also, the peptide where PPxY domain is present, contained 9 repeats of this domain interposed by another linker that facilitates the formation of cross-links between a single WW domain and a single PPxY domain ensuring the formation of a fully linked network. [36]

2. Multimeric polymers

Multimeric polymers are a great resource to generate multivalency because the end-groups of these polymers can be varied. This possibility combined with the linear or branched (multi-arm or star) structure of the polymer lets the user to create different conjugation strategies between the affinity pairs in function to the end goal. Moreover, the end groups can be the same (symmetrical) or different (asymmetrical) allowing for the possibility to form different hydrogels.^[56,57]

Polyethylene Glycol (PEG) is a polyether composed of repeated ethylene glycol units.^[58] This polymer is biocompatible, hydrophilic and non-ionic. It has been employed to create hydrogels that mainly serve as a drug-delivery system and a vehicle to promote tissue regeneration.^[59–61] Despite chemically cross-linked PEG hydrogels being the focus of most research and applications, physically cross-linked PEG hydrogels are also studied.^[7] One example of this type of hydrogels is reported by Jing^[13] in which peptides where conjugated to PEG chains to produce an hydrogel when in presence of a phosphate-buffered saline solution.

The use of polymers such as PEG as a structure building platform is highly convenient because it allows the users to vary its molecular sizes, the topologies and chemical functionalities (various functional groups such as thiol, malidemide, azide or vinyl sulfone can be added to PEG polymers) in order to create a tailored template according to the purpose of the experiment. [4,59,62] Hydrogels with longer and more flexible PEG chains are more prone to degradation due to their hydrophilic character. To contradict this difficulty, it is important to increase the number of cross-linking sites for the network to be more hydrophobic. [63]

Both Zhang^[28] and Yamaguchi^[48] have reported on the importance of incorporating multimeric polymers such as 4-arm PEG to obtain hydrogels with higher affinity when compared to similar cases of hydrogels with the same affinity pairs without the multimeric proteins.

Other polymers such as polylactic acid, poly(ethylene oxide) diacrylate, polyglycolic acid, poly(propylene oxide), poly(N-isopropylacrylamide) and N-(2- hydroxypropyl) methacrylamide have also been synthetized in a multimeric fashion. [64,65]

3. Multimeric proteins

Multimeric proteins such as the tetrameric streptavidin allow for the binding of multiple ligands.^[66] When these proteins and their respective ligands (displayed in a multivalent way) are introduced into a solution, a hydrogel network is formed.

1.2. Research Strategy

In this work, the aim is to explore chemical and physical strategies to yield hydrogels using PEG as a multicomponent polymer (Figure 1.5).

Firstly, on chapter 2, hydrogels formed by polymer condensation via the Ugi reaction will be studied by using two different 20 KDa star-shaped PEG molecules whose terminal molecular moiety is varied (one will present an amine and the other a carboxylic acid). These polymers, combined with an amine and an isocyanide, will be the participants of an Ugi condensation reaction that will result into chemically cross-linked hydrogel whose rheological behaviour is going to be analysed.

Lastly, on chapter 3, affinity-triggered assemblies are going to be explored by following two different strategies:

- 1) Conjugation of two different peptides with affinity towards each other into 20 KDa 8-arm star-shaped PEG molecules and promoting the creation of an affinity-triggered assembly. The dynamic storage modulus and loss modulus of this hydrogel is going to be observed. This work is included in the publication "Affinity-triggered assemblies based on a designed peptide- peptide affinity pair", DOI: 10.1002/biot.201800559.
- 2) Expressing and purifying GFP (Green Fluorescent Protein) in tandem aiming to create an affinity-triggered hydrogel between the tandem GFP and an Ugi based ligand A4C7 conjugated into a 20 KDa 4-arm star-shaped PEG molecule.

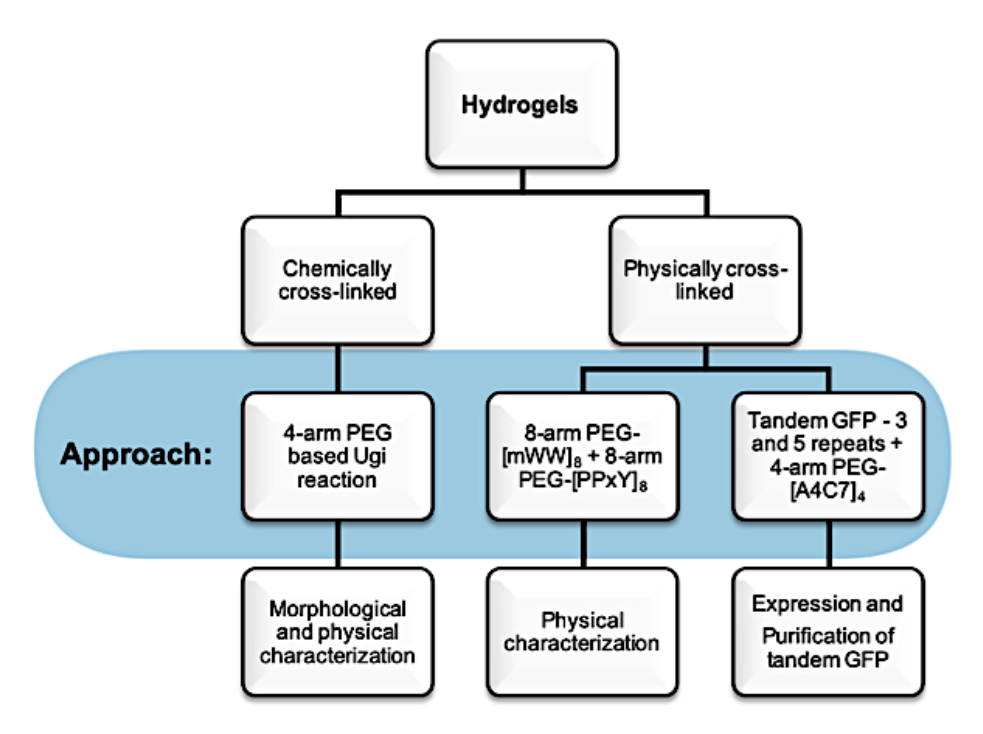


Figure 1.5 – Schematic representation of the research strategy.



MULTIFUNCTIONAL CHEMICAL HYDROGELS

2. Multifunctional Chemical Hydrogels

2.1. Hydrogels Formed by Polymer Polycondensation via the Ugi Reaction

2.1.1. Ugi Reaction

Multicomponent reactions are one-pot reactions involving three or more reagents to form a single product. Three classes of multicomponent reactions are described in the literature: (1) isocyanide-based, (2) non-isocyanide and (3) metal-catalysed reactions. Due to the high efficiency, atom economy and versatility, multicomponent reactions are emerging as a very resourceful tool in polymer science. The isocyanide-based Ugi four-component reaction is one of the most established ones.^[67] The Ugi reaction is a one-pot reaction that was first reported in 1959^[68]. This multicomponent reaction involves an amine, a carboxylic acid, an isocyanide and an aldehyde or a ketone.^[4]

Firstly, the formation of an imine 4 occurs from the reaction between the amine 1 and the ketone 2 with the loss of a water molecule (limiting step of the Ugi reaction). Subsequently, the imine 4 will be protonated by the carboxylic acid 3 and the ion iminium 5 is formed. Immediately after, the nucleophilic carbon of the isocyanide 6 attacks the iminium 5 whilst the anion of the carboxylic acid is reacting with molecule 7 to originate molecule 8. Lastly, the molecules rearrange themselves (Mumm rearrangement) by transferring the acyl group from the oxygen to the nitrogen thus forming the Ugi scaffold marked as 9 (Figure 2.1).

Figure 2.1 - Ugi reaction mechanism.

It is important to carefully select the components introduced in this one-pot reaction due to the extremely prominence of the formation of the iminium ion. If a scarcely nucleophilic amine is chosen, the reaction can either present a low yield or not take place at all. When the basic strength of an amine is low the concentration of the iminium ion will be low and, consequently, the reaction will not take place. [69] Another aspect to take into consideration is the temperature at which the reaction takes place. Even though some reactions involving amino sugar components were performed at low temperatures (-50 °C)^[70], usually the Ugi reaction is done at either 21-25 °C^[20,71-73] or at 60 °C (in some cases when methanol is the solvent of choice).^[72,73]

Concerning the solvent, although there are some reports of the Ugi reaction being performed using benzene^[72], toluene^[73] or even deep eutectic solvents such as a mixture of urea and choline chloride^[74], most commonly they are performed in a polar protic solvent^[75] such as methanol (either pure methanol^[20,71–73] or a mix between methanol and other solvents such as tetrahydrofuran^[76] or chloroform^[77]). Choosing methanol as a solvent results in higher yields because the conditions of polarity and solubility of reagents and products are facilitated by it.^[69] Also, when methanol is chosen, the imine or the isonitrile ought to be in excess to improve the yield of the reaction as proved by a statistical study on the effect of the usage of the reagents in excess.^[78] Occasionally, other alcohols such as ethanol^[79] or trifluoroethanol^[72] are used.

The Ugi reaction can be combined with other combinatorial chemistries allowing for the creation of a plethora of different compounds (example: Petassis-Ugi ligands).^[80]

Another isocyanide-based multicomponent reaction is the Passerini reaction, first described by Mario Passerini in 1921^[81,82]. Here, the amine group is missing and, instead of the formation of an ester and an amide bond, the formation of two amide bonds takes place. The major disadvantage associated with the absence of the amine group in the final product is the deficient structural diversity and thermal stability in comparison with the final products of the Ugi reaction.^[67]

2.1.2. Ugi Reaction and Hydrogel Formation

In 1999, De Nooy reported what many consider to be the first hydrogel formed by polymer condensation by the Ugi reaction. Here, a hydrogel was synthetized in water at a pH of 3.5-4 using cyclohexyl isocyanide and a selection of carboxylic acids, amines and aldehydes. These hydrogels were transparent and highly stable when in contact with a saline solution. Also, De Nooy conveyed that when the amine is in tremendous excess, the hydrogel was more resistant. In this communication, it is also stated that hydrogels' properties can be tuned by changing the components and proportions of the reactants.^[71,83]

Five years later, Bu and co-workers contributed to exploration of the importance of the effect of temperature and ratios of the components introduced into the system to create hydrogels via an Ugi condensation reaction. Bu *et al.* stated that increased temperatures accelerated the gelation process and that higher concentrations of the polymer/cross-linking agent led to an increased gelation time.^[20]

These are some examples of the ground-breaking work done related to chemically cross-linked hydrogels formed by the Ugi reaction. For more, see Table 2.1.

Amine	Ketone / Aldehyde	condensation via the Ugi reac Carboxylic acid	Isocyanide	Ref.
NH₄CI 1-(deoxylactit-1-yl) chitosan 1,5-diaminopentane	Gluteraldehyde Formaldehyde	Carboxymethyl cellulose Tartaric acid	Cyclohexyl Isocyanide	[71]
1,5-diaminopentane Lysine methylester	Formaldehyde	Hyaluronic acid Alginic Acid Carboxymethyl cellulose Carboxymethyl dextran Carboxymethyl scleroglucan C6-oxidized scleroglucan	Cyclohexyl Isocyanide N-butyl Isocy- anide	[84]
Lysine ethyl ester	Formaldehyde	Hyaluronic acid	Cyclohexyl Isocyanide	[85]
1,5-diaminopentane	Formaldehyde	Alginate	Cyclohexyl Isocyanide	[20]
1,5-diaminopentane	Formaldehyde	Pectin	Cyclohexyl Isocyanide	[86]
Deacetylation hyalu- ronic acid	Formaldehyde	Deacetylation hyaluronic acid	Cyclohexyl Isocyanide	[87]
3-(Diethylamino) propylamine 4-picolylamin 4-fluorobenzylamine Benzylamine Furfurylamine	Formaldehyde	Pectinic acid	1,4-bis(3-iso- cyanopro- pyl)piperazine	[88]
4-picolyl amine, Benzylamine Furfurylamine Isopropyl amine	Formaldehyde	Carboxymethyl cellulose	1,4-bis(3-iso- cyanopro- pyl)piperazine	[89]

2.2. Research Strategy

The aim of the study reported in this chapter is to create, for the first time, PEG-based hydrogels formed by the Ugi polycondensation reaction. Two different sets of 20 kDa 4-arm PEG molecules will be employed in the same reaction: one will carry an amine as the terminal group and the other will be set with a carboxylic acid. The PEG molecules with a terminal carboxylic acid will be previously functionalized so the -COOH group will be modified giving the possibility to tune the properties of these hydrogels. The effect of the temperature, solvent and introduction of different aldehydes and isocyanides into the reaction will also be studied. The hydrogels will be rheologically characterized. Moreover, an antimicrobial and a static biofilm assay will be performed for two hydrogels in which the aldehyde for the Ugi reaction is varied.

2.3. Materials and Methods

2.3.1. Materials

2.3.1.1 Chemicals

4-arm PEG functionalized with NHS moiety (PEG-[NHS]₄) (SUNBRIGHT PTE-200HS) and 4-arm PEG functionalized with NH₂ (PEG-[NH₂]₄) (SUNBRIGHT PTE-200PA) were purchased from NOF Europe (Frankfurt am Main, Germany).

4-(aminomethyl)benzoic acid (283746), 4-biphenyl-3'-amino-acetic acid (CDS010205), cyclohexyl isocyanide (8181510010), DL-tryptophan (T0129), gamma-amino-N-butyric acid crystalline (A2129), isopropyl isocyanide (553344), ninhydrin (151173), phenol (P1037), phenylacetaldehyde (107395), pyridine (P57506), potassium cyanide (207810) and propionaldehyde (538124) were purchased from Sigma-Aldrich (Missouri, USA).

Difco Mueller Hinton Broth (90001-822) was purchased from VWR (Pennsylvania, USA).

Ethanol (131085) was purchased from PanReac AppliChem (Chicago, USA).

Methanol (M/4056/17) was purchased from Thermo Fisher Scientific (New Hampshire, USA).

2.3.1.2 Software

ChemDraw Professional 16 was used to draw all of the structures and the reactions displayed on this chapter.

2.3.2. Methods

The reagents were weighted in a Sartorius AX423 scale (Max 420 g, d=1 mg) (Göettingen, Germany) or in a Mettler Toledo scale (Max 42 g, d=0.01 mg) (Ohio, USA) and the calibration of pH values was conducted with pHenomenal pH 1100L from VWR (Pennsylvania, USA).

The U.V measurements at 560 and 600 nm were conducted with the TECAN Infinite F200 from Tecan Trading AG (Männedorf, Switzerland) on 96-well transparent flat-bottom microplates from Sarstedt (Nümbrecht, Germany) for the Kaiser test and Nunc MicroWell 96-Well Microplates from Thermo Fisher Scientific (New Hampshire, USA) for the antimicrobial and static biofilm assays.

2.3.2.1 Multi-arm PEG Functionalization

The carboxylic acid of choice was used to functionalize 4 arm-PEG molecules with an *N*-Hydroxysuccinimide (NHS) terminal group. Both molecules were dissolved in a PBS pH 7.4 solution and later mixed. The reaction was incubated for 12 hours at 4 °C with rotational agitation (22 rpm). Afterwards, the solution was dialysed with water as a solvent using the dialysis membrane Spectra/Por 7 Dialysis Tubing 10 kDa MWCO (132120) from Spectrum (New Jersey, USA). Later, the solution was stored for at least 24 hours at -80 °C to be freeze-dried.

The percentage of functionalization was assessed by the Kaiser test using the dialysate freeze-dried. The functionalization was confirmed by ART-FTIR.

2.3.2.2 Kaiser Test

 $50~\mu L$ of 80% phenol in ethanol (w/v), $50~\mu L$ of 2% 0.001M potassium cyanide in pyridine (v/v) and $50~\mu L$ of 5% ninhydrin in ethanol (w/v) were added to 1 mL of sample. Afterwards, the mixture was heated up to $100~^{\circ}C$ in the water bath Scanvac SHC200 (Lynge, Denmark) for 5 min. After that period, the samples were diluted 1:20 and the absorbance was measured at 560 nm in a microplate reader. A calibration curve (0 – 5 μ mol mL⁻¹) was made using glycine as standard. The Kaiser test detected the amount of primary amines present in the dialysate. The concentration of amines is proportional to the concentration of the molecule that was object of functionalization (either gamma-amino-butyric acid, 4-(aminomethyl)benzoic acid, 4-biphenyl-3'-amino-acetic acid or tryptophan). If the percentage of functionalization was 100 %, there would be no amines in the dialysate.

2.3.2.3 ATR-FTIR

The ATR-FTIR spectrums were recorded in the range 400-3000 cm⁻¹ with 24 scans with a PerkinElmer FT-IR Spectrometer Spectrum Two using the UATR Two module.

The samples were put directly on top of the crystal and, when solid, compressed using a L160-1742 tip. The force gauge used diverges from sample to sample.

2.3.2.4 <u>Hydrogel Formation</u>

The appropriate mass for the PEG-[NH₂]₄ and the PEG-[COOH]₄ functionalized (concentration 1 %, 2.5 %, 5 % and 10 % w/v each) was weighted. Both substances were dissolved in the appropriate solvent and were then mixed together. Afterwards, the aldehyde and the isocyanide of choice were added to the solution, in this order, with a molar excess towards the amines in solution. The Ugi reaction took place at either 25 °C or at 60 °C. The solvent used was either methanol, water or a mixture of the two with a 1:1 ratio.

Unless it is stated otherwise, the hydrogels will be formulated with PEG-[NH₂]₄, 4-arm PEG functionalized with gamma-amino-butyric acid (PEG-[GABA]₄) as PEG-[COOH]₄, propionaldehyde as the aldehyde and isopropyl isocyanide as the isocyanide.

All of the hydrogels that gelated at 60 °C were left at this temperature for 1 day.

2.3.2.5 Gel Fraction Determination

When the gelation process occurred, the hydrogel's weight was noted. Afterwards, the hydrogel was dried at 60 °C for 24 hours and its weight was recorded (Wg). Next, 1 mL of distilled water was added for 10 minutes to the hydrogel. Then, the hydrogel was removed, and its total weight was logged. Later, the hydrogel was again submersed in water and this process was repeated until a plateau in the swelling factor vs. time curve was reached. When this stage was accomplished, 1 mL of water was added to the system and only 24 hours later, the hydrogel weight was registered. Afterwards, water was regularly replaced for 24 hours and the gel was then dried at 60 °C and its weight recorded (Wr).

By measuring the gel fraction (GF) (Equation 2.1), it is possible to quantitively assess the efficiency of the cross-linking. The gelation process takes place when a sufficient number of functional groups per molecule is present in order to reduce the amount of non-reacted precursors in the hydrogel.^[63]

Gel fraction (%) =
$$\frac{Wr}{Wg}$$
 x 100

Equation 2.1

2.3.2.6 Rheology Studies

Oscillatory amplitude and frequency sweep measurements were conducted on an Anton Paar MCR 102 using a parallel sandblasted plate with a diameter of 8 mm. For each sample, an amplitude sweep measurement was performed to determine the samples' critical strain. Afterwards, a frequency sweep measurement was performed to determine the viscous and the elastic moduli with a constant strain determined by the amplitude sweep measurements. The temperature set for these experiments were 21 °C.

2.3.2.7 Antimicrobial Assay

The bacterial strains *Escherichia coli* K-12 and *Staphylococcus aureus* ATCC 25923 were chosen as an example of Gram-positive and Gram-negative bacteria, respectively.

The bacterial strains were inoculated in Mueller Hinton broth medium and grown overnight at 37 °C with constant shaking of 180 rpm. The optical density at 600 nm of the overnight culture was 4.4 for *E. coli* and 3.96 for *S. aureus*. The culture was then diluted to an optical density at 600 nm (O.D._{600nm}) of 0.05 with Mueller Hinton broth medium. Afterwards, the cultures were pipetted into a well on a 96-well microplate and the hydrogel was inserted on top. The mixture was then incubated at 37 °C for 24 hours. After that time, the O.D._{600nm} was measured.

2.3.2.8 Static Biofilm Assays

After the antimicrobial assays, the media and the non-adherent cells were removed, and the wells were carefully washed twice in water. Then, to fix the biofilms, the adherent cells were incubated at 60 °C for one hour, without agitation. After that time, 0.006 % (w/v) of crystal violet was added to each well for 10 minutes. Afterwards, the excess stain was removed with water. Subsequently, to create a homogenous solution, 30 % of acetic acid was added and the O.D.600nm was measured.

2.4. Results and Discussion

2.4.1. Hydrogel Formation Conditions

The Ugi reaction is a one-pot reaction that involves an aldehyde/ketone, an amine, a carboxylic acid and an isocyanide. ^[3] To understand if PEG-based hydrogels could be formed by using this reaction, several conditions were varied such as the concentration of the multimerized PEG molecules, the temperature and the solvent used. To determine the best conditions, the hydrogels formed will be characterized by rheology.

The starting components were propional dehyde, an amine that was present on the terminal groups of a 4-arm PEG molecule, gamma-amino-butyric acid functionalized on the terminal groups of a 4-arm PEG molecule and isopropyl isocyanide (Figure 2.2).

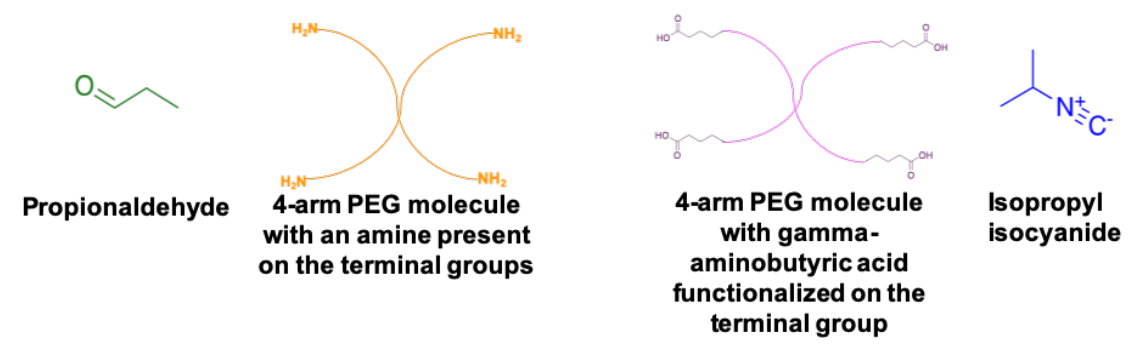


Figure 2.2 – Starting components for the formation of hydrogels via Ugi condensation reaction.

2.4.1.1 <u>Functionalization of Gamma-aminobutyric acid on 4-arm PEG</u> Molecules

A carboxylic acid-terminated PEG was not available commercially, unlike the amine-terminated 4-arm PEG. Therefore, the carboxylic acid-terminated PEG was functionalized by mixing PEG-[NHS]₄ with gamma-aminobutyric acid (GABA) *in house*. By a Kaiser test, it was possible to determine that the degree of functionalization was 99.5 %. The functionalization products and reagents were evaluated by ATR-FTIR (Figure 2.3).

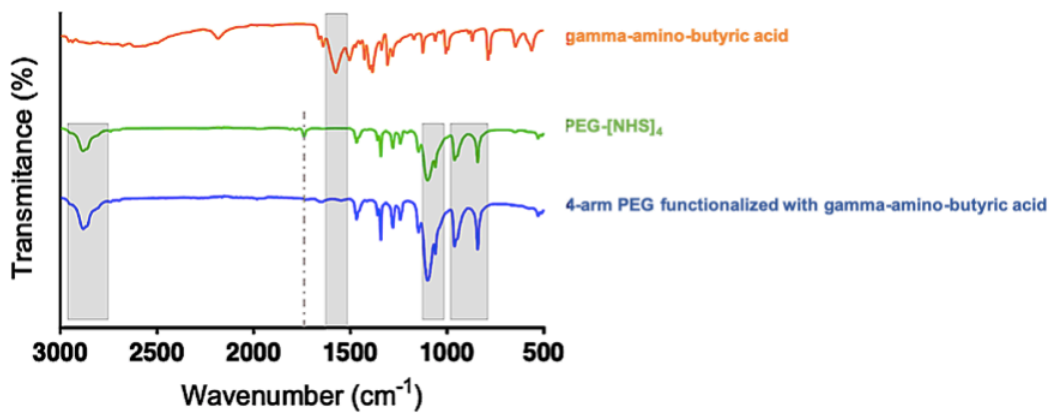


Figure 2.3 – Sample characterization by ATR-FTIR spectra to confirm functionalization.

The ATR-FTIR spectra for gamma-amino-butyric acid, in orange, shows a characteristic peak at 1560 cm⁻¹ attributed to an asymmetric stretching of the carboxylate group. The FTIR spectra for PEG-[NHS]₄, in green, presents a peak at 2860 cm⁻¹ corresponding to an O-H stretching, a peak at 1743 cm⁻¹ (marked by the dashed line) characteristic of a C=O stretching due to the presence of the ester group, confirming the presence of NHS and a peak at 1091 cm⁻¹ attributed to the ether group. The presence of alkenes (C=C bending) will be responsible for the peaks between 974 cm⁻¹ and 812 cm⁻¹. Finally, in blue, the FTIR spectra for 4-arm PEG functionalized with gamma-amino-butyric acid presents the same peaks as PEG-[NHS]₄ except for the characteristic peak that identifies the NHS component (marked by the dashed line).

2.4.1.2 Optimizing Conditions for Hydrogel Formation

To successfully employ the Ugi reaction and to obtain high product yields, there are several parameters that need to be optimized, especially since, in the literature, it has never been reported the formation of hydrogels via the Ugi reaction using multivalent PEG molecules. In this case, the optimized parameters were the temperature, aldehyde and isocyanide excess, the solvent used and the concentration of the multimerized PEG molecules (Figure 2.4). These conditions were studied using as starting materials those presented in Figure 2.2.

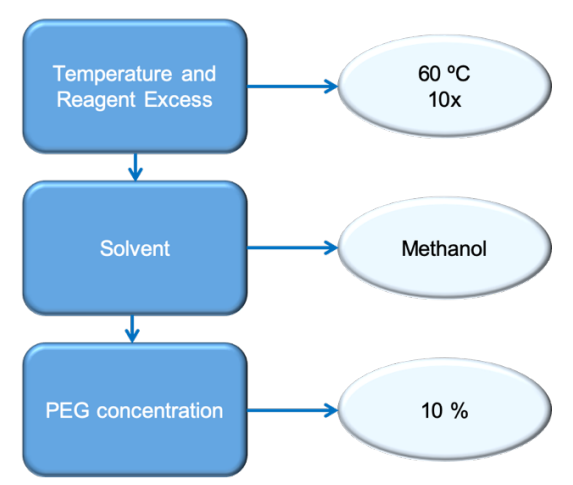


Figure 2.4 – Schematic representation of the optimization conditions process.

To understand the effect of the isocyanide, the aldehyde and the effect of the temperature in the formation of the hydrogels, two hydrogels were formed in methanol by exploring the following conditions: concentration of 10% (w/v) for both PEG-[GABA]₄ and PEG-[NH₂]₄, 10-excess molar of both isopropyl isocyanide and propionaldehyde. Other two hydrogels were formed by adding, in methanol, concentration of 10% (w/v) for both PEG-[GABA]₄ and PEG-[NH₂]₄, 1-excess molar of both isopropyl isocyanide and propionaldehyde. One of each formulation was incubated at 60 °C and the remaining was set at room temperature (25 °C) (Table 2.2).

Table 2.2 – Parameter determination of different hydrogels formed by polymer polycondensation by the Ugi reaction at different temperatures and with different isopropyl isocyanide and propionalde-

hyde molar excess in comparison to the amines in the system.

Ugi	PEG con-	on- Molar excess		Hydrogel	G';	Critical	05	
Gel N°	centration (w/v)	Cya- nide	Alde- hyde	Temp.	formed & gelation time	G " (Pa)	strain (%)	GF (%)
1	10 %	1x	1x	25	No	-	-	-
2	10 %	1x	1x	60	Yes – 1 day	5014.8±70.5; 75.8±17.4	0.01	92.7±2.8
3	10 %	10x	10x	25	No	-	-	-
4	10 %	10x	10x	60	Yes – 5 hours	2156.3±43.5; 39.6±21.2	0.01	88.9±2.9

The concentration of PEG-[GABA]₄ is 10 % (w/v) and the concentration of PEG-[NH₂]₄ is 10 % (w/v).

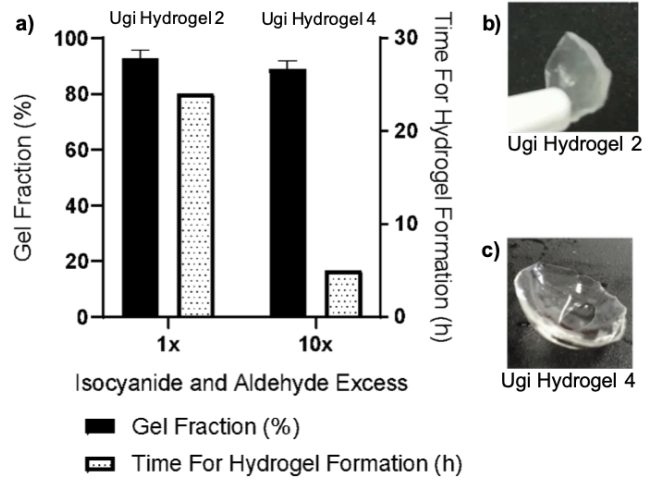


Figure 2.5 – Hydrogels formed by polymer polycondensation by the Ugi reaction with different isopropyl isocyanide and propional dehyde molar excess at 60 $^{\circ}$ C.

a) Gel fraction and Hydrogel formed & gelation time for Ugi hydrogel 2 and 4. b) Ugi hydrogel 2 – Formed at 60 °C in methanol with a concentration of 10 % (w/v) for both PEG-[GABA]₄ and PEG-[NH₂]₄, 1-excess molar of both isopropyl isocyanide and propionaldehyde, in comparison to the amines in the system. c) Ugi hydrogel 4 – Formed at 60 °C in methanol with a concentration of 10 % (w/v) for both PEG-[GABA]₄ and PEG-[NH₂]₄, 10-excess molar of both isopropyl isocyanide and propionaldehyde, in comparison to the amines in the system.

Regarding the effect of isocyanide and the aldehyde, the hydrogels were formed with 1-excess and 10-excess molar in comparison to the amines present in the system (Ugi hydrogels 2 and 4, Table 2.2 and Figure 2.5). As expected, the gelation time was lower when employing a higher molar excess since high concentrations of the reactants benefits the Ugi reaction.^[69]

Hydrogel formation was only observed when the reaction temperature was 60 °C (Ugi hydrogels 2 and 4, Table 2.2). In fact, Bu and co-workers have reported that increasing the temperature allows faster gelation because the rate of cross-linking increases at higher temperatures granting a faster connectivity of the gel network.^[20] Perhaps, there has not been enough time for the hydrogels to be formed at room temperature.

To understand the mechanical properties of the hydrogels, rheological studies were performed. The response of the hydrogels when under an applied frequency was studied. On frequency sweeps, the amplitude of deformation is kept constant and the frequency is varied. On low frequencies, the object of study is the behaviour of the hydrogel at slow changes of stress. On the other hand, at high frequencies, the hydrogel will be tested under fast loads. It is given more prominence on the overall trend and on changes of information.^[90]

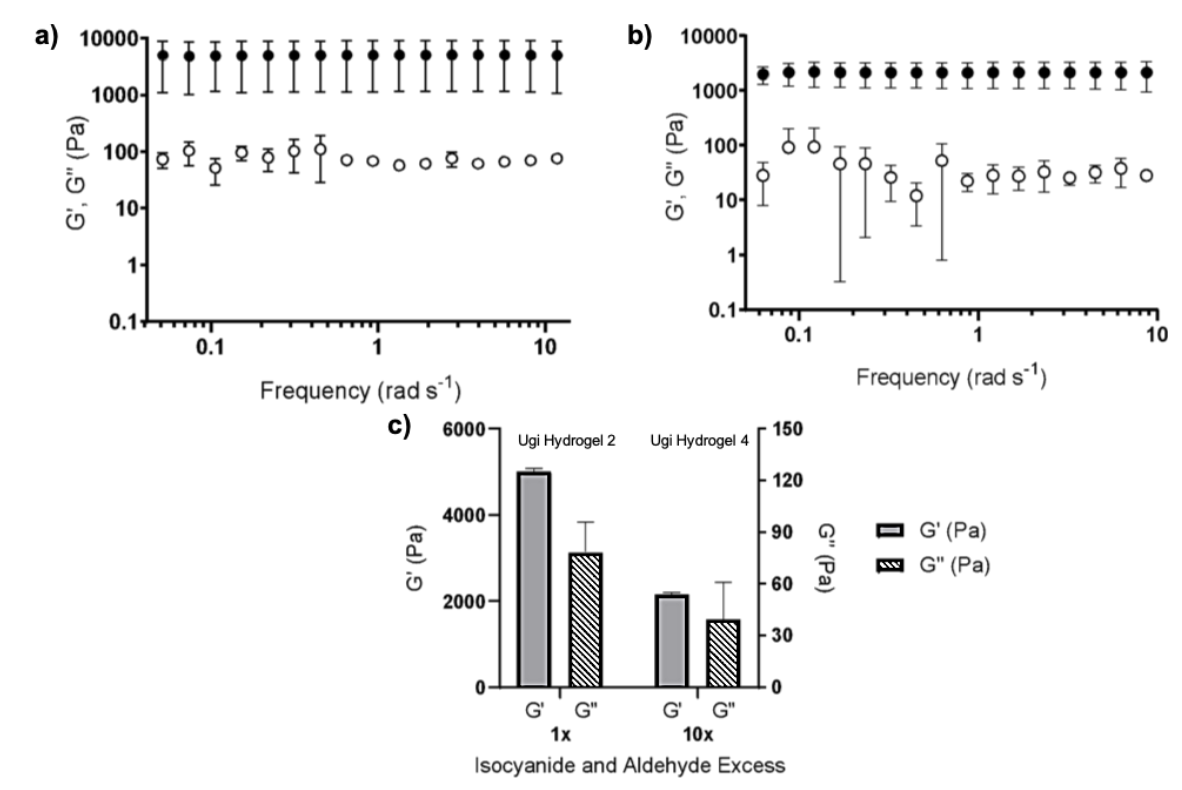


Figure 2.6 – Rheological analysis: Frequency sweeps of the hydrogels' samples from the studies on the effect of the isocyanide and aldehyde excess.

Both hydrogels are composed of a concentration of 10% (w/v) for both PEG-[GABA] $_4$ and PEG-[NH $_2$] $_4$, incubated at 60 °C in methanol. a) Ugi hydrogel 2 – The molar excess of both isopropyl isocyanide and propionaldehyde in comparison to the amines in the system is 1; b) Ugi hydrogel 4 – The molar excess of both isopropyl isocyanide and propionaldehyde in comparison to the amines in the system is 10. c) G' and G" of Ugi hydrogels 2 and 4.

Legend: ● – Storage modulus (G'); O – Loss modulus (G").

As it can be seen in Figure 2.6, Ugi hydrogels 2 and 4 present higher storage modulus than loss modulus signifying a more elastic than viscous behaviour. Moreover, the difference between the elastic or storage modulus (G') and the viscous or loss modulus (G'') combined with a lack of

dependence of the G' toward the frequency are indications of mechanically structured hydrogels.^[91] The hydrogel formed with a molar excess of 1 regarding both isopropyl isocyanide and propionaldehyde (Ugi hydrogel 2) has a higher G' (~43 %, see Table 2.2) indicating a mechanically stiffer gel in comparison to the hydrogel formed with 10 times the molar excess. This statement is supported by the higher gel fraction of the first hydrogel in comparison to the former as a superior gel fraction means that the percentage of cross-linking is higher.^[91] Perhaps, by introducing 10-excess molar of isocyanide and aldehyde there are steric effects that prevent the reaction to occur.^[92]

As the gelation kinetics of the hydrogels formed with a 10-excess molar of the isocyanide and the aldehyde (Ugi hydrogel 4) is more favourable, the hydrogels herein formed will present 10-excess molar of the isocyanide and the aldehyde in comparison to the amines in the system. The gelation kinetics will be preferred over the stiffness of the hydrogels because the order of magnitude of G' for both hydrogels is the same.

As such, the Ugi hydrogel 4, formed at 60 °C in methanol with 10 % concentration (w/v) of both PEG-[GABA]₄ and PEG-[NH₂]₄, with 10-excess molar of both isopropyl isocyanide and propionaldehyde will be named as the standard hydrogel.

Another important feature to study is the effect of the solvent. In an attempt to perform the reaction in milder conditions, the components were dissolved in water instead of methanol. When the water is the solvent used to perform the Ugi reaction, the protonation of the components needs to be taken into consideration. Bu and co-workers^[93] have studied the effect of the pH on the rheological behaviour on alginate-based hydrogels performed with the Ugi multicomponent reaction. It was observed that the viscosity of the solution increased by lowering the pH and that a hydrogel was only formed when the pH of the solution was below the pKa of the carboxylic acid groups, showing the importance of the carboxylic acid's protonation.

Since the pKa of gamma-amino-butyric acid is 4.031, PEG functionalized with the amine and the carboxylic acid were mixed together in water and the solution's pH was set to either 1, 2 or 3 using a 2 M HCl solution. Afterwards, the aldehyde and the isocyanide were added to the mixture and incubated at 60 °C. None of the solutions formed a hydrogel (Ugi hydrogel 6-10, Table 2.3). There are two possible reasons for the unsuccessful formation of a hydrogel: 1) Since water is a stronger nucleophile, it can react with the iminium ion hindering the progression of the reaction; 2) Isocyanides are not very stable when in contact with an aqueous acidic environment as they will hydrolyse and form a formamide.^[94]

Still with the intent of working in milder conditions, water and methanol were used as cosolvents in a 1:1 proportion (see Table 2.3, Ugi hydrogel 11 and Figure 2.7). By introducing methanol to the system, the iminium moiety was protected from the nucleophilic attack of the water allowing the progression of the reaction.

Table 2.3 – Parameter determination of different hydrogels formed by polymer polycondensation by the Ugi reaction in different solvents.

me of	ne Ugi reaction in different solvents.							
Ugi Gel N°	PEG concentration (w/v)	Solvent	рН	Hydrogel formed & gelation time	G '; G " (Pa)	Critical strain (%)	GF (%)	
5	10 %	Water	1.09	No	-	-	-	
6	10 %	Water	1.97	No	-	-	-	
7	10 %	Water	2.9	No	-	-	-	
8	10 %	Water	1	No	-	-	-	
9	10 %	Water	1.97	No	-	-	-	
10	10 %	Water	3	No	-	-	-	
11	10 %	Wa- ter/Meth- anol	-	Yes – 1 day	1519.9±98.4 55.5±33.3	0.01	74.1±4.4	
4	10 %	Methanol	-	Yes – 5 hours	2156.3±43.5 39.6±21.2	0.01	88.9±2.9	

The concentration of PEG-[GABA]₄ is 10 % (w/v) and the concentration of PEG-[NH₂]₄ is 10 % (w/v), the reactional temperature is 60 °C, the isopropyl isocyanide and the propional dehyde were in 10-excess molar in comparison to the amines in the system.

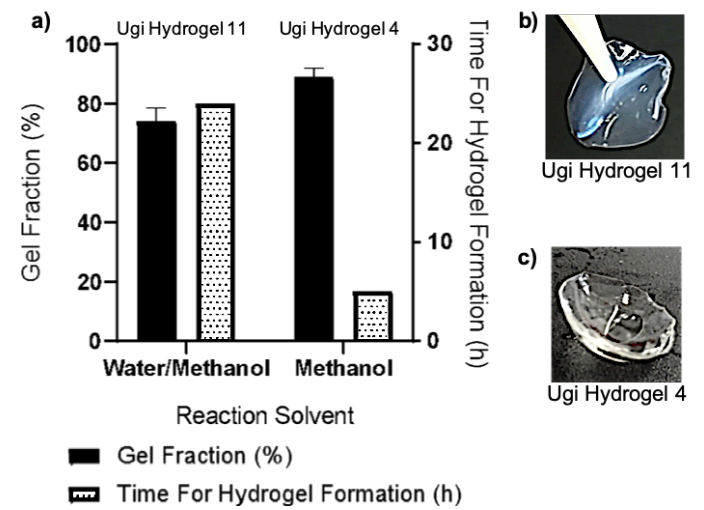


Figure 2.7 – Hydrogels formed by polymer polycondensation by the Ugi reaction with different solvents.

a) Gel fraction and Hydrogel formed & gelation time for Ugi hydrogel 11 and 4. b) Ugi hydrogel 11 – Formed at 60 °C in methanol and water (1:1) with a concentration (w/v) of 10 % for both PEG-[GABA] $_4$ and PEG-[NH $_2$] $_4$, 10-excess molar of both isopropyl isocyanide and propionaldehyde, in comparison to the amines in the system. c) Ugi hydrogel 4 – Formed at 60 °C in methanol with a concentration of 10 % (w/v) for both PEG-[GABA] $_4$ and PEG-[NH $_2$] $_4$, 10-excess molar of both isopropyl isocyanide and propionaldehyde, in comparison to the amines in the system (Standard Hydrogel).

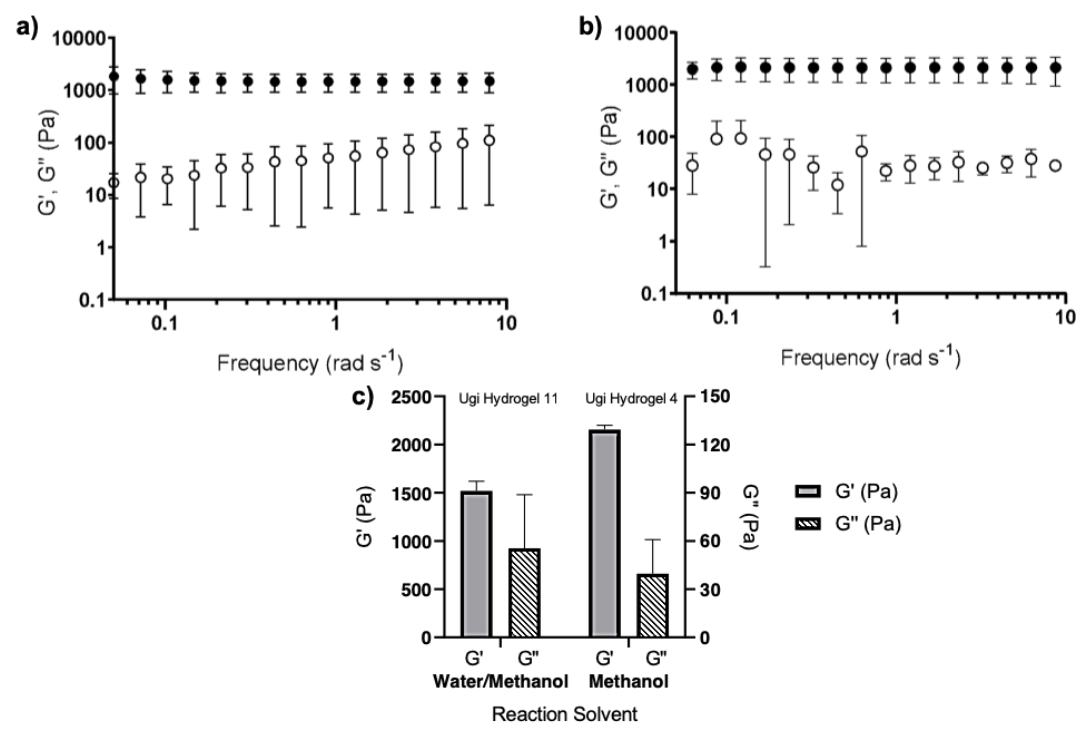


Figure 2.8 – Rheological analysis: Frequency sweeps of the hydrogels' samples from the solvent effect studies.

Both hydrogels are composed of a concentration of 10% (w/v) for both PEG-[GABA]₄ and PEG-[NH₂]₄, the molar excess of both isopropyl isocyanide and propionaldehyde is 10 and the mixture was incubated at 60 °C until the hydrogel was formed; a) Ugi hydrogel 11 – Solvent used was a mixture 1:1 of water and methanol. b) Ugi hydrogel 4 – Solvent was methanol (Standard Hydrogel). c) G' and G'' of ugi hydrogels 11 and 4. Legend: \bullet – Storage modulus (G'); O – Loss modulus (G'').

Both hydrogels (100 % methanol – Ugi hydrogel 4 or methanol/water in a proportion of 1:1 – Ugi hydrogel 11) present a larger G' than G" (Figure 2.8) indicating a dominance of the elastic force over the viscous force. However, when comparing the G' of both hydrogels, it is obvious that Ugi hydrogel 4 is stiffer, 2156.3±43.5 Pa (Ugi hydrogel 4) and 1519.9±98.4 Pa (Ugi hydrogel 11). The difference of G' leads to believe that the methanol introduced to the second system was not enough to completely protect the iminium ion, compromising a complete formation of the hydrogel. This statement can be supported by the lower value of the gel fraction of Ugi hydrogel 11 in comparison to Ugi hydrogel 4 indicating a smaller percentage of the polymer used to form Ugi hydrogel 11.^[91,95]

In regards to the solvent effect, the best condition is using only methanol because the gelation kinetics is more favourable and the hydrogel formed has better mechanical properties.

It is also important to understand what the value of the critical gel concentration is. The minimal concentration of polymer available in solution with which it is possible to form a hydrogel is named as the critical gel concentration. [96] Different hydrogels were attempted to be form with a concentration of each 4-arm PEG of 1 %, 2 % and 5 %, the aldehyde and the isocyanide were introduced to the system with a 10-excess molar, the reaction occurred in methanol and at 60 °C as it is described in Table 2.4.

Table 2.4 – Parameter determination of different polymer concentrations formed by polymer polycondensation by the Uqi reaction.

Ugi	Concentration (w/v)		Hydrogel	G';	Critical	
Gel	PEG-[GABA] ₄	PEG-[NH ₂] ₄	formed & gelation	G"	strain	GF (%)
Nº	T EG-[GABA]4	1 LO-[N1 12]4	time	(Pa)	(%)	(70)
12	1 %	1 %	No	-	-	-
13	2 %	2 %	No	-	-	-
14	5 %	5 %	Yes – 1 day	2119.5±54.2 37.3±5.2	0.1	93.1±4.5
4	10 %	10 %	Yes – 5 hours	2156.3±43.5 39.6±21.2	0.01	88.9±2.9

The reactional temperature is 60 °C and the isopropyl isocyanide and the propionaldehyde were in 10-excess molar in comparison to the amines present in the system.

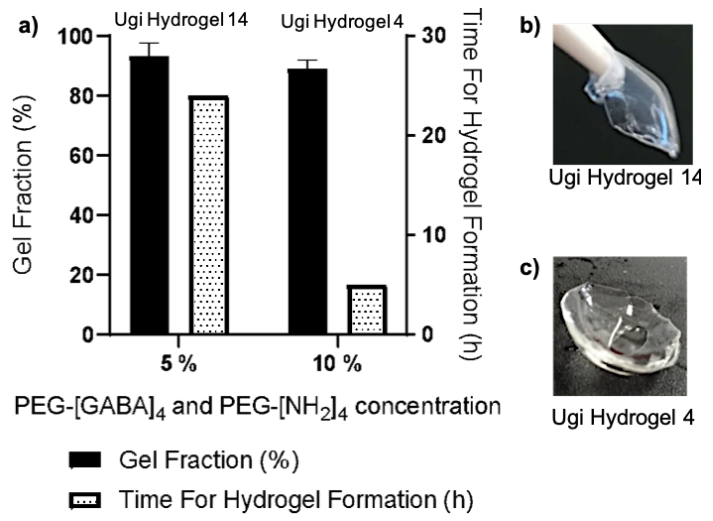


Figure 2.9 – Hydrogels formed by polymer polycondensation by the Ugi reaction with different PEG concentrations.

a) Gel fraction and Hydrogel formed & gelation time for Ugi hydrogel 14 and 4. b) Ugi hydrogel 14 – Formed at 60 °C in methanol with a concentration (w/v) of 5 % for both PEG-[GABA]₄ and PEG-[NH₂]₄, 10-excess molar of both isopropyl isocyanide and propionaldehyde, in comparison to the amines in the system. c) Ugi hydrogel 4 – Formed at 60 °C in methanol with a concentration of 10 % (w/v) for both PEG-[GABA]₄ and PEG-[NH₂]₄, 10-excess molar of both isopropyl isocyanide and propionaldehyde, in comparison to the amines in the system (Standard Hydrogel).

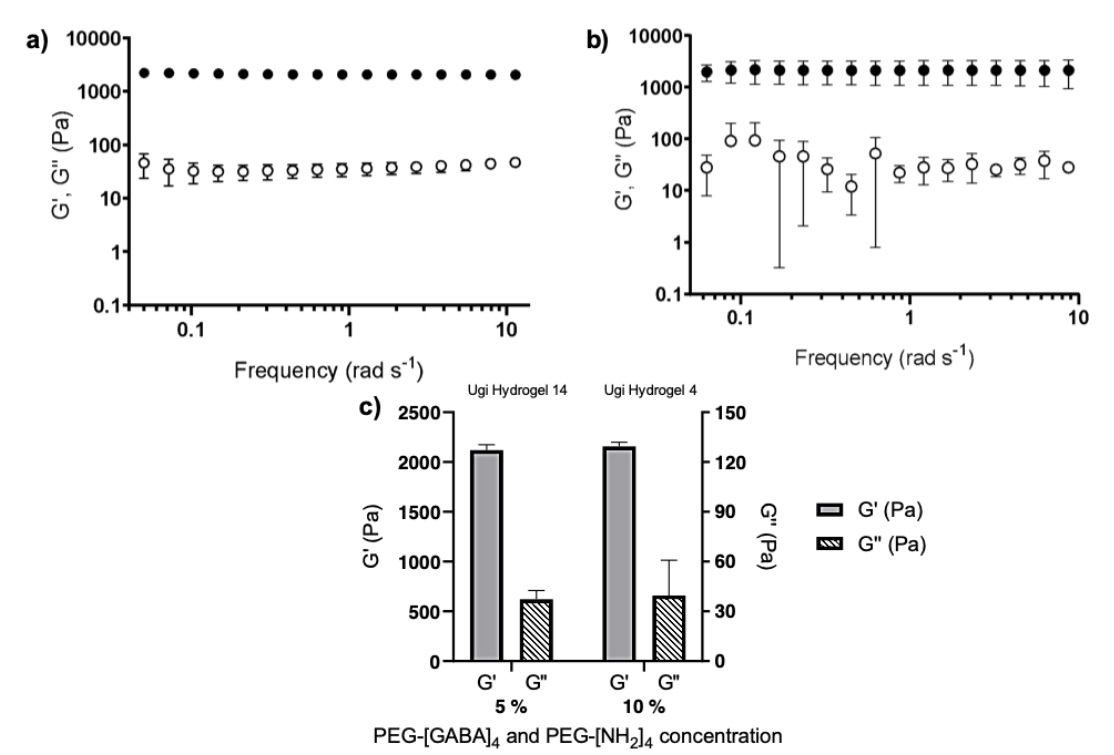


Figure 2.10 – Rheological analysis: Frequency sweeps of the hydrogels' samples from the critical gel concentration studies.

Both hydrogels were formed in methanol by introducing PEG-[GABA]₄ and PEG-[NH₂]₄, isopropyl isocyanide and propionaldehyde with the molar excess of 10 each. The mixture was incubated at 60 °C until the hydrogel was formed. a) Ugi hydrogel 14 − Concentration of 4-arm PEG molecules was 5 %. b) Ugi hydrogel 4 − Concentration of 4-arm PEG molecules was 10 % (Standard Hydrogel). c) G' and G" of hydrogels 14 and 4. Legend: ● − Storage modulus (G'); O − Loss modulus (G").

Since the hydrogels with a concentration of 1 % and 2 % (Ugi hydrogels 12 and 13) were not formed, these concentrations were below the critical gel concentration. Hydrogels with a PEG-[GABA] $_4$ and PEG-[NH $_2$] $_4$ concentration of 5 % (Ugi hydrogel 14, Figure 2.9 b) were formed and so, the critical gel concentration was determined to be 5 %, similarly with other hydrogels formed with a PEG-based system.[15]

The G' and G" of both hydrogels is very similar, 2119.5±54.2 Pa for Ugi hydrogel 14 and 2156.3±43.5 Pa for the standard hydrogel (Ugi hydrogel 4, Table 2.4, Figure 2.10). It is important to notice that the critical strain determined during amplitude sweep experiments for the standard hydrogel is ten-fold lower and so, the strain applied to the standard hydrogel was also ten-fold lower meaning the hydrogel with 5 % concentration of each 4-arm PEG can undertake higher stress rates without its structure breaking down.^[91]

The hydrogels were characterized by ATR-FTIR (Figure 2.11). All of the main peaks found in PEG-[GABA]₄ are found in the spectra correspondent to the hydrogels. With the exception, of a sharp inverted peak at 1660 cm⁻¹ which can be masked by the background (water). This peak can be attributed to C=O stretching due to the presence of an amide.

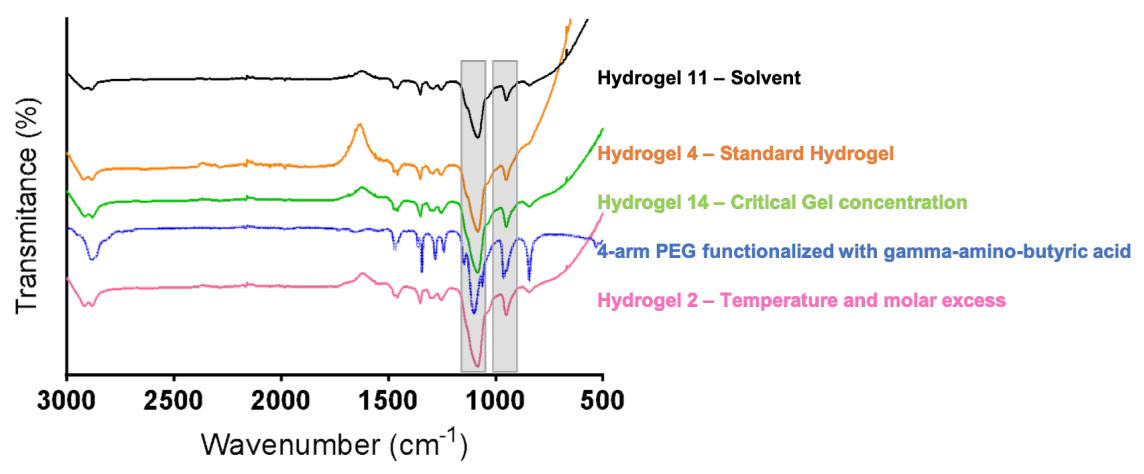


Figure 2.11 – Sample characterization by ATR-FTIR spectra of different hydrogels formulated by the starting conditions.

Legend: In black, Ugi hydrogel 11 – Gauge force 86; In orange, hydrogel 4 (Standard Hydrogel) – Gauge force 81; In green, Ugi hydrogel 14 – Gauge force 99; In blue, PEG functionalized with gamma-amino-butyric acid; In pink, Ugi hydrogel 2 – Gauge force 79.

Lastly, to ensure that all of the components used for the Ugi reaction were responsible for the formation of the hydrogels mentioned above, controls were performed, where 4 different formulations were done. Each formulation does not include one of the four components involved in the Ugi Reaction (Table 2.5). Since none of the hydrogels were formed, this shows that all of the components are essential for hydrogel to be formed. Also, it is important to mention that the Passerini reaction is not a viable strategy to employ when aiming to form chemically cross-linked hydrogels with a four arm-PEG functionalized with a carboxylic acid. Since the product of the Passerini reaction is thermally less stable^[67], it is possible to theorize that since the reaction is made at 60 °C, the Passerini reaction can be indeed taking place, however the final product may not be able to withstand the high temperature.

Table 2.5 – Components introduced into the mixture of different hydrogel to understand the influence of the Ugi reaction

Formula- tion	PEG-[GABA] ₄	PEG-[NH ₂] ₄	Propionalde- hyde	Isopropyl iso- cyanide	Hydrogel For- mation
1	No	Yes	Yes	Yes	No
2*	Yes	No	Yes	Yes	No
3	Yes	Yes	No	Yes	No
4	Yes	Yes	Yes	No	No

Legend: * Passerini Reaction

To sum up, the best conditions to obtain PEG-based hydrogels using the Ugi multicomponent condensation reaction as the cross-linking strategy, correspond to the Ugi hydrogel 4 (standard hydrogel). This statement is based on the gelation kinetics which is maximized when the conditions chosen are: 10 % (w/v) of PEG-[COOH]4, 10 % (w/v) of PEG-[NH2]4, 10-excess molar of aldehyde in comparison to the amines present in the system, 10-excess molar of isocyanide in comparison to the amines present in the system. The most appropriate reactional temperature is 60 °C and the solvent of choice is methanol. Herein, unless it is stated, the hydrogels will be formulated with these conditions and using PEG-[NH2]4, PEG-[GABA]4 as PEG-[COOH]4, propionaldehyde as the aldehyde and isopropyl isocyanide as the isocyanide.

2.4.1.3 Incorporating variability in the hydrogels

Chemically cross-linked hydrogels have many applications and the final user can tune the properties of the hydrogel by incorporating different molecules into the hydrogel's network.

The Ugi reaction involves an amine, a carboxylic acid, an aldehyde and an isocyanide.^[4] Since the amine is commercially available functionalized into a 4-arm PEG molecule, the carboxylic acid, the aldehyde and the isocyanide are the moieties that can be altered in order to introduce functionality (Figure 2.12).

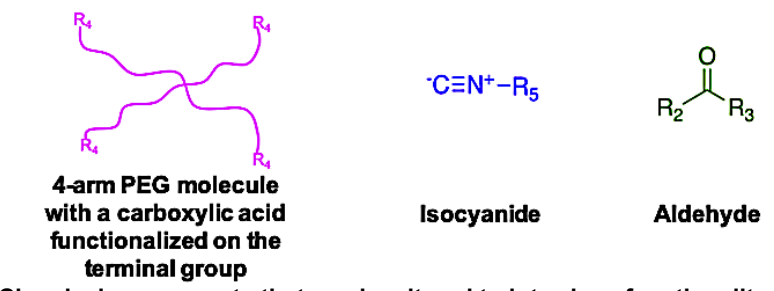


Figure 2.12 – Chemical components that can be altered to introduce functionality.

The first attempts to introduce variability were done with PEG-[COOH]₄. Aromatic carboxylic acids were functionalized into 4-arm PEG-[NHS]₄ to form PEG-[COOH]₄. For this, the presence of a terminal amine (1) in the carboxylic acid moiety is a requirement so that it reacts with the NHS group (2) forming an amide bond (3) with the PEG molecule and the NHS group (4) will be consequently released (Figure 2.13).^[97] So, three different molecules were incorporated: 4-(aminomethyl)benzoic acid, 4-biphenyl-3'-amino-acetic acid (PAMBA) and tryptophan (Figure 2.14).

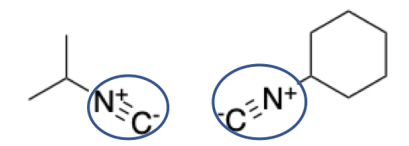
Figure 2.13 – Reaction between NHS group and an amine.

Legend: 1 – Molecule with a terminal amine; 2 – Molecule with a NHS group; 3 – Molecule with an amide bond; 4 – Leaving NHS group.

4-(aminomethyl)benzoic acid 4-biphenyl-3'-amino-acetic acid Figure 2.14 – Compounds used for the incorporation into PEG-[NHS]₄. In blue, the expected reaction point with PEG-[NHS]₄.

Tryptophan

Besides incorporating different molecules into PEG-[COOH]₄, a formulation based on the standard hydrogel was attempted. However, instead of using isopropyl isocyanide, cyclohexyl isocyanide was utilized with a 10-excess molar to the amines present in the system (Figure 2.15). This experiment was designed aiming to understand if there was any steric effect by using bulkier isocyanides for the formation of these PEG-based hydrogels and how compromised the formation of a hydrogel would be.



Isopropyl Isocyanide Cyclohexyl Isocyanide

Figure 2.15 – Isocyanide compounds used to formulate the hydrogels. In blue, the expected reaction point.

Table 2.6 – Parameter determination of different hydrogels formed by polymer polycondensation by the Ugi reaction using varied carboxylic acids.

	gi reaction using varied carboxylic acids.							
Ugi	PEG-[COO	H] ₄		G'	0			
Gel N°	-СООН	Function- alization (%)	Hydrogel formed & gelation time	G " (Pa)	Critical strain (%)	GF (%)		
15	4-(aminome- thyl)benzoic acid	98.9	Yes – 1 day	4758.4±175.66 2015.7±145.7	0.01	>100*		
4	Gamma-amino- butyric acid ¹	99.5	Yes – 5 hours	2156.3±43.5 39.6±21.2	0.01	88.9±2.9		
16	4-biphenyl-3'- amino-acetic acid	99.9	No	-	-	-		
17	Tryptophan	99.9	No	-	-	-		

The functionalization percentage was assessed with the Kaiser test method. Legend: * – Not possible to accurately determine the gel fraction; ¹ – Standard hydrogel.

The carboxylic acid compounds were successfully functionalized (>98%) into the 4-arm PEG molecules. The functionalization was assessed by the Kaiser test.

As verified in Figure 2.16, the ATR-FTIR spectra that corresponds to 4-(aminomethyl)benzoic acid presents three peaks. The peak at 1398 cm⁻¹ is representative of O-H bending due to the carboxylic acid part of the molecule. Moreover, the C-C stretching from the carbons present in the aromatic ring arise a peak at 1570 and 1591 cm⁻¹. The FTIR spectra for PEG-[NHS]₄, in green, presents four distinctive peaks: a broad band at 2860 cm⁻¹ corresponding to a O-H stretching, a peak visible at 1743 cm⁻¹ (dashed line) characteristic of a C=O stretching due to the presence of the ester group, confirming the presence of NHS. Moreover, there is a peak at 1091 cm⁻¹ attributed to the ether group and the presence of alkenes (C=C bending) is noted by the peaks between 974 cm⁻¹ and 812 cm⁻¹. Finally, in blue, the FTIR spectra for the 4-arm PEG functionalized with 4-(aminomethyl)benzoic acid (PEG-[PAMBA]₄) is full of noise however, it presents the main peaks that the PEG-[NHS]₄ spectra presents except the peak at 1743 cm⁻¹.

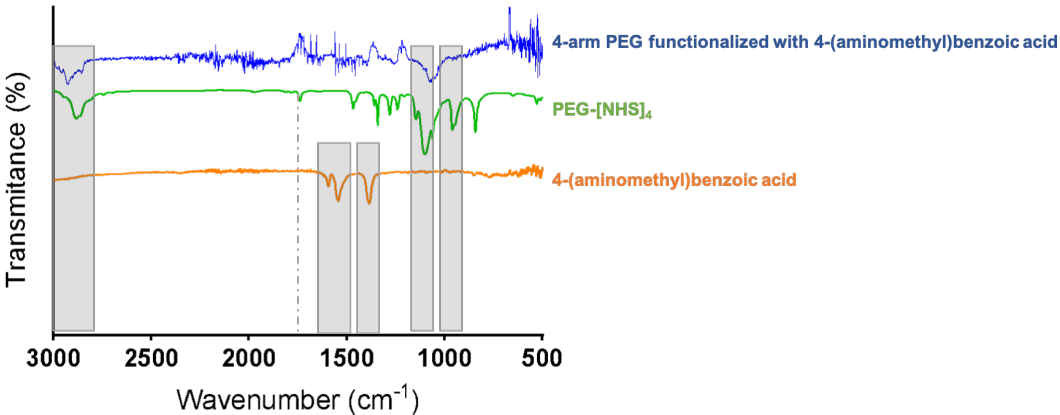


Figure 2.16 – Sample characterization by ATR-FTIR spectra.

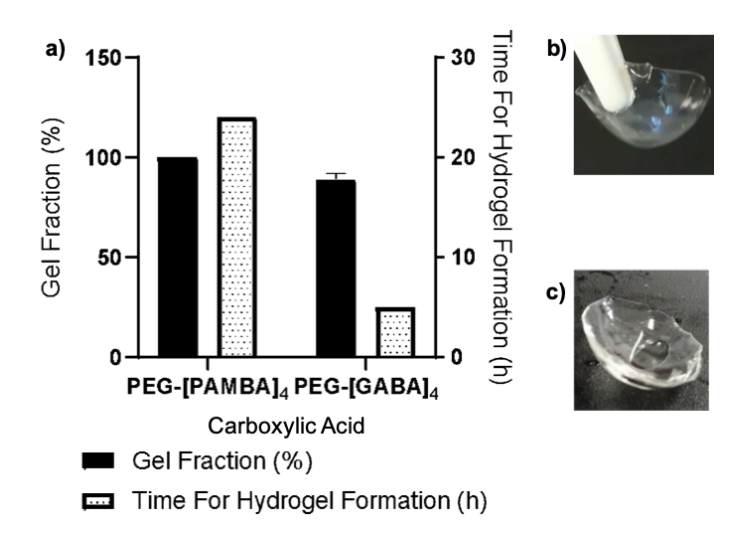


Figure 2.17 – Hydrogels formed by polymer polycondensation by the Ugi reaction with different PEG-[COOH]₄.

a) Gel fraction and Hydrogel formed & gelation time for Ugi hydrogel 15 and 4. b) Ugi hydrogel 15 – Formed at 60 °C in methanol with a concentration (w/v) of 10 % for both PEG-[4-(aminomethyl)benzoic acid]₄ and PEG-[NH₂]₄, 10-excess molar of both isopropyl isocyanide and propionaldehyde, in comparison to the amines in the system. c) Ugi hydrogel 4 – Formed at 60 °C in methanol with a concentration (w/v) of 10 % for both PEG-[GABA]₄ and PEG-[NH₂]₄, 10-excess molar of both isopropyl isocyanide and propionaldehyde, in comparison to the amines in the system (Standard Hydrogel).

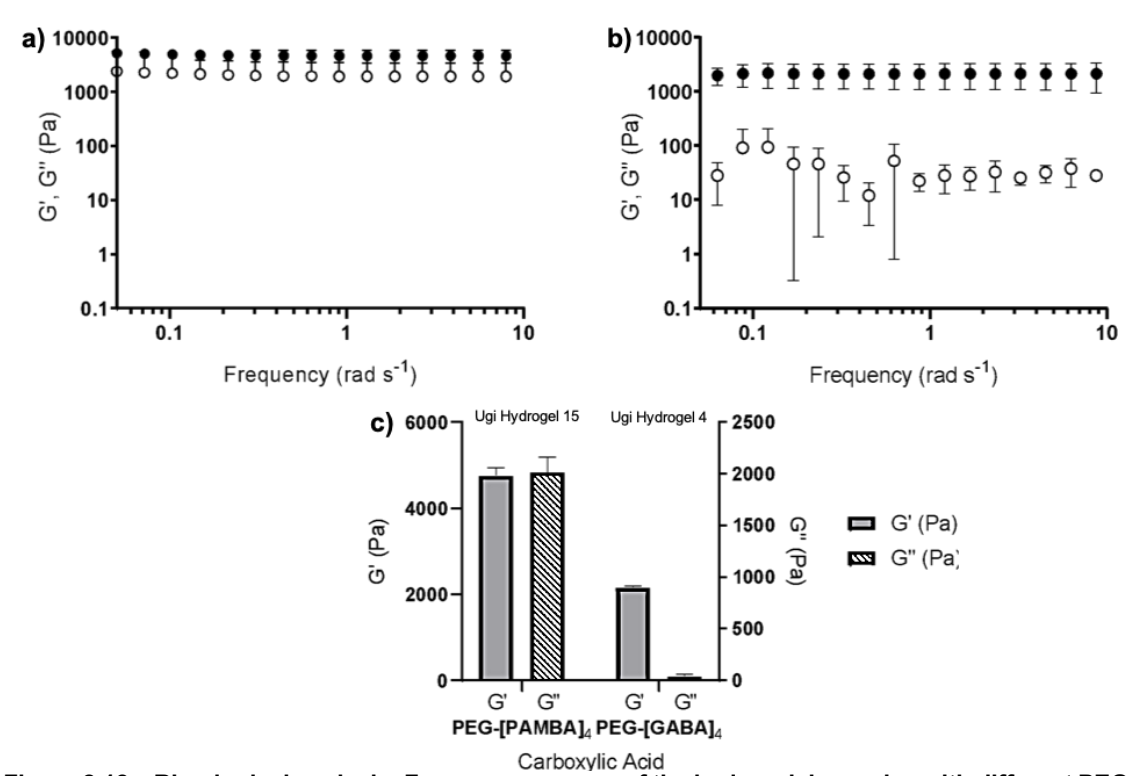


Figure 2.18 – Rheological analysis: Frequency sweeps of the hydrogels' samples with different PEG-COOH.

a) Ugi hydrogel 15 – PEG-[4-(aminomethyl)benzoic acid] $_4$ as the carboxylic acid component. b) Ugi hydrogel 4 – PEG-[Gamma-amino-butyric acid] $_4$ as the carboxylic acid component (Standard hydrogel). c) G' and G'' of Ugi hydrogels 15 and 4.

Legend: ● – Storage modulus (G'); O – Loss modulus (G").

The functionalized 4-arm PEG-[GABA]₄ molecules, PEG-[NH₂]₄, propionaldehyde and isopropyl isocyanide were mixed in methanol and left in 60 °C for the reaction to occur. Besides the standard hydrogel, the only hydrogel obtained was the one whose formulation contained the carboxylic acid 4-(aminomethyl)benzoic acid functionalized to the 4-arm PEG molecule (Ugi hydrogel 15, Table 2.6, Figure 2.17).

Table 2.7 – Parameter determination of different hydrogels formed by polymer polycondensation by

the Ugi reaction using varied isocyanides.

Ugi	(w/v) Alde-			Hydrogel formed &	G'	Critical strain	GF	
Gel N°	PEG- [GABA] ₄	PEG- [NH ₂] ₄	hyde	Isocyanide	gelation time	G " (Pa)	(%)	(%)
18	10 %	10 %	Propion-	Cyclohexyl	Yes – 1 day	9794.4±382.2 170.0±120.4	0.01	86.5±0.1
4	10 %	10 %	Propion-	Isopropyl ¹	Yes – 5 hours	2156.3±43.5 39.6±21.2	0.01	88.9±2.9

Legend: 1 – Standard hydrogel

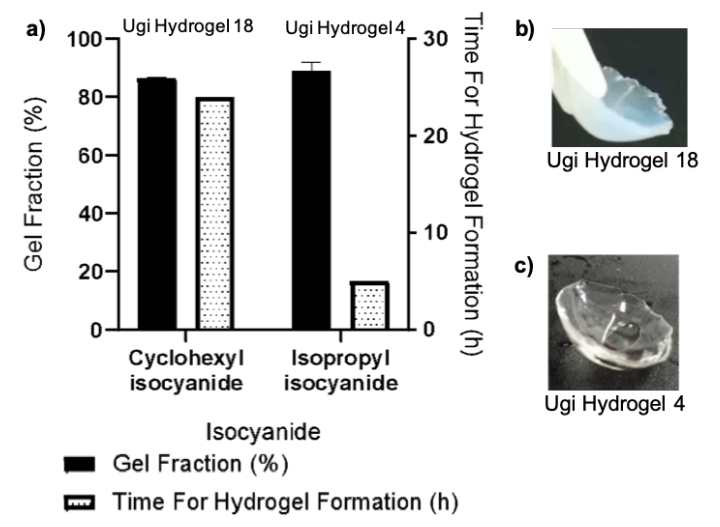


Figure 2.19 – Hydrogels formed by polymer polycondensation by the Ugi reaction with different isocyanides.

a) Gel fraction and Hydrogel formed & gelation time for Ugi hydrogel 18 and 4. b) Ugi hydrogel 18 – Formed at 60 °C in methanol with a concentration (w/v) of 10 % for both PEG-[GABA]₄ and PEG-[NH₂]₄, 10-excess molar of both cyclohexyl isocyanide and propionaldehyde, in comparison to the amines in the system. c) Ugi hydrogel 4 – Formed at 60 °C in methanol with a concentration (w/v) of 10 % for both PEG-[GABA]₄ and PEG-[NH₂]₄, 10-excess molar of both isopropyl isocyanide and propionaldehyde, in comparison to the amines in the system (Standard Hydrogel).

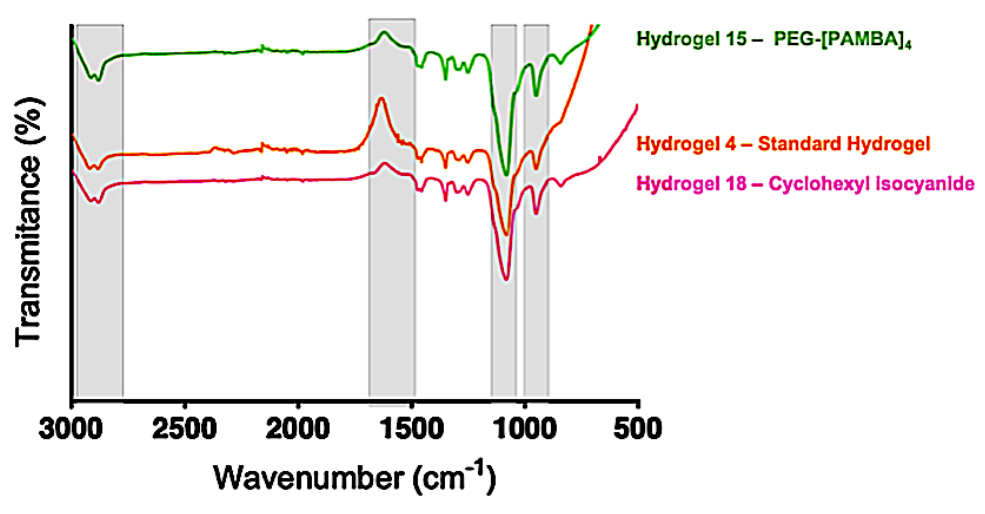


Figure 2.20 – Sample characterization by ATR-FTIR spectra of the hydrogels formulated to incorporate the function of conductivity.

Legend: In green, Ugi hydrogel 15– Gauge force 101; In orange, Ugi hydrogel 4; In pink, Ugi hydrogel 18– Gauge force 81.

As observed in Figure 2.20, all of the hydrogel samples present a broad band from 2978.5 cm⁻¹ to 2618 cm⁻¹ corresponding to a O-H stretching, a characteristic peak at 1560 cm⁻¹ attributed to a asymmetric stretching of the carboxylate group and a peak whose minimum transition is at 1405 cm⁻¹ that is credited to O-H bending. In addition, around 1660 cm⁻¹, there is a sharp inverted peak which can be masked by the spectrum of the background (water). This peak can be attributed to C=O stretching due to the presence of an amide bond.

The hydrogels' stiffness was measured by rheology (Figure 2.18 and Figure 2.21). The higher G' in comparison to G" and the non-dependence with frequency are indicators of mechanically structured hydrogels. The standard hydrogel (Ugi hydrogel 4) is the less rigid hydrogel meaning that the introduction of bulkier molecules to the system created a more robust structure. Regarding the hydrogel formed by incorporating PEG-[PAMBA]₄ as the carboxylic acid (Ugi hydrogel 15, Figure 2.18 a), the G' and the G" (4758.4±175.66 Pa, 2015.7±145.7 Pa, respectively) show an improvement on the gel's stiffness (~120 % higher). Finally, the introduction of cyclohexyl isocyanide (Ugi hydrogel 18,Table 2.7, Figure 2.19 a) lead to the highest G' and G" (9794.4±382.2 Pa and 170.0±120.4 Pa) of all the hydrogels formed (Figure 2.21 a).

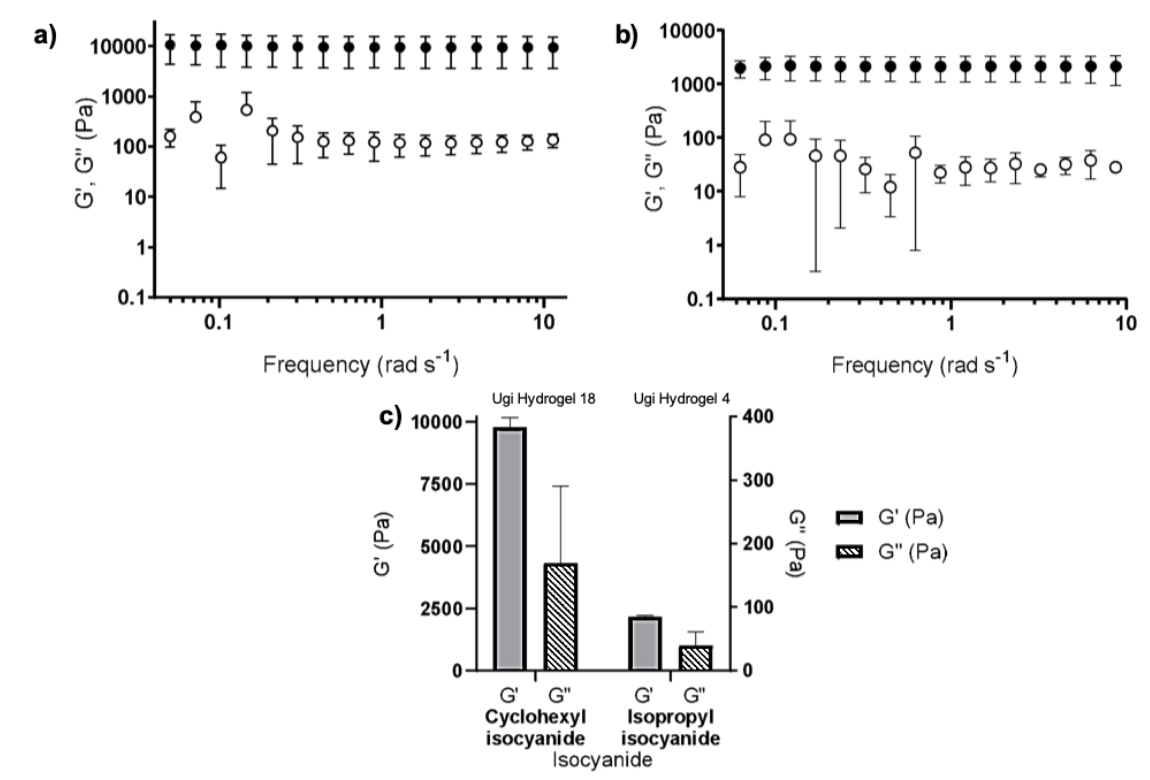


Figure 2.21 – Rheological analysis: Frequency sweeps of the conductive hydrogels' samples.
a) Ugi hydrogel 18 – Formed with cyclohexyl isocyanide for the isocyanide component. b) Ugi hydrogel 4 – Formed with isopropyl isocyanide as the isocyanide component (Standard Hydrogel). c) G' and G" of Ugi hydrogels 18 and 4.

Legend: ● – Storage modulus (G'); O – Loss modulus (G'').

Finally, it was attempted to vary the aldehyde component. The aromatic phenylacetaldehyde was introduced in the hydrogels' network as a substitute of propional dehyde (Figure 2.22).

Figure 2.22 – Aldehyde compounds used to formulate the hydrogels.

Table 2.8 – Parameter determination of different hydrogels formed by polymer polycondensation by the Ugi reaction using varied aldehydes.

Ugi	Concent (w/\		Aldahada	1	Hydrogel formed &	G'	Criti- cal	GF
Gel N°	PEG- [GABA] ₄	PEG- [NH ₂] ₄	Aldehyde	Isocyanide	gelation time	G " (Pa)	strain (%)	(%)
19	10 %	10 %	Phenyla- cet-	Isopropyl	Yes – 1 day	2112.4±15.6 114.4±13.3	0.1	74.0±4.8
4	10 %	10 %	Propion- ¹	Isopropyl	Yes – 5 hours	2156.3±43.5 39.6±21.2	0.01	88.9±2.9

Legend: 1 – Standard hydrogel

By mixing 10 % (w/v) PEG-[GABA]₄, 10 % (w/v) PEG-[NH₂]₄, 10-excess molar of phenylacetaldehyde and 10-excess molar of isopropyl isocyanide in methanol and letting the solution gelate at 60 °C, a hydrogel was formed (Table 2.8, Figure 2.23). From the ATR-FTIR spectra (Figure 2.24), it is possible to see an inverted peak around 1660 cm⁻¹ that can be attributed to C=O stretching due to the presence of an amide bond.

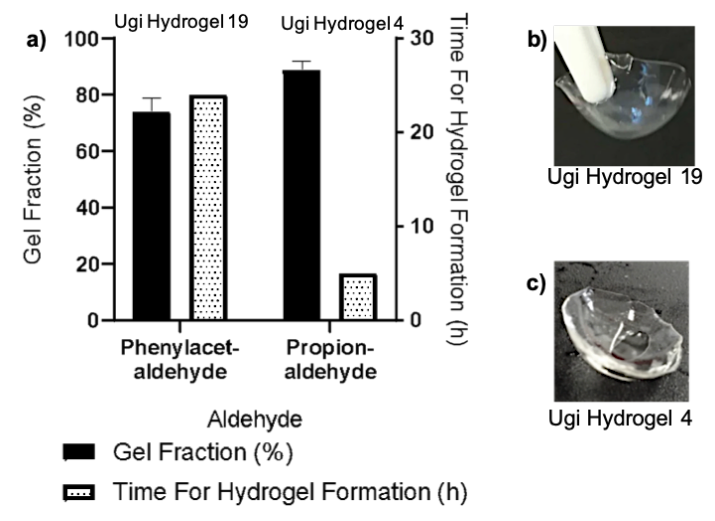


Figure 2.23 – Hydrogels formed by polymer polycondensation by the Ugi reaction with different aldehydes.

a) Gel fraction and Hydrogel formed & gelation time for Ugi hydrogel 19 and 4. b) Ugi hydrogel 19 – Formed at 60 °C in methanol with a concentration (w/v) of 10 % for both PEG-[GABA]₄ and PEG-[NH₂]₄, 10-excess molar of both isopropyl isocyanide and phenylacetaldehyde, in comparison to the amines in the system. c) Ugi hydrogel 4 – Formed at 60 °C in methanol with a concentration of 10 % (w/v) for both PEG-[GABA]₄ and PEG-[NH₂]₄, 10-excess molar of both isopropyl isocyanide and propionaldehyde, in comparison to the amines in the system (standard hydrogel).

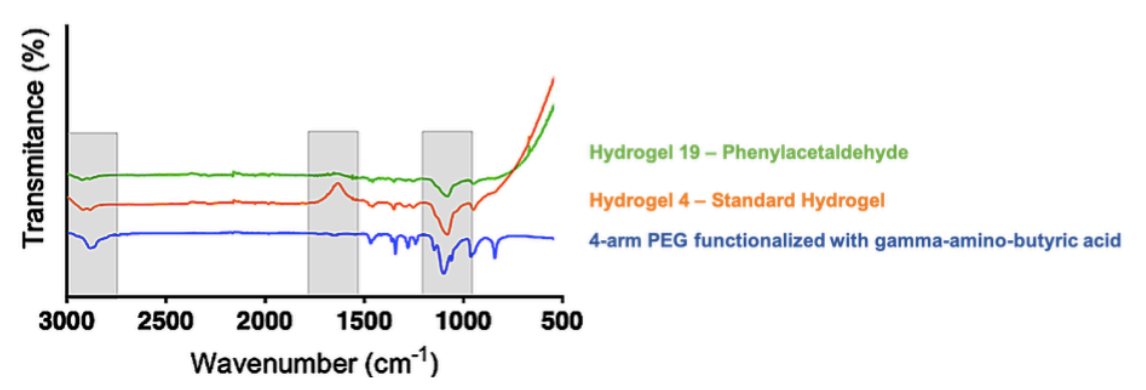


Figure 2.24 – Sample characterization by ATR-FTIR spectra of the hydrogels formulated to incorporate new functionalities.

Legend: In green, hydrogel 19 – Gauge force 94; In orange, hydrogel 4 – Gauge force 81; In blue, PEG functionalized with gamma-amino-butyric acid.

The rheological properties of the hydrogels were studied and, as verified in Figure 2.25 and Table 2.8, the storage and the loss moduli are similar: Standard hydrogel (Ugi hydrogel 4) G' is 2156.3±43.5 Pa and the G" is 39.6±21.2 Pa; hydrogel with phenylacetaldehyde (Ugi hydrogel 19) G' is 2112.4±15.6 Pa and the G" is 114.4±13.3 Pa. Although the G' of both hydrogels are very

similar, the critical strain of Ugi hydrogels 19 is 10 times higher (Table 2.8), meaning that this hydrogel can endure higher stress before breaking.

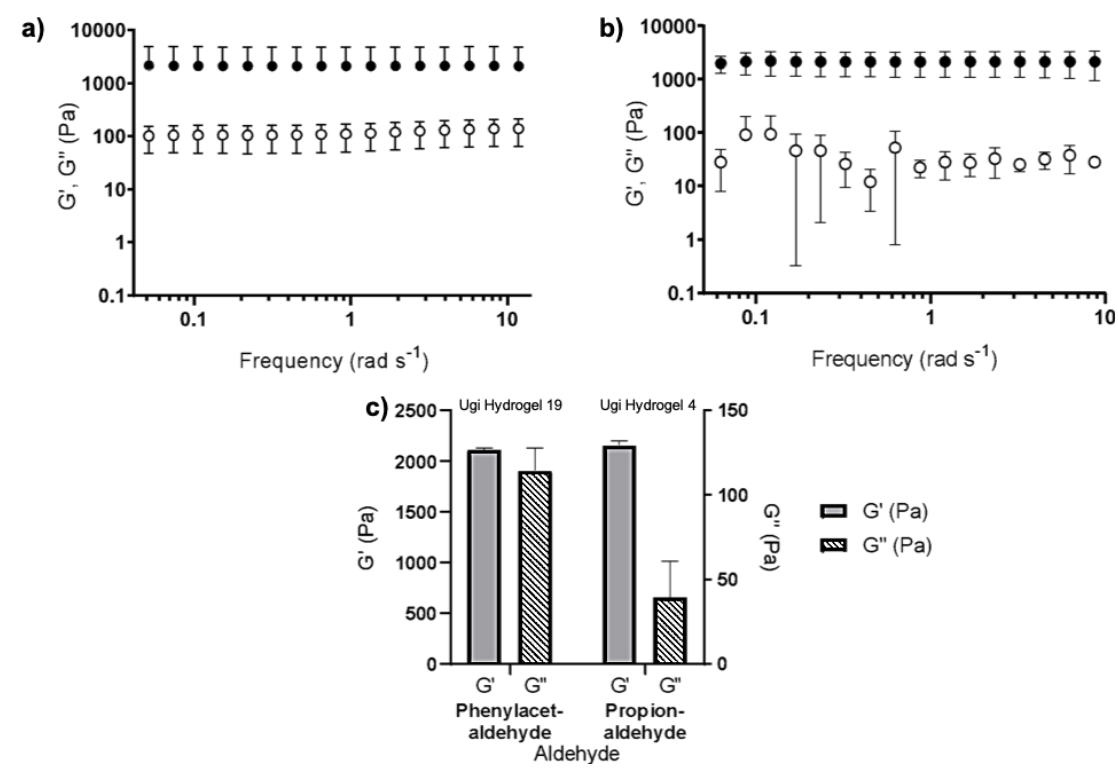


Figure 2.25 – Rheological analysis: Frequency sweeps of the antimicrobial hydrogels' samples.
a) Ugi hydrogel 19 – Formed with phenylacetaldehyde as the aldehyde component. b) Ugi hydrogel 4 – Formed with propionaldehyde as the aldehyde component (Standard Hydrogel). c) G' and G" of Ugi hydrogels 19 and 4.

Legend: ● – Storage modulus (G'); O – Loss modulus (G'').

Previously, in our lab, PEG-coated magnetic nanoparticles were functionalized with an antimicrobial peptide composed by three tandem repeats of the peptide arginine-tryptophan. ^[98] Due to the aromaticity of these dipeptides, they have the ability to penetrate the membranes leading to cell death. ^[99] This system presented excellent results in inhibiting the growth of the Gramnegative bacteria *E. coli* and in inducing cell death of the Gramnositive *B. subtilis*. ^[98] Given the success of this work, we performed preliminary assays to assess the potential antimicrobial activity of the Ugi hydrogels. As it can be verified in Figure 2.26, the aromatic component of the aldehydes (R3) and the isocyanides (R5) are more available to interact with the bacteria in comparison to the carboxylic acid (R6). Therefore, an aromatic aldehyde will be a great candidate to be incorporated into the hydrogels' network instead of an aromatic carboxylic acid.

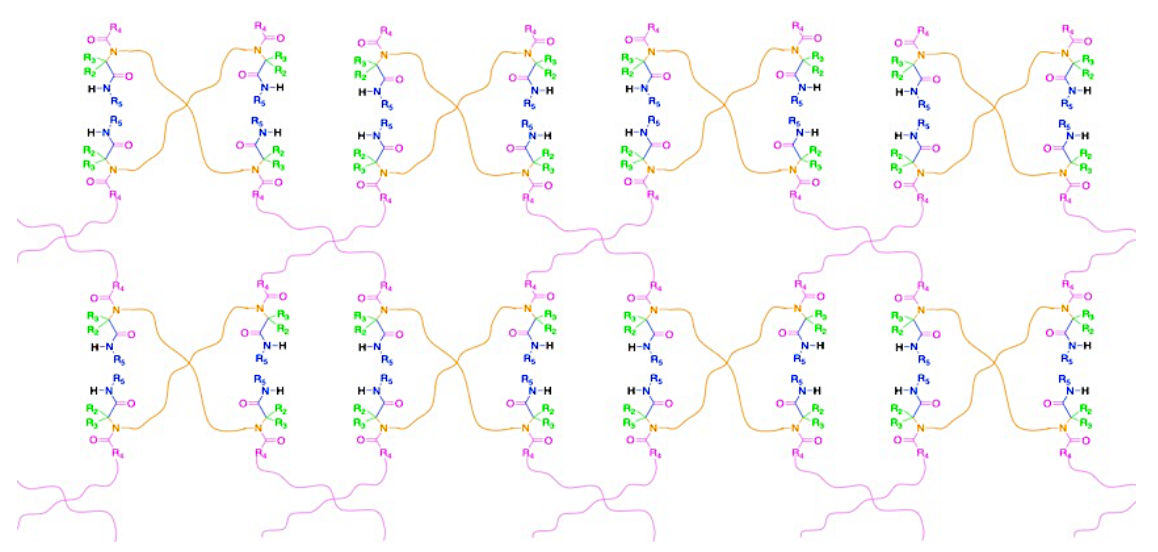


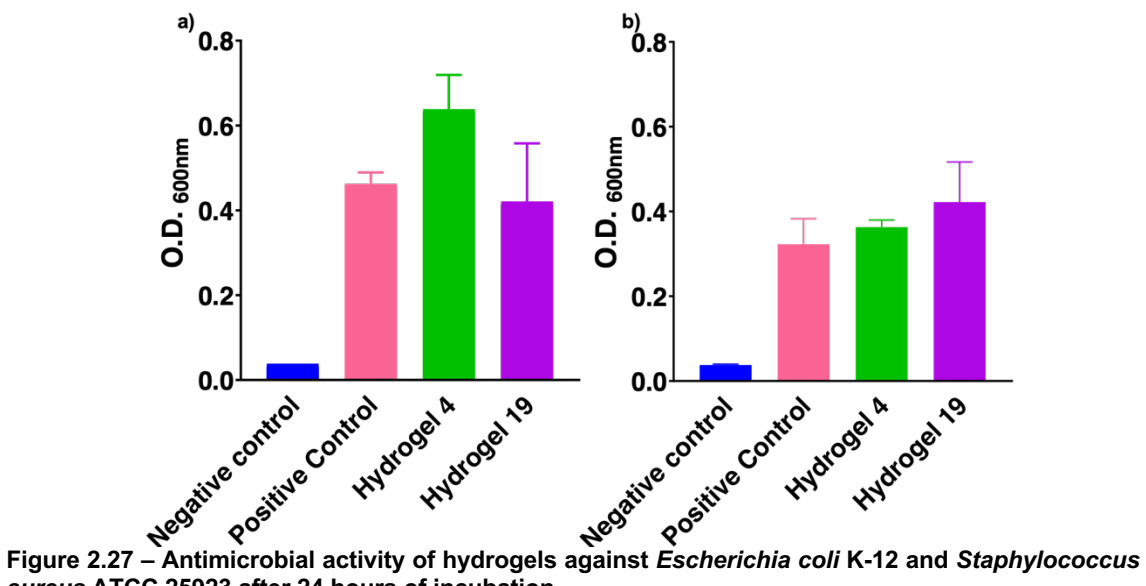
Figure 2.26 – Schematic representation of the hydrogel obtained by polycondensation via the Ugi reaction.

Legend: PEG-[NH₂]₄ is represented in orange, PEG-[COOH]₄ is represented on pink; Aldehyde is represented in green; Isocyanide is represented in blue.

To assess the antimicrobial properties of these hydrogels, each one was divided into 6 equal parts and were separately set on top of a well on 96 well microplates with the culture medium and respective cells that were grown overnight. The experiment was 24 hours long and, at the end, the O.D._{600nm} was measured.

From Figure 2.27, it is possible to conclude that the hydrogels do not present antimicrobial activity. In fact, when the hydrogel is present, the O.D._{600nm} increased in comparison to the positive control, especially on the *E. coli* culture. Here, there was a significant increase of the microbial activity when in contact with the standard hydrogel. Since the phenylacetaldehyde (Ugi hydrogel 19) was incorporated into the network, the presence of the aromatic compound in the solution may not be detected by the bacteria.

Kolewe^[100] described that the stiffer PEG-based hydrogels are, the more bacterial adhesion there is. One explanation for the increased cell density in the cultures where the hydrogel was layered could be that the platform created by the hydrogels beneficiated cell growth. It is important to notice that the mechanism to why bacteria respond to hydrogel's stiffness is not understood. Perhaps, when more is known about this phenomenon, an explanation to the increased cell density observed in Figure 2.27 will arise.

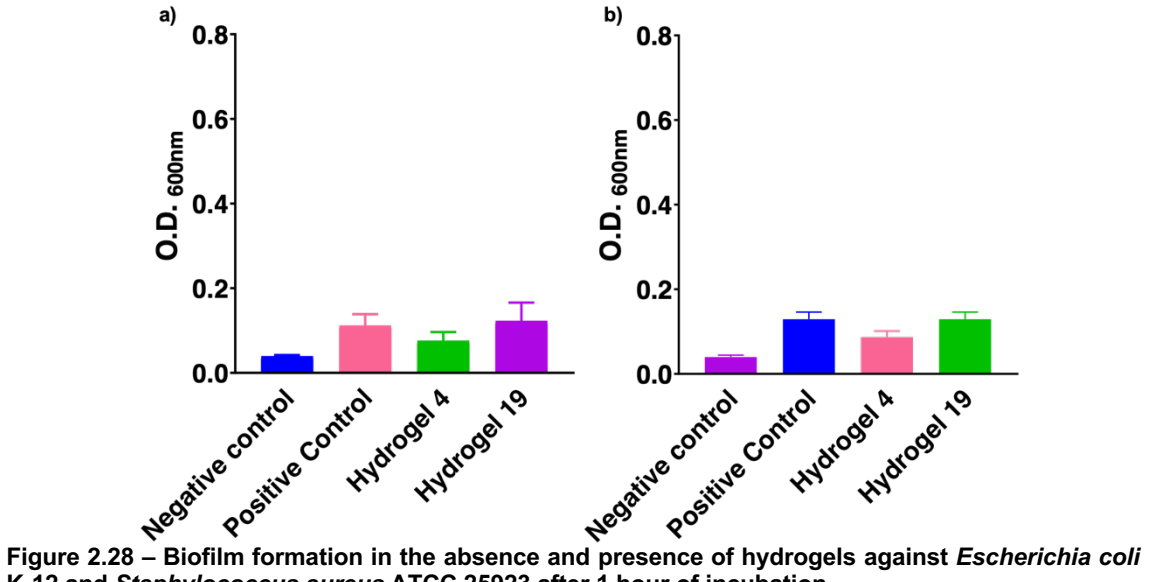


aureus ATCC 25923 after 24 hours of incubation.

Antimicrobial activity of hydrogels against Escherichia coli K-12 (a) and Staphylococcus aureus ATCC 25923

Legend: Blue - Negative control (Muller Hinton Medium); Pink - Positive control (Cell culture); Green - Ugi hydrogel 4 (Standard Hydrogel); Purple – Ugi hydrogel 19.

Afterwards, a static biofilm assay was conducted. The hydrogels also do not inhibit biofilm formation as it can be seen in Figure 2.28 that after one hour of incubation there is no significant difference in the O.D.600nm when comparing the positive control and the hydrogel samples.



K-12 and Staphylococcus aureus ATCC 25923 after 1 hour of incubation.

Escherichia coli K-12 culture (a) and Staphylococcus aureus ATCC 25923 culture (b). Legend: Blue - Negative control (Muller Hinton Medium); Pink - Positive control (Cell culture); Green - Ugi hydrogel 4 (Standard Hydrogel); Purple – Ugi hydrogel 19.

2.5. Conclusions

On this chapter, it was shown, for the first time, that it is possible to take advantage of the Ugi reaction to create chemically cross-linked hydrogels whose sole component are PEG molecules. These hydrogels were formed due to the cross-linking of 4-arm PEG molecules with an amine and a carboxylic acid as the end groups. Taking into consideration the gelation kinetics (24h vs 5h), the best conditions for hydrogel formation were: 10 % (w/v) PEG-[NH₂]₄, 10 % (w/v) PEG-[COOH]₄, 10-excess molar of aldehyde and isocyanide (in regard to the amines in solution). The reaction would have to take place at 60 °C and in methanol.

By introducing different molecules to form the network of the hydrogels, there is a variation of the hydrogels' stiffness (from G' of 9794.4±382.2 Pa – Ugi hydrogel 19 – to a G' of 1519.9±98.4 Pa – Ugi hydrogel 11, strain 0.01%). This way, it is possible to achieve a control of the convenient stiffness according to any future application. From the results obtained, the Ugi reaction participants that play a bigger role on the gel stiffness are the aldehyde's chemical structure. Even though the highest G' recorded was referred to the hydrogel sample with a different isocyanide (cyclohexyl isocyanide) – hydrogel 18, the critical strain was 10 times lower in comparison to the critical strain of the hydrogel with the different aldehyde (phenylacetaldehyde) – hydrogel 19.

It is reported in the literature that higher gel fraction results from an increase of the percentage of cross-linking. [91] Simultaneously, an increase of the degree of cross-linking usually leads to stiffer hydrogels. [95] However, this relationship between cross-liking, gel fraction and hydrogel stiffness was not always observed because the introduction of different aldehydes and carboxylic acids into the system resulted in a lower gel fraction. In contrast, the introduction of these bulkier compounds lead to a higher rigidity and it is possible that they could have counterbalanced the effect of the decrease in cross-linking degree.



AFFINITY TRIGGERED HYDROGELS

3. Affinity Triggered Hydrogels

In biomaterial science, proteins and peptides are seen as building blocks for the creation of biomaterials with fine-tuned proprieties.^[101]

There is a plethora of affinity pairs that can be exploited to form physically cross-linked hydrogels such as the WW domain/PPxY and the green fluorescent protein (GFP)/A4C7. These affinity pairs will be the subject of study on this chapter.

3.1. Affinity Pair: WW Domain and PPxY

The WW domain, first reported in $1994^{[102]}$, is a 30-40-residue peptide whose core is of hydrophobic nature. This domain has two loops and three twisted and slightly bent antiparallel β -sheets with charged amino acids that typically include 4 conserved aromatic amino acids of which two are tryptophans spaced by 20-22 amino acids, hence the name WW domain. [102-105] This domain is commonly found in proteins that participate in signalling and regulatory pathways such as dystrophin, Yellow-Black-Blue2 and Yes Associated Protein [102,104,106]

The WW domains have different binding specificities and so they are divided into four different classes: Class I domains employ hydrogen bonding to recognize and bind to peptides presenting a proline rich domain (PPxY – x represents an amino acid of choice), being the tyrosine of extreme importance for the establishment of the interaction between the affinity pair PPxY domain and the WW domain. [103,105,107] The interaction established between the WW domain and its affinity pair PPxY has been extensively studied namely due to its importance in cell signaling. [108–110] Class II that identifies PPLP motif (also known as the PL motif). Class III that identifies proline-rich segments containing arginine (PR motif) And finally, Class IV that acknowledges a motif comprising S/TPmotif. [111]

Macias^[112] has analysed several WW domain sequences and designed a folded prototype based on those sequences (see Figure 3.1) in which the residues of the first and the third strand establish hydrophobic interactions.

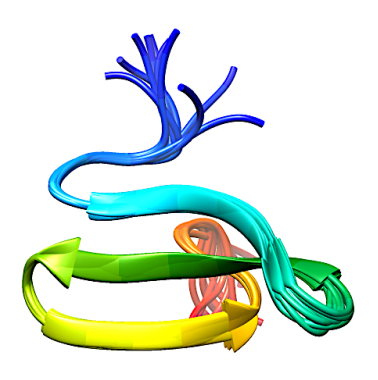


Figure 3.1 – WW domain prototype proposed by Macias *et al* via NMR experiments.^[112] Protein Data Bank ID: 1E0M.

3.2. Affinity Pair: Green Fluorescent Protein and A4C7

3.2.1. Green Fluorescent Protein

The GFP is composed by a β -barrel containing eleven strands that are neighbouring a central helix (see Figure 3.2). The GFP resembles a perfect cylinder that is 40 Å tall with a radius of 12.5 Å. [113] Inside this cylinder, in the central coaxial α -helix, there is a chromophore isolated from the solvent. [114] GFP's fluorescence does not depend on a cofactor or a substrate, only on the residues number 65 to 67 (Serine-Tyrosine-Glycine) that compose the chromophore.



Figure 3.2 – GFP structure proposed by Yang et al.[115] Protein Data Bank ID: 1GFL.

Studies on Green Fluorescent Protein go back to 1960 when Osamu Shimomura, Martin Chalfie and Roger Tsien started a ground-breaking work, worthy of a 2008 Nobel Prize in Chemistry, with *Aequorea victoria*, the jellyfish from where this 238 amino acid protein was first isolated.^[114,116] This is one of the most researched proteins because its fluorescence, high stability at pH 6-10 and at temperatures up to 65 °C^[117] and because of its possible applications^[53,117–121]. GFP is commonly used as protein tag to produce recombinant proteins^[122–124] because it is very robust, allows for easy detection of the protein of interest in a bulk cell suspension and gives information about the dynamic and association to other proteins.^[125,126]

In spite of a high demand of GFP in numerous applications, there was no specific mild and low-cost purification scheme of GFP-fusion proteins. So, our lab developed a small synthetic affinity ligand (A4C7) that can selectively recognize GFP and, consequently, could be employed to create a new and specific purification methodology.^[127]

3.2.2. A4C7: Small synthetic ligand for GFP purification

Biological, structural or synthetic affinity ligands towards a specific target (protein, peptides, cells, etc) can be designed by studying natural interactions between proteins and/or residues, using *in vitro* techniques such as phage, ribosome or yeast display and by applying combinatorial chemistry using screening and/or selection techniques.^[128,129] Our lab has already developed several affinity ligands for the purification of antibodies^[130], GFP-tagged proteins^[131] and albumin^[131].

Synthetic affinity ligands such as A4C7 are highly resistant to chemical and biological degradation, cheap, easily scalable and have low toxicity.^[127,129,132]

A4C7 is an Ugi-based ligand composed by an amine, 1-Pyrenemethylamine Hydrochloride (A4), and a carboxylic acid, Phenylacetic Acid (C7) (Figure 3.3). This small ligand presents a high binding percentage (93 %) due to the contribution of hydrophobic interactions and hydrogen-bond interactions. The affinity constant of A4C7 towards GFP is in the order of 10⁵ M⁻¹.[127]

Figure 3.3 - Chemical structure of A4C7.

3.2.3. Introducing Multivalency by Incorporating Multi-arm PEG Molecules

The availability of 2, 4 or 8-arm PEG molecules (Figure 3.4), allows for the creation of hydrogels with tunable properties. In theory, expanding the number of arms would originate stiffer hydrogels because the degree of cross-linking would be higher. However, by increasing the number of arms, the intermolecular aggregation increases as well. In conclusion, the number of arms can only be increased until a certain point before the degree of cross-linking decreases.^[133–135] This statement is supported by some studies that suggest that even though it is more advantageous to incorporate 4-arm PEG molecules in detriment of 2-arm PEG molecules, when comparing hydrogels formed with 4-arm PEG to hydrogels formed with 8-arm PEG, the first presents faster gelation time, a rougher surface and a more porous surface that can improve the swelling and water uptake.^[133,134] Moreover, hydrogels formed with 4-arm PEG molecules present higher

storage and loss moduli meaning these hydrogels are stronger and more deformable at the same time. [133]

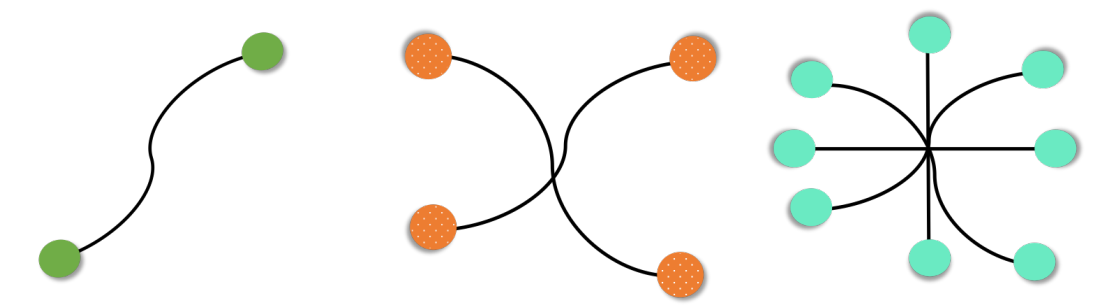


Figure 3.4 - Schematic representation of 2-arm PEG, 4-arm PEG and 8-arm PEG molecules.

3.3. Research Strategy

This chapter will focus on affinity-triggered hydrogels by exploring two different systems based on proteins/peptides and PEG. Peptide- or protein-based materials are highly attractive in the biomedical field due to the possibility of using proteins as building blocks to obtain a material with tunable proprieties and because of the non-toxicity of the degradation products.^[101] Moreover, PEG is a biocompatible polymer that is highly used to create systems

First, peptide-peptide interactions will be studied in which the proline rich peptide PPxY (KGEYPPYPPPSG) and mWW, a minimalist version of the WW domain (SMGLPPGWDEYKT) will be conjugated to an 8-arm PEG molecule and mixed together in iPSC medium to create an affinity triggered assembly (Figure 3.5) The multivalence will be obtained by the 8-arm PEG molecules conjugated with the proteins. This assembly will be characterized rheologically. The results presented in this section were included in the publication "Affinity-Triggered Assemblies Based on a Designed Peptide-Peptide Affinity Pair" [136], DOI: 10.1002/biot.201800559.

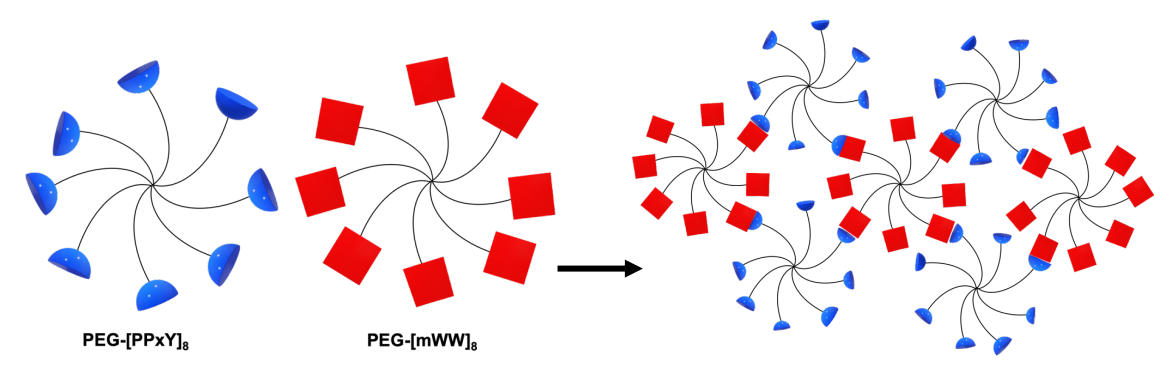


Figure 3.5 – Schematic representation of an affinity triggered assembly formed by PEG-[PPxY]₈ and PEG-[mWW]₈.

Legend: PEG-[PPxY]₈ – Peptide PPxY functionalized on an 8-arm PEG molecule; PEG-[mWW]₈ – Minimalist version of the WW peptide functionalized on an 8-arm PEG molecule.

Lastly, the interactions established between a synthetic ligand and a protein will be exploited to create hydrogels. The trigger will be the affinity of the GFP in tandem repeats (3 and 5)

and the synthetic ligand A4C7 functionalized in a 4-arm PEG molecule (Figure 3.6) creating a much more modular system in comparison to the previous one. In this case, the multivalence is granted by the tandem repeats and the multi-arm PEG molecules. Tandems of (3 and 5) GFP will be recombinantly expressed in a tandem fashion. The 3 and 5 repeats of GFP will be purified via immobilized metal affinity chromatography (IMAC), anion exchange and size-exclusion chromatography (SEC).

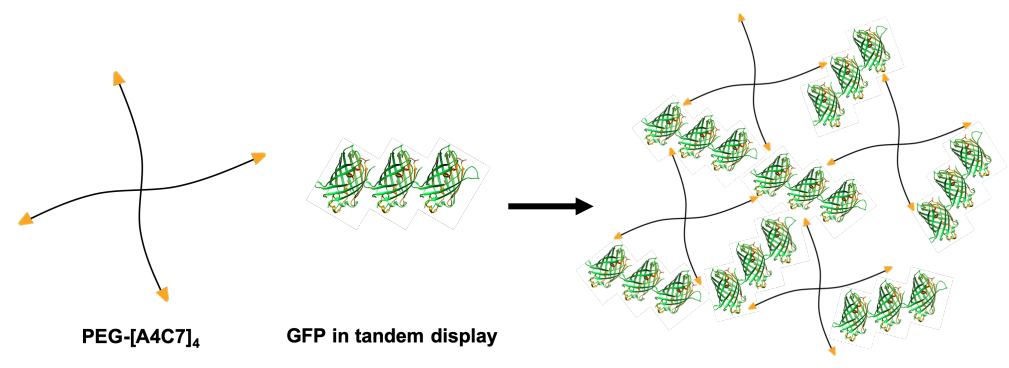


Figure 3.6 – Schematic representation of an affinity triggered assembly formed by PEG-[A4C7] $_4$ and GFP in tandem display.

Legend: PEG-[A4C7]₄ – Synthetic ligand A4C7 functionalized on a 4-arm PEG molecule.

3.4. Materials and Methods

3.4.1. Materials

3.4.1.1 Chemicals

NHS-terminated 8-arm PEG 20 kDa (SUNBRIGHT HGEO-200GS*) and maleimide terminated 8-arm PEG 20 kDa (SUNBRIGHT PTE-200MA) were purchased from NOF Europe (Frankfurt am Main, Germany).

Peptide PPxY (KGEYPPYPPPYPSG, 98% purity) was purchased from GeneCust (Boynes, France) or produced at the Department of Chemistry and Biochemistry of the Faculty of Sciences of the University of Porto, Portugal. The minimalist version of the peptide WW (SMGLPPGWDEYKT) was also produced at the Department of Chemistry and Biochemistry of the Faculty of Sciences of the University of Porto.

10% SDS solution (1610416), 30% Acrylamide/bis-acrylamide solution, 37.5:1 (1610158), Fixative Enhancer Concentrate (1610461), Image development reagent (1610464), Reduction moderator solution (1610463) and Silver Stain Plus Kit (1610449) were purchased from Bio-Rad (California, USA).

Tetramethylethylenediamine (23673), Ammonium persulphate (9592) was purchased from Carl Roth (Karlsruhe, Germany).

Methanol (10675112), Solution 1-StepTM TMB-Blotting Substrate (34018) and Pierce Clear Milk Blocking Buffer 10x (37587) was purchased from ThermoFisher Scientific (Massachusetts, USA).

Coomasie brilliant blue R-250 (27816), ethylenediamine tetraacetic acid (ED3SS-1), imidazole (I202), glycerol (G9012), sodium phosphate dibasic heptahydrate (431478) and sodium phosphate monobasic (S3522-2), were purchased from Sigma (Missouri, USA).

Acetic acid glacial (101830) and Tween20 detergent (655204) were purchased from Merck (Darmstadt, Germany).

LB Broth (MB02802), NZYTech Miniprep (MB010), GreenSafe Premium (MB132), NZY-DNA Loading Dye (MB131), agarose (MB05201), agar (MB02902), Tris Base (MB01601), ampicilin (MB02101), tetracycline (MB02202) and chloramphenicol (MB02402) were purchased to NZYTech (Lisbon, Portugal).

3.4.1.2 Biochemicals

iPSC medium TeSR2 Basal medium (05861) was purchased from StemCell Technologies (Grenoble, France).

The plasmid pET21b (69741-3) and BLR (DE3) cells were purchased to Merck (Darmstadt, Germany).

The Rosetta cells were kindly given by Dr. Inês Grilo from UCIBIO, Requimte.

NZYDNA III (MB04401) was purchased from NZYTech (Lisbon, Portugal).

Precision Plus Protein Dual Xtra prestained protein standard (1610377) was purchased from Bio-Rad (California, USA).

Anti-Mouse IgG (Whole Molecule) Peroxidase Conjugate (A 4416) was purchased to Sigma-Aldrich (Missouri, USA).

Anti-GFP rabbit IgG fraction (A11121) was purchased to Life Technologies (Paisley, UK).

3.4.1.3 Software

Chimera 1.13.1 program was used to render the structures of the WW domain and the structures of the GFP molecule. ChemDraw Professional 16 was resorted to draw the structure of the A4C7 molecule.

3.4.2. Methods

The reagents were weighted in a Sartorius AX423 scale (Max 420 g, d=1 mg) (Göettingen, Germany) or in a Mettler Toledo scale (Max 42 g, d=0.01 mg) (Ohio, USA) and calibration of pH was conducted with pHenomenal pH 1100L from VWR (Pennsylvania, USA).

The measurements of the fluorescence were performed in a TECAN Infinite F200 from Tecan Trading AG (Männedorf, Switzerland), using BRAND GMBH 96 U Bottom Black Polystyrene microplates from Sigma (Missouri, USA). Unless stated otherwise, the measurements in the visible spectra were also made in the TECAN Infinite F200 on 96-well transparent flat-bottom microplates from Sarstedt (Nümbrecht, Germany).

3.4.2.1 Functionalization of WW domain and PPxY domain

The minimalist version of the WW peptide was previously functionalized with the malei-mide-terminated 8-arm PEG (PEG-[Mal]₈) (PhD work from Cláudia Fernandes).

The PPxY peptide was dissolved in PBS pH 7.4. The N-hydroxysuccinimide-terminated 8-arm PEG (PEG-[NHS]₈) was also dissolved in PBS pH 7.4. The solutions were mixed with a molar ratio of 1:1. Afterwards, the mixture was left incubating for 16 hours with rotational agitation (22 rpm). The solution was then dialysed using a Spectra/Por 7 Dialysis Tubing against water. 24 hours later, the mixture was stored at -80 °C and lyophilized.

To determine the yield of PPxY functionalization on the NHS-terminated 8-arm PEG, the amount of peptide PPxY in the sample, before and after dialysis, was measured by recording the fluorescence intensity. The excitation wavelength was of 280 nm and the emission wavelength was of 340 nm and a gain of 41. The degree of functionalization was estimated to be 93 %.

For the controls used in the rheological characterization, PEG-[Mal]₈ was dissolved in PBS pH 7.4, left incubating for 16 hours with rotational agitation (22 rpm), dialysed using a Spectra/Por 7 Dialysis Tubing against water, stored at -80 °C and lyophilized. The same protocol was adopted for PEG-[NHS]₈.

3.4.2.2 <u>Formation of a Hydrogel Between the Functionalized WW and PPxY domains</u>

Both peptides functionalizated into the respective 8-arm PEG were individually dissolved in iPSC medium and mixed together with a 1:1 ratio, each contributing to 20 % of the total hydrogel volume. The pH of the mixture was set to 8-8.2 using a 1 M solution of NaOH. This hydrogel formed by the mixture of the minimalist version of the WW peptide functionalized on an 8-arm

PEG molecule and the peptide PPxY functionalized on an 8-arm PEG molecule will herein be referred to as the hydrogel in study.

PEG-[Mal]₈ and PEG-[NHS]₈ were also separately dissolved in iPSC medium and joined together with a 1:1 ratio, each contributing to 20 % of the total hydrogel volume. The pH of the mixture was set to 8-8.2 using a 1 M solution of NaOH. This mixture will be referred, in this section, as the negative control.

3.4.2.3 Rheological Studies

The hydrogel samples examined presented a total volume of 100 μ L. A HAAKE MARS III controlled stress rheometer with a temperature unit (Peltier element) set to 20 ±0.5 °C was used. Stress sweeps and frequency sweeps tests were performed using a cone-plate geometry with a diameter of 35 mm, cone angle of 2° and a gap of 0.125 mm.

3.4.2.4 <u>Isolate, Quantify and Evaluate the Integrity of Plasmid DNA of Bacterial Cells</u>

 $5~\mu L$ of transformed Rosetta cells with the plasmid pET21b carrying the gene of interest ([GFP-HS] $_5-5$ repeats of the GFP followed by the hydrophilic spacer complex) were added to 10 mL of Luria-Bertani (LB) medium containing 100 μg mL $^{-1}$ ampicillin and 30 μg mL $^{-1}$ chloramphenicol and incubated overnight at 37 °C with 200 rpm of orbital agitation.

The gene codifying for [GFP-HS]_x (x repeats of the GFP followed by the hydrophilic spacer complex) is cloned on the expression vector pET 21b (Figure 3.7).

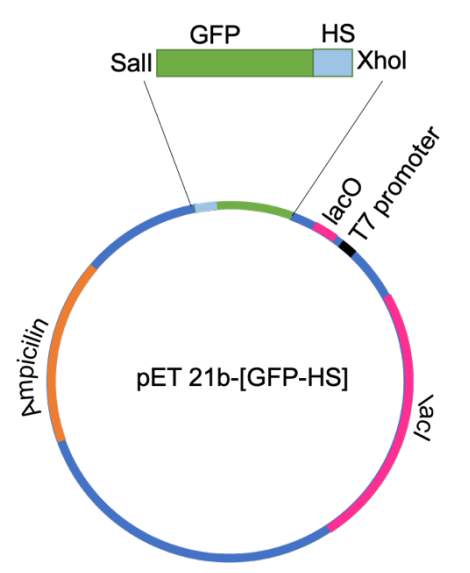


Figure 3.7 – Graphic representation of the plasmid carrying the [GFP-HS] gene.

The LB medium was prepared by dissolving 25 g of LB per litter of distilled water.

The DNA isolation procedure was performed with the NZYMiniPrep kit. The pre-inoculum was centrifuged in a VWR MicroStar12 centrifuge using the rotor GRF-m2.0-12.b (Pennsylvania, EUA) for 3 minutes at 11000 xg. Next, the supernadant was discharged. The pellet was then resuspended in 500 μ L of A1 buffer by vortexing. Following, 500 μ L of A2 buffer were added to the mixture and gently mixed. Then, it was left incubating for 4 minutes at room temperature. This

step was followed by the addition of 600 μ L of A3 buffer. Afterwards, the mixture was centrifuged for 10 minutes at 11000 xg and the pellet was discharged. The supernatant was introduced in a silica-based gel column and centrifuged for 2 minutes at 11000 xg. Subsequently, the flow-through was discharged. Afterwards, 500 μ L of previously heated AY buffer was added into the column followed by centrifugation of 2 minutes at 11000 xg. The flow-through was discharged, 600 μ L of A4 buffer were added and three cycles of centrifugation for 2 minutes at 11000 xg began intercalated by the discharged of the flow through. The elution process began by adding 30 μ L of previously heated autoclaved and deionized water followed by the introduction of the eppendorf containing the mix into the water bath Scanvac SHC200 (Lynge, Denmark) set at 42 °C for one minute. Afterwards, the samples were centrifuged for two minutes at 11000 xg. The product of the first elution was stored while the second elution took place. Finally, 50 μ L of of previously heated autoclaved and deionized water were added to the eppendorf and the samples were once again centrifuged for two minutes at 11000 xg.

The recovered DNA was quantified via Nanodrop 1000 from Thermo Scientific (Massachusetts, USA) and its purity and integrity were evaluated via an electrophoresis with an 0.8 % (w/v) agarose gel. This gel was prepared by dissolving pure grade agarose in TAE buffer (40 mM Tris Base, 20 mM glacial acetic acid and 1 mM ethylenediamine tetraacetic acid) and adding 3 μL of stain Green Safe Premium per 100 mL TAE buffer. The samples were prepared by diluting 4 μL of each plasmid in 2 μL of milliQ water and in 1 μL of loading dye, resulting in 7 μL loaded into the gel. 5 μL of the molecular marker NZYDNA Ladder III was directly applied into the gel. The agarose gel was casted and run in Mini-Sub Cell GT Systems from Bio-Rad (California, USA) with PowerPacTM Basic Power Supply (300V, 4.0A, 75W) from Bio-Rad (California, USA). The electrophoresis was run for 60 minutes at 100 V. Afterwards, the gel was revealed using Molecular Imager GelDocTM XR+ from Bio-Rad (California, USA) in a UV Transiluminator.

For [GFP-HS]₃ (3 repeats of the GFP followed by the hydrophilic spacer complex) the same protocol was implemented.

3.4.2.5 <u>Transformation of Competent Cells E. coli BLR (DE3) With the Plasmid pET-21B</u>

 $5~\mu L$ of the plasmid DNA of interest were added to $50~\mu L$ of competent *E. coli* BLR (DE3) cells and $1~\mu L$ of the control plasmid was added to $20~\mu L$ of competent cells. These solutions were left on ice for 30~minutes. The heat shock protocol began by introducing each of the solutions for 40~seconds into a 42~°C water bath, followed by 2~minutes on ice. Then, LB medium was added until the total volume of each solution was 1~mL. These mixtures were left for 1~minute hour at 37~°C with an orbital agitation of $225~rpm.50~\mu L$ and $150~\mu L$ of each mixture were added into different LB agar plates. The remaining volume was centrifuged at 1700~xg, the supernatant was discharged, the pellet was resuspended in LB medium and plated.

The LB agar medium was prepared by adding 15 g of agar and 25 g of LB per litter of distilled water. This mixture was autoclaved and 100 μ g mL⁻¹ of ampicillin and 12.5 μ g mL⁻¹ of tetracycline was then added.

3.4.2.6 Protein Expression

3.4.2.6.1 1 Litter of Culture Medium

Firstly, a pre-inoculum was performed with 6 mL of LB medium supplemented with 100 μ g mL⁻¹ ampicillin and 30 μ g mL⁻¹ chloramphenicol and with a single colony of competent *E. coli* Rosetta (DE3) cells harbouring a plasmid for the [GFP-HS]₅ for 6 hours at 37 °C and 225 rpm of orbital agitation on a IKA KS 4000 ic control VWR incubator (Radnor, Pennsylvania, USA). Afterwards, 1 mL of the pre-inoculum was used to inoculate overnight at 37 °C and 225 rpm of orbital agitation with 50 mL of the LB medium with 100 μ g mL⁻¹ ampicillin and 30 μ g mL⁻¹ chloramphenicol. Then, 50 mL of the previous inoculum was added to 1 L of LB medium with 100 μ g mL⁻¹ ampicillin and 30 μ g mL⁻¹ chloramphenicol and left with 200 rpm of orbital agitation at 37 °C until the optimal density at 600 nm (O.D.₆₀₀) reached 0.6-0.8. At this point, an aliquot was collected and 1mM of isopropyl β -D-1 thiogalactopyranoside (IPTG) was used to induce expression. The culture was then incubated at 30 °C with 200 rpm of orbital agitation. Every two hours until the 6 hours time point, aliquots were collected. After 22 hours of induction, a final aliquot was collected.

The cell expression from the moment before induction up until the 22 hours time point (time course) was evaluated via O.D.600 in an Evolution 201 UV-Visible spectrophotometer from Thermo Scientific (Massachusetts, USA), fluorescence spectroscopy and sodium dodecyl sulfate—polyacrylamide gel electrophoresis (SDS-PAGE) gels. The polyacrylamide gels were casted and run in Mini-Protean Tetra Cell System with PowerPacTM HC High Current Power Supply (250V, 3.0A, 300W) from Bio-Rad (California, USA). The gels were stirred in an Enduro Minimix orbital shaker from Labnet (New Jersey, USA) for staining and also revealed in the Molecular Imager GelDocTM XR+, Bio-Rad (California, USA).

For [GFP-HS] $_3$ expression the same protocol was implemented. For protein expression in BLR(DE3) cells, instead of chloramphenicol, 12.5 μ g mL $^{-1}$ of tetracycline was used.

3.4.2.6.2 2.5 Litter of Culture Medium

The protocol implemented was the same as the one used for the protein expression in 1 L of culture medium. However, the 50 mL inoculum was added to 2.5 L of LB medium supplemented with the antibiotics.

3.4.2.6.3 Cell Fractionation

After 22h protein expression, the cells were harvest by centrifugation in a HERAEUS Multifuge X3R centrifuge using the rotor Fibralite F14 - 6x250 LE from Thermo Scientific (Massachusetts, USA) for 15 minutes at 4 °C and 1500 rpm. The supernatant was discarded, and the pellet was resuspended in 20 mM sodium phosphate, 0.5 M NaCl pH 7. Afterwards, the suspension went through 3 cycles of freeze (-80 °C)/ thaw (room temperature). The suspension was stored at -20 °C until further use.

Then 10% of DNase I was added to the mix, and the sample was incubated on ice. 30 minutes later, the cells were disrupted in a French Press homogenizer from Thermo Scientific (Massachusetts, USA) for 3 cycles under 4000 psi. Then, the cells were centrifuged at 10 000 xg for 40 minutes at 4 °C. The resulting pellet was resuspended in 20 mM sodium phosphate, 0.5 M NaCl pH 7 and the supernatant was ultracentrifuged using a Beckman Optima LE-80 centrifuge using the rotor 45Ti (California, USA) at 204710 xg for 1 hour and 30 minutes at 4 °C. The pellet

was resuspended in 20 mM sodium phosphate, 0.5 M NaCl pH 7 and the supernatant was collected and stored at -20 °C.

The cell fractionation was assessed via fluorescence and SDS-PAGE gels.

3.4.2.7 Purification

For the purification, the AKTA avant 25 automated system GE Healthcare (Uppsala, Sweden) was used. The columns used for purification were the HisTrap FF 1mL, HiTrap Q HP 5 mL and the HiLoad 16/600 Superdex 75 prep grade column, all from GE Healthcare (Uppsala, Sweden).

To concentrate and/or to exchange buffer, Merck Amicon ultra centrifugal filters 10 kDa (UFC901024) from Merck (Darmstadt, Germany), Merck Amicon ultra-0.5 mL centrifugal filters 10 kDa (UFC501096) from Merck (Darmstadt, Germany) and Spectra/Por 7 Dialysis Tubing 50 kDa MWCO (10031954) from Spectrum (New Jersey, USA) were used. To dialyse the functionalization product of the peptides on the 8-arm PEG molecules, Spectra/Por 7 Dialysis Tubing 10 kDa MWCO (132120) from Spectrum (New Jersey, USA).

3.4.2.7.1 Immobilized Metal Affinity Chromatography

For IMAC a pre-packed 1 mL HisTrap FF column was used. The column was connected to the AKTA avant 25 system under the flow rate of 0.5 mL min⁻¹ and equilibrated (5 column volume – C.V. – of 10 mM sodium phosphate, 0.5 M NaCl pH 7.4) with a constant flow rate of 1 mL min⁻¹. The sample was loaded and the column was washed with 10 C.V. of 10 mM sodium phosphate, 0.5 M NaCl, pH 7.4. Then, the elution was performed by using a gradient elution with increasing concentration of imidazole until 0.5 M imidazole. Fractions of 1 mL were collected in a 96-deep well block. The sample content was evaluated through fluorescence and SDS-PAGE gels.

The column was regenerated by using 5 C.V. of milliQ water, 2 C.V. of 1 M NaCl followed by with 5 C.V. of milliQ water, 2 C.V. of 1 M NaOH followed by 5 C.V. of milliQ water. Finally, the column was equilibrated with 5 C.V. of 10 mM sodium phosphate, 0.5 M NaCl pH 7.4.

The column was stored at 4 °C after being equilibrated with 10 C.V. of milliQ water and 5 C.V. of ethanol 20 %.

3.4.2.7.2 Size-Exclusion Chromatography

Size-exclusion chromatography was performed using a HiLoad 16/600 Superdex 75 prep grade column. The column was connected to the AKTA avant 25 system under a 0.5 mL min⁻¹ flow rate and equilibrated with 1 C.V. of distilled water and 2 C.V. of PBS buffer pH 7.4 with a constant flow rate of 1 mL min⁻¹.

A sample of 1 mL was loaded on a 5 mL loop and the column was washed with 1.5 C.V. of PBS buffer pH 7.4 with a constant flow of 1 mL min⁻¹. Fractions of 1 mL were also collected in a 96-deep well block. Before storing the column at 4 °C, it was regenerated with 1.2 C.V. of 1 M NaCl and 2 C.V. of milliQ water. The column was left with 20% ethanol.

The sample content was evaluated through fluorescence and SDS-PAGE gels.

3.4.2.7.3 Anion Exchange Chromatography

For the anion exchange chromatography, a prepacked 5 mL HiTrap Q HP column from GE Healthcare was used. This column was connected to the AKTA avant 25 system under a 0.5 mL

min⁻¹ flowrate and equilibrated with 5 C.V. of 20 mM Tris-HCl pH 8 with a constant flow of 1 mL min⁻¹.

The sample was loaded on a 5 mL loop. A first washing step with 8 C.V. of 20 mM Tris-HCl pH 8 was performed. Afterwards, the elution was performed with a gradient of 20 mM Tris-HCl pH 8 to 20 mM Tris-HCl 0.5 M NaCl. This was followed by a final step with 20 mM Tris-HCl 0.5 M NaCl pH 8. Fractions of 1 mL were collected in a 96-deep well block. The sample content was evaluated through fluorescence and SDS-PAGE gels.

To store the column at 4 $^{\circ}$ C, it was first regenerated with 5 C.V. of distilled water and 3 C.V. of 20% ethanol.

3.4.2.7.4 SDS-PAGE Electrophoresis Analysis

Polyacrylamide gels of 12.5 % were prepared with a 30 % solution of acrylamide/Bis 37.5:1 to analyse the samples form time course, cell fractioning and purification. Two different method of sample preparation were used: One to evaluate the time course and another for the evaluation of fractioning and purification.

To evaluate the time course, the volume of the samples was dictated by the following equation:

Volume sample (mL) =
$$\frac{1.2}{0.D_{-600 \text{ nm}}}$$
 Equation 3.1

Each sample was centrifuged for 5 minutes at 5000 xg, the supernatant was discarded and the pellet was resuspended in 50 μ L of sample buffer. Afterwards, the samples were boiled for 10 minutes. Regarding the fractionation and purification samples, 5 μ L of each sample were dissolved in 5 μ L of sample buffer and boiled for 10 minutes.

The polyacrylamide gels were run for eighty minutes at a constant voltage of 120 V. Then, the SDS-PAGE gels were stained by either comassie blue staining or by silver staining. When the method of comassie blue staining was used, the gels were stained for 30 minutes with a Comassie Brilliant Blue solution and then distained with a solution comprising of 7.5 % acetic acid and 45 % methanol.

When the method for staining was silver staining, the Silver Stain Plus kit was used and the supplier instructions were followed.

Two polyacrylamide gels were run for two hours at a constant voltage of 80 V. One of the gels was stained with silver staining and the other one was used for Western-blotting.

A filter paper, a nitrocellulose membrane, the polyacrylamide gels and a filter paper were assembled by this order and assembled in a cassette. This cassette was placed on the electrophoresis tray with a chill unit (-20 $^{\circ}$ C). Cold transfer buffer (Tris 25 mM, Glycine 192 mM and 20 % methanol, pH 8.1-8.4) was deposited into the electrophoresis tray. Afterwards, the transfer occurred at 100 V for 1 hour.

The membrane was then blocked for one hour with 15 mL of milk in TBST (TBS with 0.05 % Tween 20) 1x at room temperature. Then, the membrane was washed twice with TBST for one minute at room temperature. Subsequently, the primary antibody Anti-GFP rabbit IgG fraction was diluted 1:2000 in TBST and then added to the membrane overnight at 4 °C with mild agitation. Posteriorly, the membrane was washed twice for one minute at room temperature. Then, the

membrane was incubated with mild agitation for one hour at room temperature with a solution comprising of the secondary antibody Anti-Mouse IgG diluted 1:2000 in TBST. The membrane was then washed three times with TBST for 10 minutes.

The method of detection utilized was the colorimetric method which consisted on adding 15 minutes of the 1-Step TMB-Blotting Substrate Solution until a blue colour was observed.

3.4.2.7.6 Fluorescence Intensity Quantification

To measure the fluorescence intensity, 200 μ L of each sample were pipetted into a 96-well black microplate and the fluorescence was measured in an infinite Tecan Microplate Reader. The excitation wavelength used was 485 nm and the emission wavelength used was 535 nm and the gain (41) was previously determined with a GFP calibration curve. Finally, the GFP concentration was determined by the following equation:

Sample fluorescence = $487016 \times [GFP - HS]_x + 279.24$ Equation 3.2

77

3.5 Results and Discussion

3.5.1 Affinity-triggered Assemblies Based on a Peptide-Peptide Affinity Pair

A minimalist version of the WW domain (SMGLPPGWDEYKT – Figure 3.8, in orange) was used to create a hydrogel triggered by the affinity of this pair towards the small peptide PPxY (KGEYPPYPPPYPSG). This minimalist version presents all of the amino acids required for the recognition of the PPxY domain, namely the two proline residues that are essential to establish interactions with the proline residues of the target molecule and, the aspartic acid and glutamic acid, necessary for the establishment of hydrogen bond interactions to the target due to their hydrophilic and charged character. [112]

The WW domain is hydrophobic and so, its biological production in the soluble form would be very difficult. By using this minimalist version, it is possible to synthetize the peptide by solid-phase peptide synthesis. This technique allows for the cheaper production of small peptides.^[137]

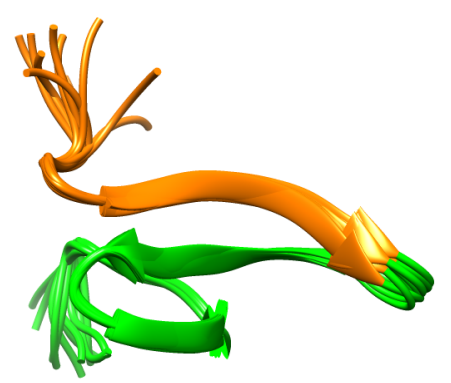


Figure 3.8 – WW domain prototype proposed by Macias *et al.*^[112] Protein Data Bank ID: 1E0M. In orange, the structure of the minimalist version of the WW peptide.

Even though a minimalist version of the peptide was used to produce affinity triggered hydrogels, its affinity constant towards the PPxY peptide is in the same order of magnitude in comparison to the full peptide (Table 3.1).

Table 3.1 – Comparison between the affinity constant of minimalist version and the full version of WW domain towards the PPxY domain.

WW domain	K _A (M ⁻¹)	Method K _A determination	Ref.
mWW	1.6x10 ⁵	Microscale thermophoresis	[136]
CC43	2.2x10 ⁵	Isothermal Titration Calorimetry	[36]
Nedd4.3	1.6x10 ⁴	Isothermal Titration Calorimetry	[36]

In terms of mechanical proprieties of the hydrogels triggered by the affinity between a WW domain and PPxY, the storage modulus is always low (Table 3.2). Furthermore, the G' and the G" are always very similar.[36,47,136]

From these examples, it is possible to conclude that for these systems, the introduction of multivalency to form the hydrogels by either multivalent polymers or by tandem proteins does not affect greatly the mechanical proprieties of the hydrogel.

Table 3.2 - Comparison of storage modulus between different affinity-triggered hydrogels compris-

ing of the pair WW and PPxY domains.

WW domain	PPxY	G ' (Pa)	Ref.
PEG-[mWW] ₈	PEG-[PPxY] ₈	20	[136]
Tandem Nedd4.3	Tandem	9	[36]
Tandem CC43	PEG-[PPxY] ₈	15	[47]

From the frequency sweep assays (Figure 3.9), the hydrogel in study is a viscoelastic liquid, as it is a mechanically weak assembly. Despite presenting a similar behaviour to the negative control, the hydrogel in study presents a tendency to have a more predominant elastic component. This proves the beneficial contribution of the affinity between the PPxY and the mWW on the material.

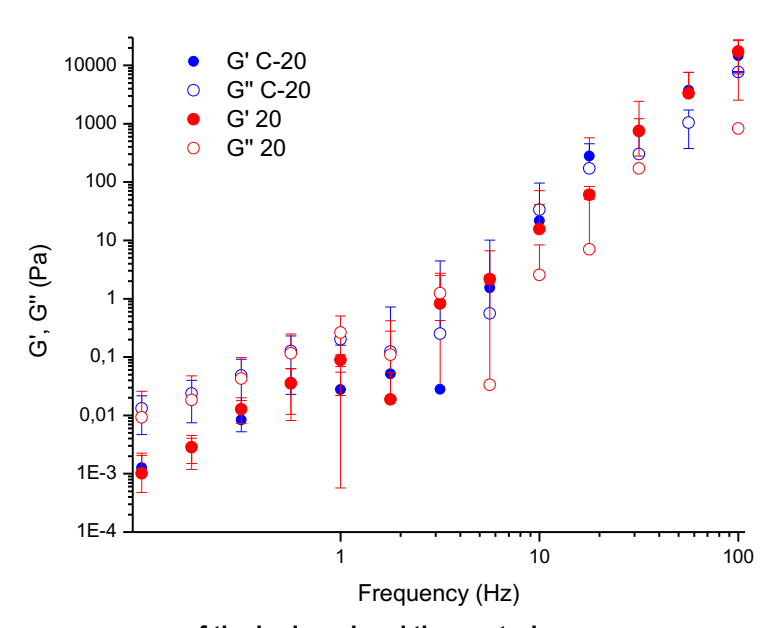


Figure 3.9 – Frequency sweeps of the hydrogel and the control. In blue, the storage modulus (G') and the loss modulus (G") of the control sample that is comprised of a mixture (20 % w/v - C-20) between PEG-[Mal]₈ and PEG-[NHS]₈. In red, the storage modulus (G') and the loss modulus (G") of the hydrogel formed by PEG-[mWW]8 and PEG-[PPxY]8. The close and open symbols represent the storage (G') and the loss (G") moduli, respectively.

The mechanical behaviour of the hydrogel in study shows a dependency of the frequency as an increase of the frequency leads to higher storage and loss moduli. Moreover, in higher frequencies, there is a shift on the behaviour and the storage modulus is increasingly higher in comparison to the loss modulus.

3.5.2 Affinity-triggered Assemblies Based on a Protein-synthetic ligand Affinity Pair

On this section, the aim is to express and purify multimeric GFP tandem proteins and to produce an affinity-triggered hydrogel based on the reported affinity between A4C7 and GFP. The two components of these hydrogels are: a multimeric GFP tandem protein and the synthetic ligand functionalized in a 4-arm PEG molecule. The multimeric protein was expressed in tandems of 3 and 5 GFP molecules to later analyse the difference of hydrogel formation and its proprieties caused by the difference of avidity between the different tandems and the ligand A4C7.

The final aim is to recombinantly produce protein-based biomaterial, by exploiting the affinity between the synthetic ligand A4C7 and GFP, as they are a promising and versatile class of materials.

The plasmid containing the gene of interest was grown overnight in Rosetta cells competent cells. Then, the plasmid DNA was extracted and isolated with the aid of a MiniPrep kit. The results obtained are shown on Table 3.3 and Figure 3.10.

Table 3.3 - Quantification and purity evaluation of the DNA extracted with the MiniPrep Kit.

	[DNA] (ng μL ⁻¹)	Abs ₂₆₀ /Abs ₂₈₀	Abs ₂₆₀ /Abs ₂₃₀
pET-[GFP-HS] ₃	41.8	1.81	2.1
ET IOED HOL	97.2	1.86	1.92
pET-[GFP-HS]₅	31.2	1.79	2.13

For pET 21b-[GFP-HS]₃, the values presented correspond to the second elution. For pET 21b-[GFP-HS]₅, the values on top correspond to the first elution and the ones on the bottom correspond to the second elution.

To assess the purity of the extracted DNA, absorbances at 260, 280 and 230 nm were read to detect the presence of protein contamination, contamination of aromatic moieties such as phenol and urea and to detect the presence of nucleic acids, respectively. [138] In the presence of pure plasmid DNA, the ratio Abs₂₆₀/Abs₂₈₀ should be between 1.8 and 2.0 and the ratio Abs₂₆₀/Abs₂₃₀ should be over 1.8. [139] Therefore, the extracted DNA presented good purity with very little contamination. In the case of the plasmid DNA of pET-[GFP-HS]₅, the second elution was chosen to proceed to the transformation because it presented higher Abs₂₆₀/Abs₂₃₀ ratio. On Table 3.3 and Figure 3.10 the first DNA elution of pET-[GFP-HS]₃ is not represented because this elution did not present enough volume to assess the quantification, purity and integrity.

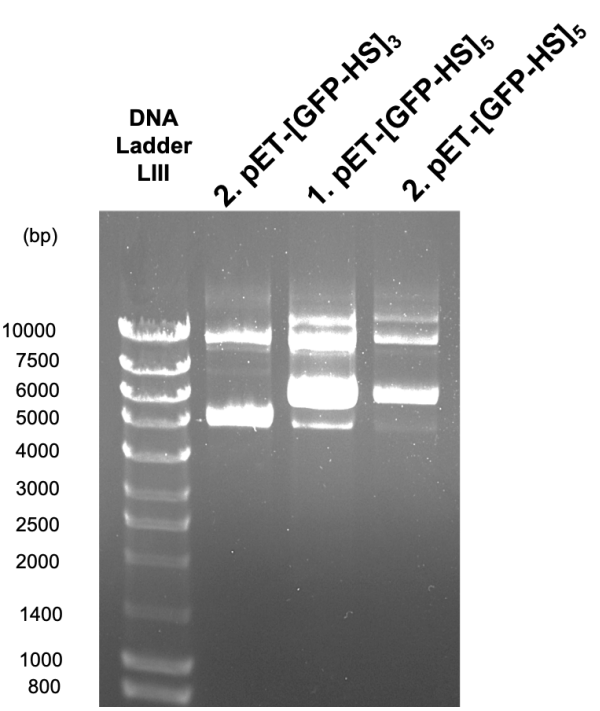


Figure 3.10 – Integrity evaluation of plasmid DNA.
Legend: 2. pET-[GFP-HS]₃ represents the second DNA elution, 1. pET-[GFP-HS]₅ and 2. pET-[GFP-HS]₅ represents the first and the second DNA elution, respectively.

From Figure 3.10, on the first and second elution of pET-[GFP-HS]₅, it is possible to distinguish the four forms of the plasmid: nicked, linear, supercoiled and circular (from top to bottom) being the most prominent band the one related to the supercoiled form and the least prominent the one demonstrating the circular form. In contrast, on the second DNA elution correspondent to pET-[GFP-HS]₃, it is only possible to distinguish the nicked, linear and the supercoiled forms of the plasmid (from top to bottom). In opposition to the band representing the linear band being very faint, the supercoiled one is very prominent.

3.5.2.1 Protein Expression

Bacterial recombinant protein expression is very advantageous because it is relatively inexpensive, the culture conditions are simple and easily scalable. [140] In opposition, one of the main disadvantages of using recombinant protein expression are the low yields (usually below 50 mg of protein per litter of expression). [1]

The proteins [GFP-HS]₃ and [GFP-HS]₅ (for the molecular weight of each tandem repeat, see Table 3.4) were expressed using two different *E. coli* strains (Rosetta (DE3) and BLR (DE3)) and in two different culture volumes (1 L and 2.5 L) using BLR (DE3) cells.

Table 3.4 – Molecular weight of the tandem GFP protein.

	Molecular weight (KDa)
[GFP-HS] ₁	32.13
[GFP-HS] ₂	60.47
[GFP-HS] ₃	88.81
[GFP-HS] ₄	117.27
[GFP-HS]₅	145.61

The estimated molecular weight was calculated by an online tool by Innovagen known as pepcalc^[141]. Legend: [GFP-HS]₁ - 1 repeat of the GFP followed by the hydrophilic spacer complex; [GFP-HS]₂ - 2 repeats of the GFP followed by the hydrophilic spacer complex; [GFP-HS]₃ - 3 repeats of the GFP followed by the hydrophilic spacer complex; [GFP-HS]₄ - 4 repeats of the GFP followed by the hydrophilic spacer complex; [GFP-HS]₅ - 5 repeats of the GFP followed by the hydrophilic spacer complex.

The Rosetta strain (characterized by Novagen) is used to improve protein expression as it supplies tRNAs for rare codons that are commonly not found in *E. coli*, allowing for an "universal" translation.^[142] As the goal is to express GFP in tandem which is a more complex protein than a single GFP molecule, this strain was preferred over the commonly used BL21 (DE3).

BLR (DE3) cells are *lon* and *ompT* deficient and carrying a chromosomal copy of the gene encoding for the T7 RNA polymerase under control of the lacUV5 promoter, like the Rosetta cells previously used. However, it also presents a *recA* delection, minimizing the recombination of long and repetitive DNA sequences and so it enables the expression of tandem sequences of the same protein.^[143–145]

3.5.2.1 Expression in Rosetta (DE3) Cells

The expression was carried out for 22 hours at 30 °C with 200 rpm of orbital agitation after being induced with 1 mM of IPTG when O.D._{600nm} reached 0.6-08. The expression conditions used of GFP (time and temperature of induction, concentration of IPTG and velocity of agitation) were optimized *in house*.

After induction, the expression was followed over 22 hours (Figure 3.11-a and Figure 3.11-b) by measuring the optical density at 600 nm (Figure 3.11-c and Figure 3.11-d). To assess if the protein of interest was being produced, the fluorescence was also measured (Figure 3.11-c and Figure 3.11-d).

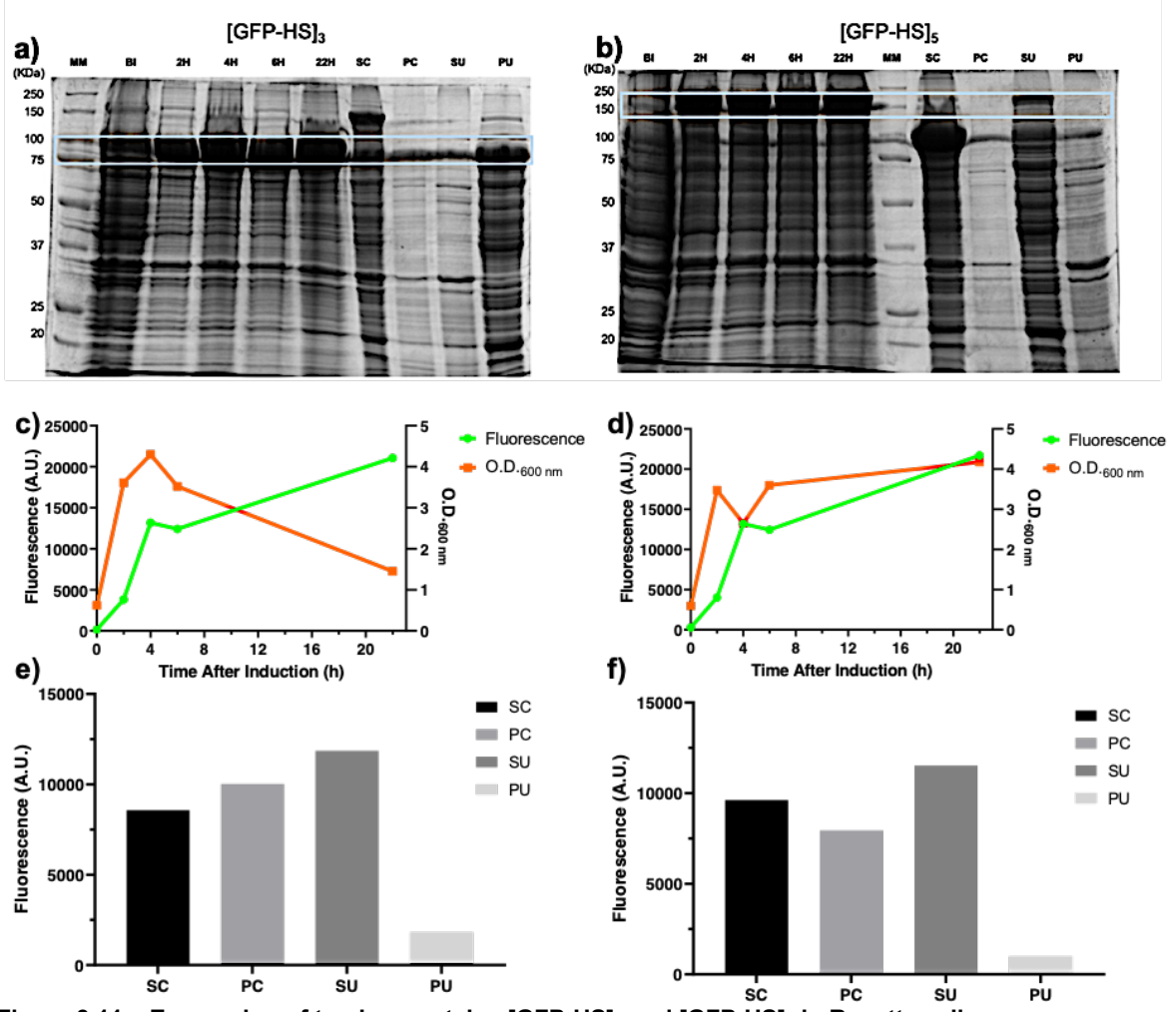


Figure 3.11 – Expression of tandem proteins [GFP-HS]₃ and [GFP-HS]₅ in Rosetta cells. SDS-PAGE gel of the fractions collected through expression (time course) and fractioning for [GFP-HS]₃ (a) and for [GFP-HS]₅ (b). Fluorescence intensity and O.D. $_{600nm}$ of fractions collected throughout expression for [GFP-HS]₃ (c) and for [GFP-HS]₅ (d). Fluorescence intensity of the protein of interest during the several fractioning stages for [GFP-HS]₃ (e) and for [GFP-HS]₅ (f). Both gels were stained with comassie blue staining.

Legend: MM - Molecular weight Marker; BI - Before Induction; 2h - 2 hours after induction; 4h - 4 hours after induction; 6h - 6 hours after induction; 22h - 22 hours after induction; 3C - Supernatant collected after the first Centrifugation; 3C - Supernatant collected after the Ultracentrifugation; 3C - Supernatant collected after the Ultracentrifugation; 3C - Supernatant collected after Ultracentrifugation.

It is possible to perceive, on the time course gels, that the protein [GFP-HS]₃ is being produced because of the presence of one intense band at 89 KDa is noted (Figure 3.11-a). Also, [GFP-HS]₅ is being expressed as confirmed by an intense band at 145 KDa (Figure 3.11-b). These statements are also established by an increase of the fluorescence registered during the expression for both proteins in tandem and without being displayed in tandem (Figure 3.11-c and Figure 3.11-d).

After cell fractionation, the samples were analysed by SDS-PAGE gels (Figure 3.11-a and Figure 3.11-b) and quantified by fluorescence measurements gels (Figure 3.11-e and Figure 3.11-f). As it can be seen on Figure 3.11, and on Table 3.5, a great amount of protein is produced on the soluble fraction after ultracentrifugation.

Table 3.5 – Concentration of GFP in tandem display on the various stages of fractioning.

	Supernatant af- ter the centrifu- gation	Pellet after the centrifugation	Supernatant af- ter the ultracen- trifugation	Pellet after the ultracentrifuga-
[GFP-HS] ₃	17.03	20.00	23.76	3.17
(µg mL ⁻¹)	17.03	20.00	23.70	3.17
[GFP-HS]₅	19.19	15.74	23.07	1.47
(µg mL ⁻¹)	19.19	15.74	25.07	1.47

It is important to mention the presence of two distinct bands between 25 and 37 KDa. It is possible that one of these bands can correspond to one repeat of the GFP with the hydrophilic spacer, whose molecular weight is 32.1 KDa (Table 3.3). This can be the indication of homologous recombination, probably due to the presence of the RecA protein. Even though this protein increases the stability of average plasmids, this recombinase can also instigate plasmids with numerous repeats to become unstable, causing a deletion in it. Afterwards, when the protein expression begins, instead of expressing the desired protein with tandem display, the end result is a protein with only one repeat. [146,147] The strategy to avoid these problems is to insert the plasmid into an *E. coli* strain with a *recA* mutation, such as the BLR (DE3) strain.

3.5.2.2 Expression in BLR (DE3) Cells

For the BLR (DE3) strain, two different culture volumes were used: 1 L and 2.5 L to test the efficiency of production and possible scale-up applications. After isolating the plasmid from the Rosetta cells, the competent BLR (DE3) cells were transformed with the plasmid of interest. Afterwards, the GFP tandem in pET21b was expressed according to the procedures described in the section 3.4.2.6 Protein Expression.

1 L of expression medium

When the O.D._{600nm} reached 0.6-0.8, the expression was induced using IPTG. Later, the expression was followed over 22 hours for [GFP-HS]₃ and 17 hours for [GFP-HS]₅ (Figure 3.12-a and Figure 3.12-b). Also, the optical density at 600 nm was measured (Figure 3.12-c and Figure 3.12-d) and, to assess if the protein of interest was being produced, the fluorescence was also measured (Figure 3.12-c and Figure 3.12-d).

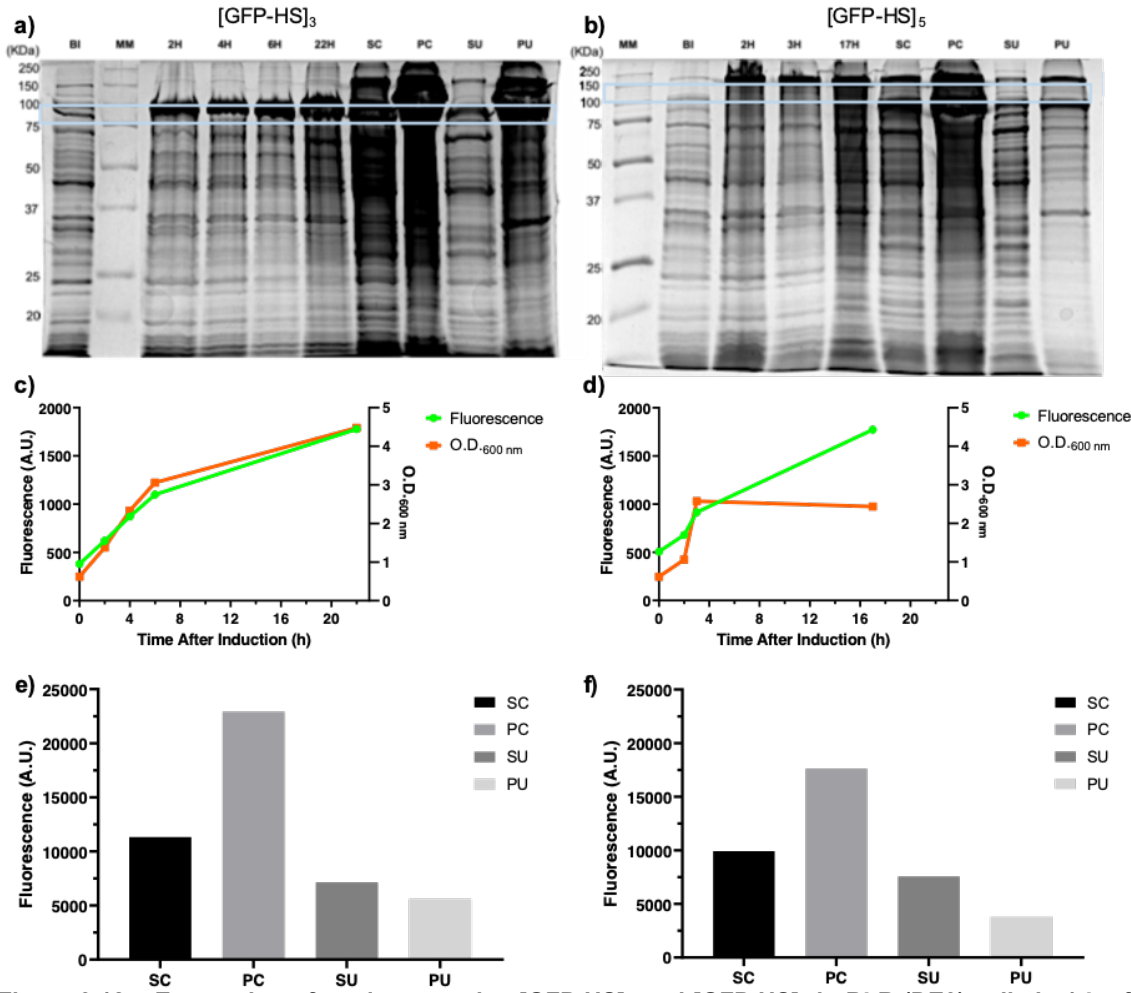


Figure 3.12 – Expression of tandem proteins [GFP-HS]₃ and [GFP-HS]₅ in BLR (DE3) cells in 1 L of culture volume.

SDS-PAGE gel of the fractions collected through expression (time course) and fractioning for [GFP-HS] $_3$ (a) and for [GFP-HS] $_5$ (b). Fluorescence intensity and O.D. $_{600nm}$ of fractions collected throughout expression for [GFP-HS] $_3$ (c) and for [GFP-HS] $_5$ (d). Fluorescence intensity of the protein of interest during the several fractioning stages for [GFP-HS] $_3$ (e) and for [GFP-HS] $_5$ (f). Both gels were stained with comassie blue staining. Legend: MM – Molecular weight Marker; BI – Before Induction; 2h-2 hours after induction; 4h-4 hours after induction; 6h-6 hours after induction; 22h-22 hours after induction; SC – Supernatant collected after the first Centrifugation; PC – Pellet collected after the first Centrifugation; PU – Pellet collected after Ultracentrifugation.

There is an intense band that marks the production of the desired proteins – 89 KDa for [GFP-HS]₃ (Figure 3.12-a) and 145 KDa for [GFP-HS]₅ (Figure 3.12-b). It appears that the band corresponding to [GFP-HS]₃ (Figure 3.12-a) is more intense than the band corresponding to [GFP-HS]₅ (Figure 3.12-b). There is also an increase of the measured fluorescence while the time after induction is progressing, indicating the production of proteins with fluorescence (protein in tandem repeats and protein without tandem repeats). (Figure 3.12-c and Figure 3.12-d). Once again, the two distinct bands between 25 and 37 KDa seen in Figure 3.11-a and Figure 3.11-b are also present, perhaps indicating the presence of GFP without being displayed in tandem fashion. Furthermore, on Figure 3.12-a, there is a very distinctive band at around 150 KDa which is the approximate molecular weight of [GFP-HS]₅, despite the protein being produced is [GFP-HS]₃.

After expression, cell harvest, mechanical lysis, the cells were fractionated, and aliquots were reserved to analyse the cell fractioning process by SDS-PAGE (Figure 3.12-a and Figure

3.12-b). The fluorescence was also measured (Figure 3.12-e and Figure 3.12-f). As it can be observed by the SDS-PAGE gels and on Table 3.6, the protein was mostly produced on the insoluble form. However, there was also protein production on the soluble form in which, 4 to 5 % was the protein of interest (Table 3.7). The fraction of the supernatant collected after the ultracentrifugation was the one that progressed for the purification (See section 3.5.2.2 Protein Purification).

Table 3.6 – Concentration of GFP in tandem display on the various stages of fractioning.

	Supernatant af- ter the centrifu- gation	Pellet after the centrifugation	Supernatant af- ter the ultracen- trifugation	Pellet after the ultracentrifuga-tion
[GFP-HS] ₃	22.67	46.48	14.07	10.90
(μg mL ⁻¹) [GFP-HS]₅	40.00			
(µg mL ⁻¹)	19.82	35.58	14.96	7.22

Table 3.7 - Percentage of the protein of interest expressed in the soluble form.

	[GFP-HS] _x	Total protein	% [GFP-HS] _x
	(µg mL ⁻¹)	(µg mL ⁻¹)	
[GFP-HS] ₃	14.07	264.1	4.11
[GFP-HS]₅	14.96	364.64	5.30

The expression in BLR (DE3) cells presents lower protein expression in the soluble form in comparison to the expression in Rosetta (DE3) cells. Moreover, when using BLR (DE3) cells, it seems that there is high production of protein in the insoluble form.

The insoluble form contains inclusion bodies (aggregates of expressed protein that present undefined hydrophobic interactions). A reason for the formation of these insoluble aggregates can be the hydrophobicity of the proteins being expressed. [148,149] As it is well known, the GFP is a hydrophobic protein [150] and the proteins that are being expressed might be equally or even more hydrophobic than the GFP protein alone. To decrease the hydrophobicity of the protein, a hydrophilic spacer ([AGAGAGPEG]₂) was introduced between the GFPs present in the tandems. This spacer was previously used by several other authors in previous studies. [36,47,57,151–153] It is possible that the hydrophilic spacer might not be enough to counterbalance the hydrophobicity of the whole molecule. It would be important to add buffers to control pH fluctuations during growth, and co-expression of chaperones to either prevent aggregation during the folding process or to assist in the solubilization of misfolded proteins. [154]

Since the majority of the protein is in the insoluble form, using either high concentration of denaturants and chaotropes such as guanidine hydrochloride or non-denaturing solubilization agents like DMSO would be interesting approaches to undertake in order to solubilize these aggregates.^[149]

2.5 L of expression medium

To assess the possibility of scaling up, both proteins of interest were expressed in 2.5 L of LB medium instead of 1 L. The conditions of temperature, concentration of IPTG and antibiotics were the same as when the expression occurred on one litter of LB. The expression was also followed by SDS-PAGE (Figure 3.13-a and Figure 3.13-b), and by measuring the optical density at 600 nm and the fluorescence (Figure 3.13-c and Figure 3.13-d).

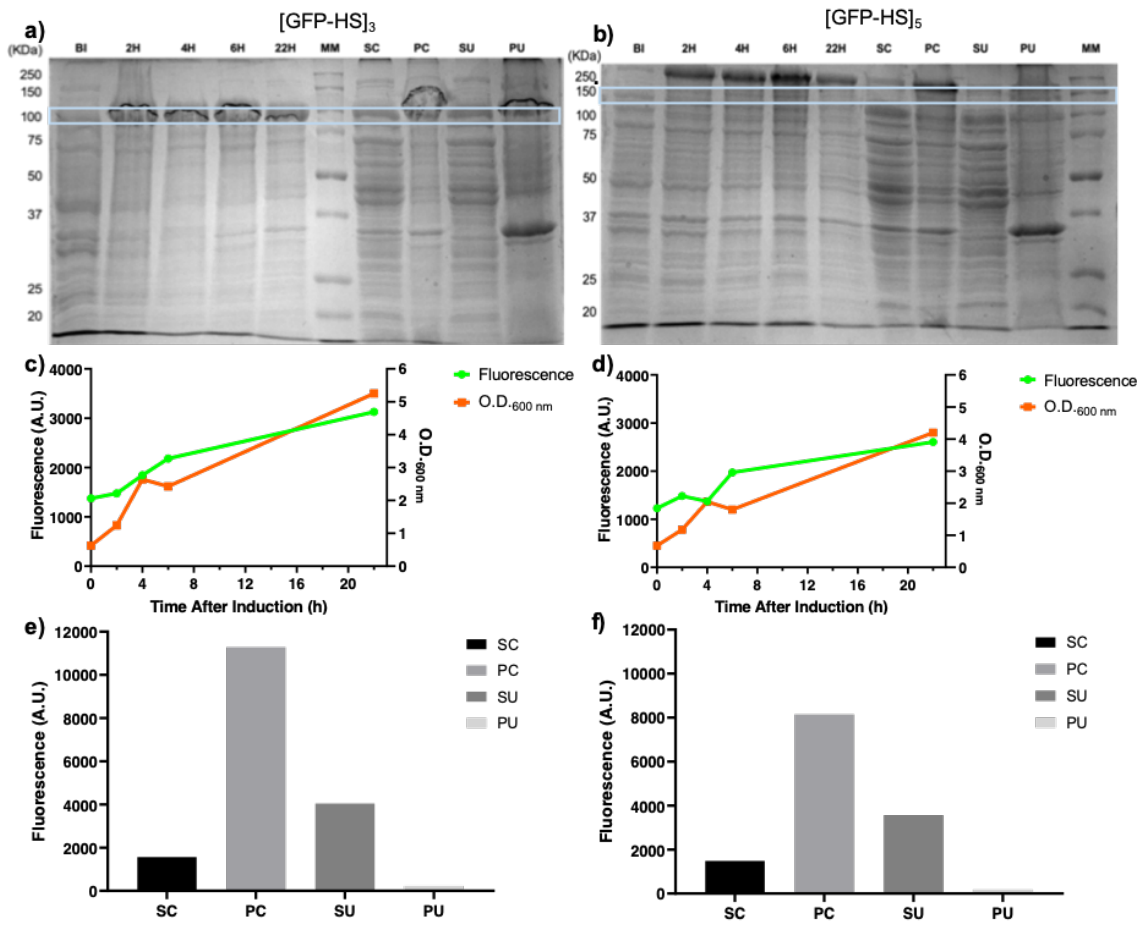


Figure 3.13 – Expression of tandem proteins [GFP-HS]₃ and [GFP-HS]₅ in BLR (DE3) cells in 2.5 L of culture volume

SDS-PAGE gel of the fractions collected through expression (time course) and fractioning for [GFP-HS] $_3$ (a) and for [GFP-HS] $_5$ (b). Fluorescence intensity and O.D. $_{600}$ of fractions collected throughout expression for [GFP-HS] $_3$ (c) and for [GFP-HS] $_5$ (d). Fluorescence intensity of the protein of interest during the several fractioning stages for [GFP-HS] $_3$ (e) and for [GFP-HS] $_5$ (f). Both gels were stained with comassie blue staining. Legend: MM – Molecular weight Marker; BI – Before Induction; 2h-2 hours after induction; 4h-4 hours after induction; 6h-6 hours after induction; 22h-22 hours after induction; 3h-4 hours after the first Centrifugation; 3h-4 hours after the first Centrifugation have 3h-4 hours after the first Centrifugati

By analysing the SDS-PAGE gels, it can be seen that protein with the desired molecular weight is being produced as there is an intense band at 89 KDa corresponding to [GFP-HS]₃ (Figure 3.13-1). Also, in Figure 3.13-b, it is possible to observe an intense band at 145 KDa that matches to the molecular weight of [GFP-HS]₅. Moreover, as it can be seen in Figure 3.13-c and Figure 3.13-d, the fluorescence is increasing along with the progression of the expression meaning that fluorescent proteins are being produced.

The two bands found between the molecular weight marker of 25 KDa and 37 KDa are also present but are more visible on the pellet collected after ultracentrifugation fraction.

On Table 3.8, the concentration of [GFP-HS]₃ and [GFP-HS]₅ on each fraction after cell lysis is represented. Analogous to the case of the expression on BLR (DE3) in 1 L of culture volume, the protein was expressed mostly on the insoluble fraction.

Table 3.8 – Concentration of GFP in tandem display on the various stages of fractionation.

	Supernatant af- ter the centrifu- gation	Pellet after the centrifugation	Supernatant af- ter the ultracen- trifugation	Pellet after the ultracentrifuga-tion
[GFP-HS]₃ (µg mL ⁻¹)	7.45	38.03	7.72	3.27
[GFP-HS] ₅ (µg mL ⁻¹)	7.05	27.3	6.75	2.52

Table 3.9 – Concentration of GFP in tandem display expressed using different strains and culture volumes.

	Concentration of the soluble fraction (μg mL ⁻¹)			
Strain	Rosetta (DE3) BLR (DE3)			
Culture volume	1 L	1 L	2.5 L	
[GFP-HS] ₃	23.76	14.07	7.45	
[GFP-HS]₅	23.07	14.96	7.05	

To sum up, concerning the expression of [GFP-HS]₃ and [GFP-HS]₅, on both Rosetta (DE3) and BLR (DE3) cells, homologous recombination appears to take place even though BLR (DE3) cells presents a *recA* delection. With BLR (DE3) cells it was expected that the protein would be mostly expressed in tandem however, a band that can possibly be representing [GFP-HS]₁ is very visible. It appears that the production of GFP in tandem over single GFP was favourable. This can be explained because GFP in tandem presents, in proportion, more hydrophobic residues than [GFP-HS]₁, forcing the cell to go through a higher metabolic burden when producing [GFP-HS]₃ and [GFP-HS]₅ in comparison to [GFP-HS]₁.

When the vehicle of expression was Rosetta (DE3) cells, most proteins went to the soluble fraction. In opposition, when BLR (DE3) cells were used, most protein was expressed on the insoluble fraction. This can be due to an increase of the energetic burden of the cell to express the proteins in a multimeric tandem fashion instead of only one monomer.

When testing different culture volumes, the most profitable one – regarding the concentration of protein expressed – was 1 L instead of 2.5 L (Table 3.9). Since the culture volume was lower, the quantity of cells was also lower. This could have led to a production of less protein but with the correct folding.

Finally, it would be important to perform a Western-blot with a primary antibody anti-GFP on the fractionation samples, to understand if the bands between the 25 and 37 KDa are GFP or another protein that is being produced at the same time as the multimeric GFP proteins.

3.5.2.2 Protein Purification

The fractions from the supernatant of the ultracentrifuge of the expression in Rosetta (DE3) and of the expression in BLR (DE3) were purified using different chromatography techniques.

The soluble fraction was purified via immobilized metal affinity chromatography, size-exclusion chromatography and anion exchange (Figure 3.14).

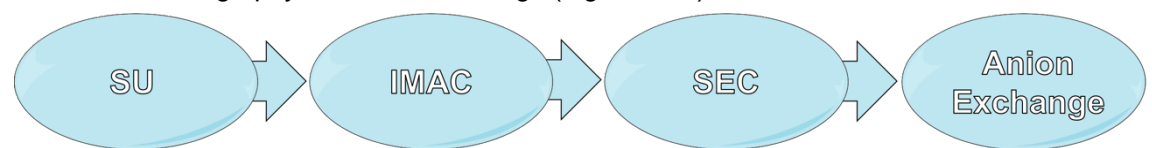


Figure 3.14 - Schematic of the purification steps of [GFP-HS]₃ crude extract.

Immobilized metal affinity chromatography was firstly introduced in 1975 by Porath^[155]. This is one of the most used chromatography systems to date. Because IMAC metal ion ligands interact with imidazole rings present on the Histidine residues present in his-tag, the protein of interest will bind to the column whilst other proteins will be washed away with the binding buffer. To elute the fraction of interest, a compound such as imidazole who can act like a metal ion ligand is used in excess.^[156]

The crude extract containing the soluble fraction of the [GFP-HS]₃ expression from BLR (DE3) was loaded in a 1 mL Histrap FF which is a prepacked column consisting on an agarose with an immobilized chelating ligand charged with nickel ions. See Figure 3.15 for the chromatogram representative of the metal affinity chromatography. 57 % of protein of interest bound to the columns and 71 % of the bounded protein was eluted.

The high absorbance values are indicative of the proteins that were not able to bind to the column, including proteins that present fluorescence. At 40 mL, the concentration of imidazole begins to increase gradually forcing the proteins that bound to the column to be eluted. At 55 mL, there is an absorbance and a fluorescence peak indicating that the protein of interest was eluted.

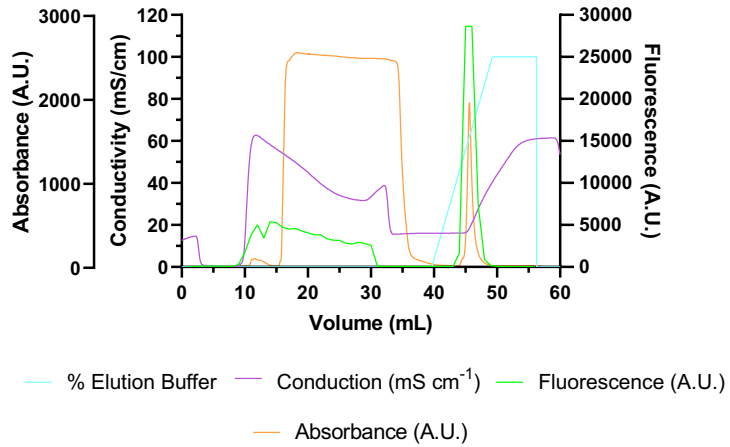


Figure 3.15 – Chromatogram of immobilized affinity chromatography of the $[GFP-HS]_3$ soluble fraction.

The samples that contained the eluted protein of interest were concentrated to a final volume of 1 mL and loaded into a 5 mL loop to be purified by size-exclusion chromatography. This

type of gel filtration chromatography consists on separating the proteins by size. Each column is composed by beads which have pores of different sizes. Proteins with higher molecular weight cannot enter all of the beads and will flow through the column much faster than smaller proteins. [157] The column used was a HiLoad Superdex 75 pg that can resolve proteins with a molecular weight ranging from 30 KDa to 70 KDa. As the molecular weight of both [GFP-HS]₃ and [GFP-HS]₅ is over 70 KDa, the proteins will be eluted in the void volume.

From the chromatogram in Figure 3.16, it is possible to observe that a major fraction of proteins were eluted between 50 and 55 mL, meaning that most of these proteins present a molecular weight over 70 KDa, like [GFP-HS]₃. Later, between 100 and 120 mL, other proteins that do not present fluorescence were eluted.

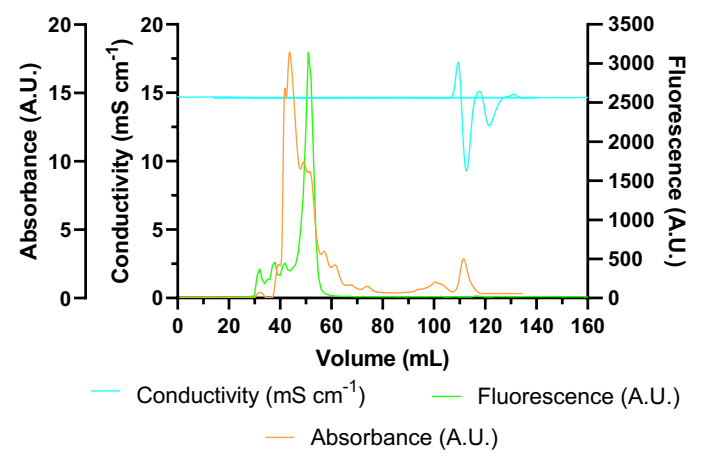


Figure 3.16 – Chromatogram of size-exclusion chromatography of the [GFP-HS]₃ soluble fraction from the expression in BLR (DE3) cells.

To confirm whether the proteins eluted between 40 and 55 mL were GFPs expressed in a tandem fashion, a Western-blot against anti-GFP was used.

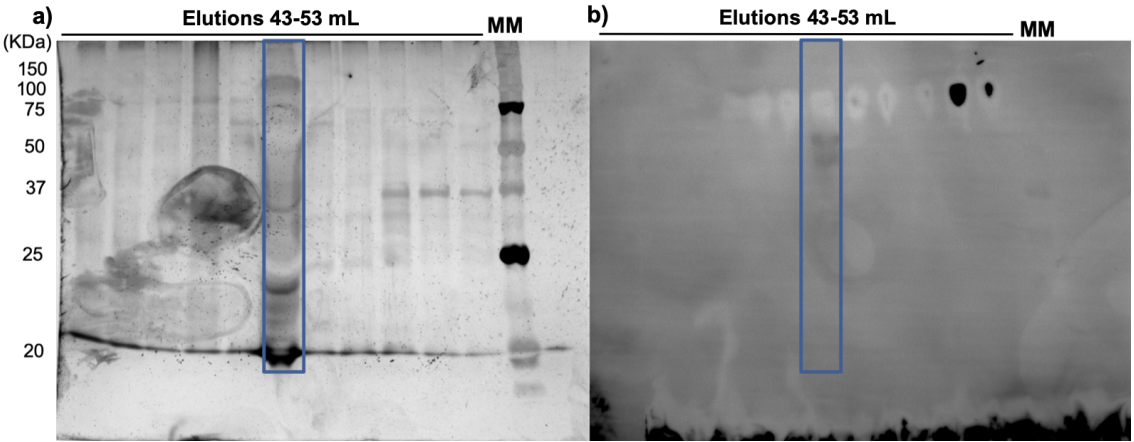


Figure 3.17 – Evaluation of the samples purified by size-exclusion.a) the SDS-PAGE gel of the samples eluted between 43 and 53 mL, b) the Western-blot using anti-GFP. The SDS-PAGE gel (12.5 %) was stained with silver staining.

Legend: MM – Molecular marker.

Figure 3.17 confirms the presence of GFPs expressed in a tandem fashion. However, as the molecular marker does not show up on the Western due to the washing steps, it is difficult to assess the molecular weight of the two bands.

Afterwards, the buffer of the sample highlighted by the blue box on Figure 3.17 was changed to Tris-HCl pH 8 and it was purified by anion exchange. This technique was used after the size-exclusion chromatography because there seems to be a difficulty in purifying the protein, so a different approach was tried to separate the GFP extract containing other proteins and other potential contaminates.

Anion exchange allows for the separation of proteins based on their charge. Negatively charged proteins will bind to the positively charged resin and will then be eluted by either increasing the salt concentration or by decreasing the pH.^[158] The column used is a 5 mL HiTrap Q HP which is a prepacked column consisting on a matrix that was functionalized with positively charged groups. The theoretical isoelectric points of each repeat are stated in Table 3.10. At pH 8, the protein of interest will be negatively charged, so the buffer chosen as the binding buffer was 20 mM Tris-HCl. To elute the proteins, a gradient of sodium chloride was used.

Table 3.10 - Molecular weight and isoelectric point of each tandem GFP protein.

	Molecular weight (KDa)	Isoelectric point
[GFP-HS]₁	32.131	5.67
[GFP-HS] ₂	60.473	5.53
[GFP-HS] ₃	88.814	5.46
[GFP-HS] ₄	117.270	5.4
[GFP-HS]₅	145.612	5.38

The estimated molecular weight and the isoelectric point was calculated by an online tool designed by Innovagen known as pepcalc^[141].

Legend: $[GFP-HS]_1 - 1$ repeat of the GFP followed by the hydrophilic spacer complex; $[GFP-HS]_2 - 2$ repeats of the GFP followed by the hydrophilic spacer complex; $[GFP-HS]_3 - 3$ repeats of the GFP followed by the hydrophilic spacer complex; $[GFP-HS]_4 - 4$ repeats of the GFP followed by the hydrophilic spacer complex; $[GFP-HS]_5 - 5$ repeats of the GFP followed by the hydrophilic spacer complex.

The sample was then loaded into a 5 mL loop, there seems that no contaminants were washed before the elution process began (Figure 3.18). Also, 100 % of the proteins that present fluorescence bound to the column.

After the concentration of NaCl began to rise, some contaminants were eluted and when the concentration reached 0.5 M (100%), the protein of interest was eluted.

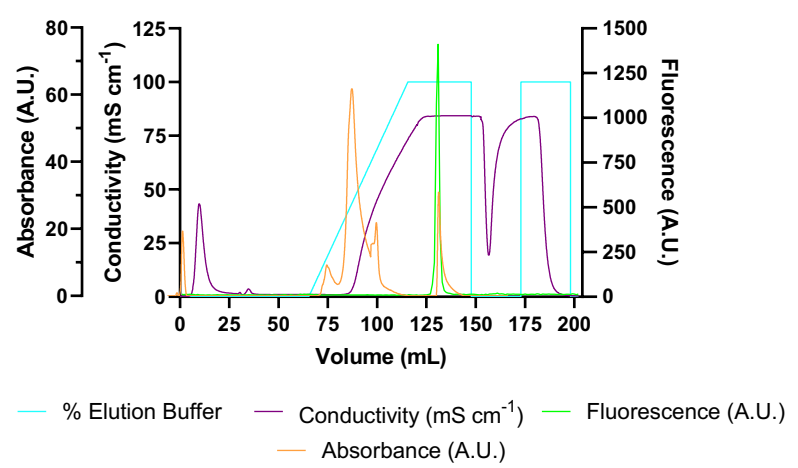


Figure 3.18 – Chromatogram of anion exchange chromatography of the [GFP-HS]₃ soluble fraction from the expression in BLR (DE3) cells.

Contrary to what was expected, the purification process was not efficient as there were still contaminants left and the fluorescent proteins were able to bound to the column. The protein of interest was eluted at 130 mL, approximately, and only 29 % of the protein with fluorescence loaded into the column was eluted. The protein of interest present in this final purification step is in very low concentrations when compared to the other contaminants (Figure 3.19).

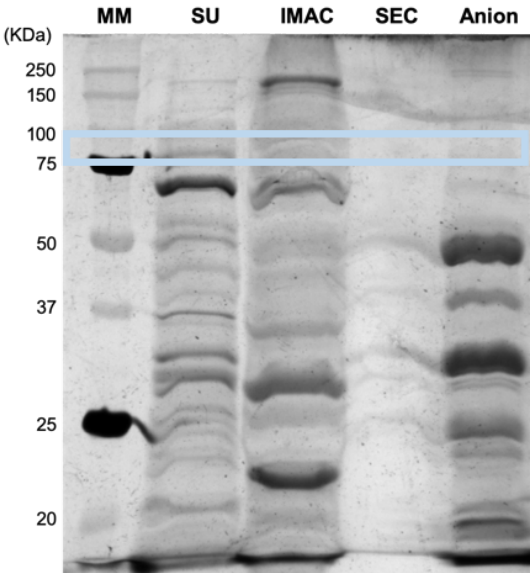


Figure 3.19 – Evaluation of the purification methods used for [GFP-HS]₃. The SDS-PAGE gel (12.5 %) was stained with silver staining.

Legend: MM – Molecular Marker, SU – Supernatant collected after the Ultracentrifugation; IMAC – Immobilized Metal Affinity Chromatography; SEC – Size-Exclusion Chromatography; Anion – Anion exchange chromatography.

3.5.2.2.2 [GFP-HS]₅

The soluble fraction was purified via immobilized metal affinity chromatography and size-exclusion chromatography (Figure 3.20).



Figure 3.20 - Schematic of the purification steps of [GFP-HS]₅ crude extract.

The soluble fraction from the ultracentrifuge was loaded into a 1 mL HisTrap FF and purified. In this case, there was also a great amount of unbound protein, even though 63 % of proteins with fluorescence bound to the column. After the elution process with a gradient of imidazole began, the protein of interest was eluted on 53-58 mL as proven by the fluorescence and the absorbance peaks (see Figure 3.21). Here, 61 % of the bounded fluorescent protein was eluted.

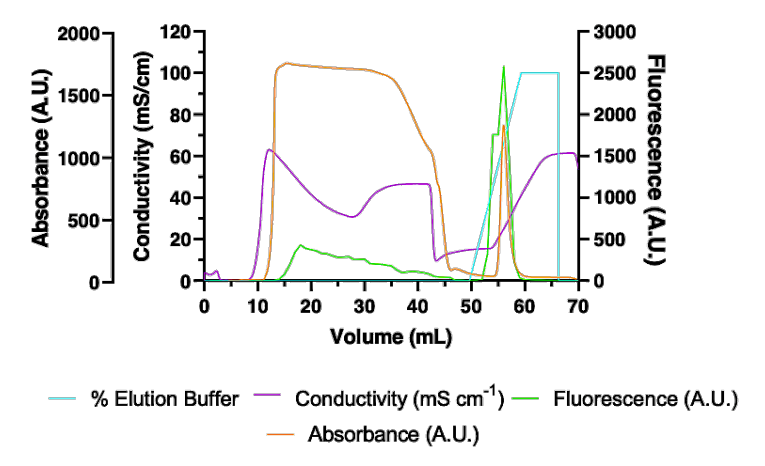


Figure 3.21 – Chromatogram of size-exclusion chromatography of the [GFP-HS] $_5$ soluble fraction from the expression in BLR (DE3) cells.

Then, the fractions of interest were concentrated to 1 mL and loaded into a 5 mL loop to be purified by SEC (Figure 3.22).

The chromatogram shows multiple absorbance peaks between 30 and 60 mL and the protein of interest was eluted at 50 mL.

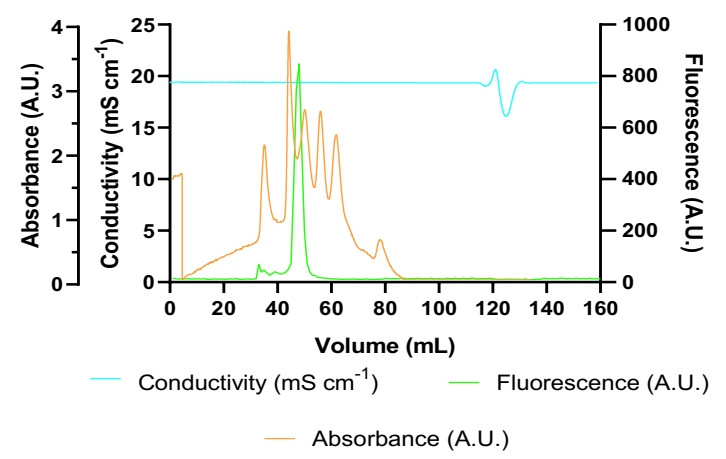


Figure 3.22 – Chromatogram of size-exclusion chromatography of the [GFP-HS]₅ soluble fraction from the expression in BLR (DE3) cells.

Once again, as proven by Figure 3.23, the protein was not pure after the purification steps.

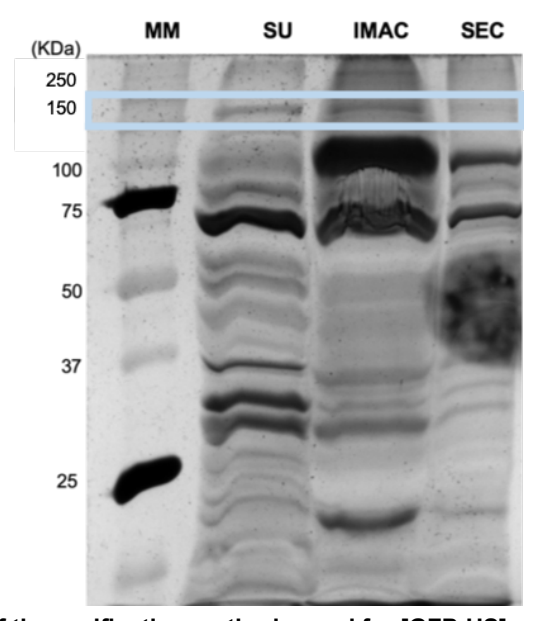


Figure 3.23 – Evaluation of the purification methods used for [GFP-HS]₅. The SDS-PAGE gel (12.5 %) was stained with silver staining.

Legend: MM – Molecular Marker, SU – Supernatant collected after the Ultracentrifugation; IMAC – Immobilized Metal Affinity Chromatography; SEC – Size-Exclusion Chromatography.

To sum up, the purification of the soluble fractions of [GFP-HS]₃ and [GFP-HS]₅ by using the steps of IMAC, SEC and anion exchange chromatography (for the [GFP-HS]₃ extract) still require optimization as most of the protein of interest is lost during the purification process (Table 3.11) and, in the final purification steps, it still contains many impurities.

Table 3.11 – Yield associated with each purification step.

	Yield (%)		
Purification Step	[GFP-HS]₃	[GFP-HS]₅	
IMAC	39.9	33.6	
SEC	39.3	10.2	
Anion exchange	19.7	-	

3.6 Conclusions

On this chapter, the main goal was to study two affinity pairs to form affinity-triggered hydrogels. The peptides and the proteins used in this work were produced in two different ways. The minimalistic version of the WW domain and the PPxY domain were obtained by chemical syntehsis (outsourced to a specialised company). The multimeric GFP proteins (3 and 5 repeats in tandem) were produced by recombinant expression in bacterial cells.

Whilst chemical synthesis is more suitable for the production of peptides, production of proteins with higher molecular weight is more manageable on cells using a recombinant DNA-based system. [137] Nonetheless, recombinant protein expression systems, specially of repeating units of a hydrophobic protein, has several challenges, namely the formation of inclusion bodies, low expression yields, protein inactivity and difficulty in purifying the crude extract. This is a process that needs extensive and thorough optimization. [140] In this work, two of these challenges were faced.

For the first time, a minimalist version of the WW domain was explored to study the effect of its affinity towards a proline-rich peptide in a polymer-polymer system. [136] The multivalency was achieved by conjugating both peptides PPxY and mWW into 8-arm PEG molecules instead of resorting to multiple repeats of the peptide. By mixing PPxY and mWW functionalized to the 8-arm PEG molecules, an assembly with weak mechanical proprieties was obtained. In the future, materials based on the assembly of this peptide-peptide affinity pair could be used for drug delivery and cell encapsulation for cell and tissue engineering.

When comparing the hydrogels formed between PEG-[mWW]₈ and PEG-[PPxY]₈ and the hydrogels that would be formed between [GFP-HS]₃ or [GFP-HS]₅ and A4C7, it would be expected that the last system (tandem proteins combined with a multimeric polymer functionalized with the proteins affinity pair) would present a larger storage modulus because this arrangement, in contrast to the first system, is a modular system and so, the flexibility of the affinity pairs to connect in different points is higher allowing for the hydrophobic interactions to be established more freely without any additional stereochemical hindrance.



CONCLUSIONS AND FUTURE PERSPECTIVES

4. Conclusions and Future Perspectives

This work aimed to explore PEG-based hydrogels using innovative methods based on chemical and physical interactions.

In the first chapter, it is reported for the first time, PEG-based chemically cross-linked hydrogels via the Ugi condensation reaction. These gels present stiff networks with a G' varying from 9794.4±382.2 Pa to 1519.9±98.4 Pa, depending on the chemistry of the compounds incorporated into the network. In the future, other hydrogels will also be formed using isocyanides that possess aromatic rings, such as phenyl isocyanide. Moreover, the electric conductance of these hydrogels will be measured.

Since the gelation kinetics was preferred over the stiffness of the hydrogels, the incorporation of the different carboxylic acids, aldehydes and isocyanides was made with a 10 % concentration of polymer instead of 5 % which provided networks ~120 % stiffer. So, it is important to study the incorporation of the different compounds when the concentration of PEG is 5 % to determine if the stiffness of the hydrogels can be further tuned. Also, the swelling behaviour of these hydrogels will also be studied in order to be employed as real-time biosensors.

In this work, two different applications were thought for the Ugi hydrogels: 1) Introducing molecules with aromatic rings to implement a conductive system into the hydrogel; 2) Incorporating molecules to create an antimicrobial system. There has always been an increasing search for conductor/semiconductor materials that are easy to fabricate and to tune. [159] Hence electroconductive hydrogels are being designed where the hydrogel network presents conducting polymer chains. Potentially, the introduction of aromatic compounds into the structure of the hydrogel can generate an electron and proton conductive system, especially since carboxylic acids and amino groups (hydrogen donating and accepting groups) are also present in the gel network. [160–163] Despite the lack of antimicrobial activity observed in our preliminary results, the Ugi hydrogels appear to promote cell adhesion despite the fact that PEG itself is an antifouling agent. [164] This feature can be further explored to, eventually, develop a system for biofilm washing.

In the second chapter, affinity triggered physically cross-linked hydrogels were explored in which the affinity pairs were displayed in different multivalent configurations: the first affinity pair was conjugated to 8-arm PEG and one of the binding participants of the second affinity pair was also conjugated to a 4-arm PEG while the remaining one was displayed in tandem. The binding of the first affinity pair (mWW and PPxY) originated a new soft affinity-triggered assembly (G' 20 Pa).

Regarding the second affinity pair (GFP and A4C7), GFP in tandem display of 3 and 5 repeats was recombinantly expressed and purified. If I was able to successfully express the protein of interest in high yields and purify the soluble fractions, a gel of 100 µL, 10 % (w/v) would be

made. The fluorescence of the GFP, would be a great asset for creating hydrogels to be applied as drug delivery systems because it would allow the medical specialist to quantitively assess the delivery of the therapy to a certain region in order to tune the treatment in function of the progression of the patient's health. ^[165,166]					

Bibliography

- [1] M. Guvendiren, H. D. Lu, J. A. Burdick, Soft Matter **2012**, *8*, 260–272.
- [2] E. Caló, V. V. Khutoryanskiy, Eur. Polym. J. 2015, 65, 252–267.
- [3] G. M. Raghavendra, R. Sadiku, M. M. Yallapu, T. Jayaramudu, K. Varaprasad, *Mater. Sci. Eng. C* **2017**, 79, 958–971.
- [4] B. O. Okesola, A. Mata, Chem. Soc. Rev. 2018, 47, 3721–3736.
- [5] O. Wichterle, D. Lím, Nature 1960, 185, 117-118.
- [6] I. Gibas, H. Janik, Chem. Technol. 2010, 4, 297–304.
- [7] S. J. Buwalda, K. W. M. Boere, P. J. Dijkstra, J. Feijen, T. Vermonden, W. E. Hennink, *J. Control. Release* **2014**, *190*, 254–273.
- [8] J. Kopecek, D. Lím, J. Polym. Sci. Part A-1 Polym. Chem. 1971, 9, 147–154.
- [9] R. W. Korsmeyer, N. A. Peppas, J. Memb. Sci. 1981, 9, 211–227.
- [10] R. M. Nalbandian, R. L. Henry, H. S. Wilks, J. Biomed. Mater. Res. 1972, 6, 583–590.
- [11] Y. Ye, X. Hu, J. Nanomater. 2016, 2016, 1–8.
- [12] K. Ishihara, M. Kobayashi, N. Ishimaru, I. Shinohara, *Polym. J.* **1984**, *16*, 625–631.
- [13] P. Jing, J. S. Rudra, A. B. Herr, J. H. Collier, *Biomacromolecules* **2008**, 9, 2438–2446.
- [14] G. L. Fiore, J. L. Klinkenberg, A. Pfister, C. L. Fraser, Biomacromolecules 2009, 10, 128– 133.
- [15] S. J. Buwalda, L. Calucci, C. Forte, P. J. Dijkstra, J. Feijen, *Polymer (Guildf)*. 2012, 53, 2809–2817.
- [16] M. Ebara, Y. Kotsuchibashi, K. Uto, T. Aoyagi, Y.-J. Kim, R. Narain, N. Idota, J. M. Hoffman, in *Science (80-.).*, Springer Japan, **2014**, pp. 9–65.
- [17] E. M. Ahmed, J. Adv. Res. 2015, 6, 105–121.
- [18] A. S. Hoffman, Adv. Drug Deliv. Rev. 2002, 54, 3–12.
- [19] H. A. Essawy, M. B. M. Ghazy, F. A. El-Hai, M. F. Mohamed, *Int. J. Biol. Macromol.* **2016**, 89, 144–151.
- [20] H. Bu, A.-L. Kjøniksen, K. D. Knudsen, B. Nyström, Biomacromolecules 2004, 1470–1479.
- [21] R. Kishi, H. Ichijo, O. Hirasa, J. Intell. Mater. Syst. Struct. 1993, 4, 533–537.
- [22] T. H. Tran, H. Okabe, Y. Hidaka, K. Hara, Carbohydr. Polym. 2017, 157, 335–343.
- [23] J. Wang, J. Wei, Appl. Surf. Sci. 2016, 382, 202–216.
- [24] Q. S. Zhao, Q. X. Ji, K. Xing, X. Y. Li, C. S. Liu, X. G. Chen, *Carbohydr. Polym.* **2009**, 76, 410–416.
- [25] D. C. Tuncaboylu, M. Sari, W. Oppermann, O. Okay, *Macromolecules* **2011**, *44*, 4997–5005.
- [26] M. Kimura, K. Fukumoto, J. Watanabe, K. Ishihara, *J. Biomater. Sci. Polym. Ed.* **2004**, *15*, 631–644.

- [27] Y. S. Zhang, A. Khademhosseini, *Science* (80-.). **2017**, 356, eaaf3627.
- [28] L. Zhang, E. M. Furst, K. L. Kiick, J. Control. Release 2006, 114, 130–142.
- [29] I. Ghidoni, T. Chlapanidas, M. Bucco, F. Crovato, M. Marazzi, D. Vigo, M. L. Torre, M. Faustini, *Cytotechnology* **2008**, *58*, 49–56.
- [30] F. Lim, A. Sun, Science (80-.). 1980, 210, 908–910.
- [31] B. Jeong, Y. K. Choi, Y. H. Bae, G. Zentner, S. W. Kim, J. Control. Release 1999, 62, 109–114.
- [32] B. Jeong, Y. H. Bae, D. S. Lee, S. W. Kim, *Nature* **1997**, 388, 860–862.
- [33] J. Huang, C. L. Hastings, G. P. Duffy, H. M. Kelly, J. Raeburn, D. J. Adams, A. Heise, *Biomacromolecules* **2013**, *14*, 200–206.
- [34] Y.-L. Chiu, S.-C. Chen, C.-J. Su, C.-W. Hsiao, Y.-M. Chen, H.-L. Chen, H.-W. Sung, *Biomaterials* **2009**, *30*, 4877–4888.
- [35] S. Toledano, R. J. Williams, V. Jayawarna, R. V. Ulijn, J. Am. Chem. Soc. 2006, 128, 1070–1071.
- [36] C. T. S. Wong Po Foo, J. S. Lee, W. Mulyasasmita, A. Parisi-Amon, S. C. Heilshorn, Proc. Natl. Acad. Sci. 2009, 106, 22067–22072.
- [37] U.-J. Kim, J. Park, C. Li, H.-J. Jin, R. Valluzzi, D. L. Kaplan, *Biomacromolecules* **2004**, *5*, 786–792.
- [38] R. V Ulijn, N. Bibi, V. Jayawarna, P. D. Thornton, S. J. Todd, R. J. Mart, A. M. Smith, J. E. Gough, *Mater. Today* **2007**, *10*, 40–48.
- [39] A. M. Jonker, D. W. P. M. Löwik, J. C. M. van Hest, Chem. Mater. 2012, 24, 759–773.
- [40] J. L. Mann, A. C. Yu, G. Agmon, E. A. Appel, *Biomater. Sci.* **2018**, 6, 10–37.
- [41] T. Nolan, N. Singh, C. R. McCurdy, in *Methods Mol. Biol.* (Ed.: A.C.A. Roque), Humana Press, Totowa, NJ, **2010**, pp. 13–29.
- [42] T. Miyata, N. Asami, T. Uragami, *Nature* **1999**, 399, 766–769.
- [43] A. A. Obaidat, K. Park, *Biomaterials* **1997**, *18*, 801–806.
- [44] A. A. Obaidat, K. Park, *Pharm. Res.* **1996**, *13*, 989–995.
- [45] M. Ehrbar, R. Schoenmakers, E. H. Christen, M. Fussenegger, W. Weber, *Nat. Mater.* **2008**, 7, 800–804.
- [46] M. S. Thompson, M. V. Tsurkan, K. Chwalek, M. Bornhauser, M. Schlierf, C. Werner, Y. Zhang, *Chem. A Eur. J.* **2015**, *21*, 3178–3182.
- [47] W. Mulyasasmita, L. Cai, R. E. Dewi, A. Jha, S. D. Ullmann, R. H. Luong, N. F. Huang, S. C. Heilshorn, *J. Control. Release* **2014**, *191*, 71–81.
- [48] Y. N., K. K.L., Biomacromolecules 2005, 6, 1921–1930.
- [49] C. Fasting, C. A. Schalley, M. Weber, O. Seitz, S. Hecht, B. Koksch, J. Dernedde, C. Graf, E.-W. Knapp, R. Haag, *Angew. Chemie Int. Ed.* **2012**, *51*, 10472–10498.
- [50] D. Guan, M. Ramirez, L. Shao, D. Jacobsen, I. Barrera, J. Lutkenhaus, Z. Chen, *Biomacromolecules* **2013**, *14*, 2909–2916.
- [51] F. Ito, K. Usui, D. Kawahara, A. Suenaga, T. Maki, S. Kidoaki, H. Suzuki, M. Taiji, M. Itoh, Y. Hayashizaki, et al., *Biomaterials* **2010**, *31*, 58–66.
- [52] J. Wang, J. Zhang, X. Zhang, H. Zhou, *PLoS One* **2013**, *8*, 1–6.
- [53] S. H. Mejias, D. Romera, A. L. Cortajarena, A. Aires, P. Couleaud, *Biochem. Soc. Trans.* **2015**, *43*, 825–831.
- [54] R. L. DiMarco, S. C. Heilshorn, *Adv. Mater.* **2012**, *24*, 3923–3940.

- [55] M. B. Charati, J. L. Ifkovits, J. A. Burdick, J. G. Linhardt, K. L. Kiick, Soft Matter 2009, 5, 3412.
- [56] J. Zhu, *Biomaterials* **2010**, *31*, 4639–4656.
- [57] L. Cai, R. E. Dewi, S. C. Heilshorn, Adv. Funct. Mater. 2015, 25, 1344–1351.
- [58] A. A. D'souza, R. Shegokar, Expert Opin. Drug Deliv. 2016, 13, 1257–1275.
- [59] C.-C. Lin, K. S. Anseth, Pharm. Res. 2009, 26, 631-643.
- [60] N. A. Peppas, J. Z. Hilt, A. Khademhosseini, R. Langer, Adv. Mater. 2006, 18, 1345–1360.
- [61] J. Zhu, Biomaterials **2010**, 31, 4639–4656.
- [62] E. Bakaic, N. M. B. Smeets, T. Hoare, RSC Adv. 2015, 5, 35469–35486.
- [63] L. J. Macdougall, V. X. Truong, A. P. Dove, ACS Macro Lett. 2017, 6, 93–97.
- [64] A. Singh, J. Elisseeff, J. Mater. Chem. 2010, 20, 8832–8847.
- [65] L. Tao, C. S. Kaddis, R. R. Qgorzalek Loo, G. N. Grover, J. A. Loo, H. D. Maynard, Macromolecules 2009, 42, 8028–8033.
- [66] C. M. Dundas, D. Demonte, S. Park, Appl. Microbiol. Biotechnol. 2013, 97, 9343–9353.
- [67] A. Llevot, A. C. Boukis, S. Oelmann, K. Wetzel, M. A. R. Meier, *Top. Curr. Chem.* 2017, 375, 66.
- [68] I. Ugi, R. Meyr, U. Fetzer, C. Steinbrückner, Angew. Chemie 1959, 71, 373–388.
- [69] S. Marcaccini, T. Torroba, Nat. Protoc. 2007, 2, 632.
- [70] M. Goebel, I. Ugi, Synthesis (Stuttg). 1991, 1991, 1095–1098.
- [71] A. E. J. de Nooy, G. Masci, V. Crescenzi, *Macromolecules* **1999**, *32*, 1318–1320.
- [72] P. Cristau, J.-P. Vors, J. Zhu, Org. Lett. 2001, 3, 4079–4082.
- [73] T. Ngouansavanh, J. Zhu, *Angew. Chemie Int. Ed.* **2007**, *46*, 5775–5778.
- [74] N. Azizi, S. Dezfooli, M. M. Hashemi, Comptes Rendus Chim. 2013, 16, 1098–1102.
- [75] A. Madej, D. Paprocki, D. Koszelewski, A. Żądło-Dobrowolska, A. Brzozowska, P. Walde, R. Ostaszewski, *RSC Adv.* **2017**, *7*, 33344–33354.
- [76] D. Lee, J. K. Sello, S. L. Schreiber, Org. Lett. 2000, 2, 709–712.
- [77] P. Xu, W. Lin, X. Zou, Synthesis (Stuttg). 2002, 2002, 1017–1026.
- [78] J.-C. Bradley, K. Baig Mirza, T. Osborne, A. Wiliams, K. Owens, *J. Vis. Exp.* **2008**, DOI 10.3791/942.
- [79] P. Chacko, K. Shivashankar, *Chinese Chem. Lett.* **2017**, 28, 1619–1624.
- [80] Í. L. Batalha, A. C. A. Roque, J. Chromatogr. B **2016**, 1031, 86–93.
- [81] M. Passerini, Gazz. Chim. Ital 1921, 51, 181–189.
- [82] M. Passerini, L. Simone, Gazz. Chim. Ital 1921, 51, 126-129.
- [83] A. Sehlinger, M. A. R. Meier, in *Adv. Comput. Simul. Approaches Soft Matter Sci. I*, **2014**, pp. 61–86.
- [84] A. E. J. de Nooy, D. Capitani, G. Masci, V. Crescenzi, *Biomacromolecules* **2000**, *1*, 259–267.
- [85] V. Crescenzi, A. Francescangeli, D. Capitani, L. Mannina, D. Renier, D. Bellini, *Carbohydr. Polym.* **2003**, *53*, 311–316.
- [86] B. Werner, H. Bu, A. L. Kjøniksen, S. A. Sande, B. Nyström, *Polym. Bull.* 2006, 56, 579–589.

- [87] V. Crescenzi, A. Francescangeli, A. L. Segre, D. Capitani, L. Mannina, D. Renier, D. Bellini, *Macromol. Biosci.* **2002**, *2*, 272–279.
- [88] M. A. Mironov, I. D. Shulepov, V. S. Ponomarev, V. A. Bakulev, *Colloid Polym. Sci.* 2013, 291, 1683–1691.
- [89] I. D. Shulepov, K. V. Kozhikhova, Y. S. Panfilova, M. N. Ivantsova, M. A. Mironov, *Cellulose* **2016**, 23, 2549–2559.
- [90] K. P. Menard, N. Menard, in *Encycl. Anal. Chem.*, John Wiley & Sons, Ltd, Chichester, UK, **2017**, pp. 1–25.
- [91] S. M. Stark, S. P. Rowland, J. Appl. Polym. Sci. 1966, 10, 1777–1786.
- [92] K. Nakamae, T. Nishino, K. Kato, T. Miyata, A. S. Hoffman, *J. Biomater. Sci. Polym. Ed.* **2004**, *15*, 1435–1446.
- [93] H. Bu, A. L. Kjøniksen, B. Nyström, Eur. Polym. J. 2005, 41, 1708–1717.
- [94] K. Sung, C. C. Chen, *Tetrahedron Lett.* **2001**, *42*, 4845–4848.
- [95] D. C. Schoenmakers, A. E. Rowan, P. H. J. Kouwer, Nat. Commun. 2018, 9, 2172.
- [96] B. Jeong, D. S. Lee, J. I. Shon, Y. H. Bae, S. W. Kim, J. Polym. Sci. Part A Polym. Chem. 1999, 37, 751–760.
- [97] G. T. Hermanson, in *Bioconjugate Tech.*, Elsevier, **2013**, pp. 229–258.
- [98] A. S. Pina, Í. L. Batalha, C. S. M. Fernandes, M. A. Aoki, A. C. A. Roque, *Water Res.* **2014**, 66, 160–168.
- [99] X. Chen, M. Zhang, C. Zhou, N. R. Kallenbach, D. Ren, Appl. Environ. Microbiol. 2011, 77, 4878–4885.
- [100] K. W. Kolewe, J. Zhu, N. R. Mako, S. S. Nonnenmann, J. D. Schiffman, ACS Appl. Mater. Interfaces 2018, 10, 2275–2281.
- [101] D. Sengupta, S. C. Heilshorn, Tissue Eng. Part B Rev. 2010, 16, 285–293.
- [102] P. Bork, M. Sudol, Trends Biochem. Sci. 1994, 19, 531–533.
- [103] H. I. Chen, M. Sudol, Proc. Natl. Acad. Sci. 1995, 92, 7819–7823.
- [104] O. Staub, D. Rotin, Structure **1996**, 4, 495–499.
- [105] M. J. Macias, M. Hyvönen, E. Baraldi, J. Schultz, M. Sudol, M. Saraste, H. Oschkinat, Nature 1996, 382, 646–649.
- [106] M. Sudol, P. Bork, A. Einbond, K. Kastury, T. Druck, M. Negrini, K. Huebner, D. Lehman, J. Biol. Chem. 1995, 270, 14733–14741.
- [107] M. J. Macias, S. Wiesner, M. Sudol, FEBS Lett. 2002, 513, 30-37.
- [108] C. Montespan, C. M. Wiethoff, H. Wodrich, J. Virol. 2017, 91, 1–20.
- [109] C. B. McDonald, S. K. N. McIntosh, D. C. Mikles, V. Bhat, B. J. Deegan, K. L. Seldeen, A. M. Saeed, L. Buffa, M. Sudol, Z. Nawaz, et al., *Biochemistry* 2011, 50, 9616–9627.
- [110] H. Wodrich, D. Henaff, B. Jammart, C. Segura-Morales, S. Seelmeir, O. Coux, Z. Ruzsics, C. M. Wiethoff, E. J. Kremer, *PLoS Pathog.* **2010**, *6*, DOI 10.1371/journal.ppat.1000808.
- [111] Y. Kato, K. Nagata, M. Takahashi, L. Lian, J. J. Herrero, M. Sudol, M. Tanokura, J. Biol. Chem. 2004, 279, 31833–31841.
- [112] M. J. Macias, V. Gervais, C. Civera, H. Oschkinat, Nat. Am. 2000, 7, 375–379.
- [113] S. J. Remington, Protein Sci. 2011, 20, 1509–1519.
- [114] T. D. Craggs, Chem. Soc. Rev. 2009, 38, 2865–2875.
- [115] Y. Fan, L. G. Moss, G. N. P. Jr, Nat. Biotechnol. 1996, 14, 303-308.

- [116] O. Shimomura, F. H. Johnson, Y. Saiga, J. Cell. Comp. Physiol. 1962, 59, 223–239.
- [117] R. Y. Tsien, Annu. Rev. Biochem. 1998, 67, 509-44.
- [118] P. P. Chapagain, C. K. Regmi, W. Castillo, J. Chem. Phys. 2011, 135, 0-6.
- [119] M. J. J. Moreau, I. Morin, P. M. Schaeffer, Mol. Biosyst. 2010, 6, 1285–1292.
- [120] M. R. Abedi, G. Caponigro, A. Kamb, Nucleic Acids Res. 1998, 26, 623-630.
- [121] E. R. G. Main, J. J. Phillips, C. Millership, Biochem. Soc. Trans. 2013, 41, 1152–1158.
- [122] M. Maniak, R. Rauchenberger, R. Albrecht, J. Murphy, G. Gerisch, Cell 1995, 83, 915–924.
- [123] T. Hazelrigg, J. H. Mansfield, Methods Biochem. Anal. 2005, 47, 227–257.
- [124] S. Stretton, S. Techkarnjanaruk, A. M. McLennan, A. E. Goodman, *Appl. Environ. Microbiol.* **1998**, *64*, 2554–9.
- [125] E. Snapp, Curr. Protoc. Cell Biol. 2005, 27, 21.4.1-21.4.13.
- [126] W. W. Ward, in *Methods Biochem. Anal.*, **2005**, pp. 39–65.
- [127] A. S. Pina, A. M. G. C. Dias, F. I. Ustok, G. El Khoury, C. S. M. Fernandes, R. J. F. Branco, C. R. Lowe, A. C. A. Roque, J. Chromatogr. A 2015, 1418, 83–93.
- [128] A. S. Pina, C. R. Lowe, A. C. A. Roque, Biotechnol. Adv. 2014, 32, 366–381.
- [129] M. Linhult, S. Gulich, S. Hober, Protein Pept. Lett. 2005, 12, 305–310.
- [130] S. D. F. Santana, V. L. Dhadge, A. C. A. Roque, ACS Appl. Mater. Interfaces 2012, 4, 5907–5914.
- [131] A. S. Pina, S. Carvalho, A. M. G. C. Dias, M. Guilherme, A. S. Pereira, L. T. Caraça, A. S. Coroadinha, C. R. Lowe, A. C. A. Roque, *J. Chromatogr. A* **2016**, *1472*, 55–65.
- [132] R. dos Santos, C. Figueiredo, A. C. Viecinski, A. S. Pina, A. J. M. Barbosa, A. C. A. Roque, J. Chromatogr. A 2019, 1583, 88–97.
- [133] H. H. Lin, Y. L. Cheng, *Macromolecules* **2001**, *34*, 3710–3715.
- [134] H. Tan, A. J. DeFail, J. P. Rubin, C. R. Chu, K. G. Marra, J. Biomed. Mater. Res. Part A 2010, 92, 979–987.
- [135] L. J. Macdougall, M. M. Pérez-Madrigal, M. C. Arno, A. P. Dove, *Biomacromolecules* 2018, 19, 1378–1388.
- [136] C. S. M. Fernandes, A. S. Pina, A. J. Moura Barbosa, I. Padrão, F. Duarte, C. A. S. Teixeira, V. Alves, P. Gomes, T. G. Fernandes, A. M. G. Carvalho Dias, et al., *Biotechnol. J.* 2019, 1800559.
- [137] F. Guzman, S. Barberis, A. Illanes, Electron. J. Biotechnol. 2007, 10, 279-314.
- [138] S. R. Gallagher, P. R. Desjardins, in Curr. Protoc. Protein Sci., John Wiley & Sons, Inc., Hoboken, NJ, USA, 2008, p. A.4K.1-A.4K.21.
- [139] J. Sambrook, D. W. Russell, Molecular Cloning: A Laboratory Manual, 2001.
- [140] G. L. Rosano, E. A. Ceccarelli, Front. Microbiol. 2014, 5, 1–17.
- [141] S. Lear, S. L. Cobb, J. Comput. Aided. Mol. Des. 2016, 30, 271–277.
- [142] S. E. Bane, J. E. Velasquez, A. S. Robinson, *Protein Expr. Purif.* **2007**, *52*, 348–355.
- [143] F. W. Studier, B. A. Moffatt, J. Mol. Biol. 1986, 189, 113–130.
- [144] M. Schmidt, L. Römer, M. Strehle, T. Scheibel, Biotechnol. Lett. 2007, 29, 1741–1744.
- [145] D. C. Chow, M. R. Dreher, K. Trabbic-Carlson, A. Chilkoti, Biotechnol. Prog. 2006, 22, 638–646.

- [146] A. I. Roca, M. M. Cox, S. L. Brenner, Crit. Rev. Biochem. Mol. Biol. 1990, 25, 415–456.
- [147] M. M. Cox, *BioEssays* **1993**, *15*, 617–623.
- [148] A. Mitraki, B. Fane, C. Haase-Pettingell, J. Sturtevant, J. King, Science (80-.). 1991, 253, 54–58.
- [149] A. Singh, V. Upadhyay, A. K. Upadhyay, S. M. Singh, A. K. Panda, *Microb. Cell Fact.* **2015**, *14*, 1–10.
- [150] H. Umakoshi, M. Nishida, K. Suga, H. T. Bui, T. Shimanouchi, R. Kuboi, Solvent Extr. Res. Dev. 2009, 16, 145–150.
- [151] A. Parisi-Amon, W. Mulyasasmita, C. Chung, S. C. Heilshorn, *Adv. Healthc. Mater.* **2013**, 2, 428–432.
- [152] W. Mulyasasmita, L. Cai, Y. Hori, S. C. Heilshorn, Tissue Eng. Part A 2014, 20, 2102–2114.
- [153] M. Greenwood-Goodwin, E. S. Teasley, S. C. Heilshorn, *Biomater. Sci.* 2014, 2, 1627–1639.
- [154] R. Arya, J. S. M. Sabir, R. S. Bora, K. S. Saini, in *Insoluble Proteins Methods Protoc.* (Ed.: E. García-Fruitós), Springer New York, New York, NY, **2015**, pp. 45–63.
- [155] J. Porath, J. Carlson, I. Olsson, G. Belfrage, Nature 1975, 258, 598–599.
- [156] H. Block, B. Maertens, A. Spriestersbach, N. Brinker, J. Kubicek, R. Fabis, J. Labahn, F. Schäfer, in *Methods Enzymol.*, **2009**, pp. 439–473.
- [157] E. Stellwagen, in *Methods Enzymol.*, **2009**, pp. 373–385.
- [158] A. Jungbauer, R. Hahn, in *Methods Enzymol.*, **2009**, pp. 349–371.
- [159] K. Tao, P. Makam, R. Aizen, E. Gazit, Science (80-.). 2017, 358, DOI 10.1126/science.aam9756.
- [160] G. Álvarez, M. González, S. Isabal, V. Blanc, R. León, AMB Express 2013, 3, 1.
- [161] R. Balint, N. J. Cassidy, S. H. Cartmell, Acta Biomater. 2014, 10, 2341–2353.
- [162] M. Kumar, N. L. Ing, V. Narang, N. K. Wijerathne, A. I. Hochbaum, R. V. Ulijn, *Nat. Chem.* 2018, 10, 696–703.
- [163] D. Mawad, A. Lauto, G. G. Wallace, in *Polym. Compos. Mater.* (Ed.: S. Kalia), Springer International Publishing, Cham, 2016, pp. 19–44.
- [164] J. L. Dalsin, P. B. Messersmith, *Mater. Today* **2005**, *8*, 38–46.
- [165] N. S. White, R. J. Errington, Adv. Drug Deliv. Rev. 2005, 57, 17-42.
- [166] Q. Lin, H. Huang, J. Chen, G. Zheng, in *Vivo Fluoresc. Imaging Methods Protoc.* (Ed.: M. Bai), Springer New York, New York, NY, **2016**, pp. 153–166.